

**Characterization of  
PratA and Tic22 proteins for functions  
in membrane biogenesis in *Synechocystis* sp.  
PCC 6803**

Dissertation der Fakultät für Biologie

der

Ludwig-Maximilians-Universität München

vorgelegt von

**Ingo Wolf**

München

2012

Erstgutachter: Prof. Dr. Jürgen Soll

Zweitgutachter: Prof. Dr. Jörg Nickelsen

Tag der mündlichen Prüfung: 28.08.2012

## Summary

*Synechocystis* sp. PCC 6803 is a cyanobacterium and successor of the ancient endosymbiont that was the origin of today's chloroplasts in algae and higher plants. Since the majority of proteins is nuclear encoded a complex translocation machinery in the outer (TOC) and inner (TIC) membrane of chloroplasts has been evolved. Tic22 is a component of the TIC complex and located within the intermembrane space. It is supposed to coordinate delivery processes between the TOC and TIC complexes, but not much has been unveiled about its precise function. The participation of the cyanobacterial homolog SynTic22 (Slr0924) in sorting processes is an exciting notion, because it could shed light on at least two questions. Compared to chloroplasts, there is no need for bacteria to import proteins. Biochemical and functional characterization of SynTic22 could therefore reveal information on its role in membrane biogenesis from a more ancient perspective. It could also help to answer the still unsolved question if, in *Synechocystis*, plasma membrane and thylakoid membrane are in direct contact or not, and how proteins are sorted into them. In this work, the attempted knockout of the gene failed under the growth conditions used, confirming the essentialness of the protein for cell survival. However, production of a strain with the endogenous gene substituted by a His<sub>6</sub>-tagged version was possible. In contrast to published data, the results in this work suggested localization of the protein mainly within the periplasm and not the thylakoid lumen. Moreover, *in vivo* pull-down experiments with recombinant and endogenous expressed SynTic22-His, followed by mass spectrometric analysis identified several putative SynTic22 interaction partners. Subsequent yeast two-hybrid analysis suggested that SynTic22 does interact neither with itself nor with the Sll1784 protein.

Studying PrtA, a protein involved in PSII biogenesis, processes of membrane biogenesis should be visualized in a time-resolved manner. A complex construct for inducible expression of *prtA* was designed, assembled and inserted into the endogenous *prtA* gene. Thereby, visualization of its influence on the maturation and sorting of extrachromosomally encoded eCFP::D1 protein between plasma and thylakoid membrane was intended. The functionality was shown *in vivo* but the affinity of the eCFP::D1 encoding vector for homologous recombination prevented further microscopic analysis. Therefore, a new construct for stable integration of a GFP::D1 protein into the inducible strains was produced for future use.

## Zusammenfassung

*Synechocystis* sp. PCC 6803 ist ein Cyanobakterium und damit ein Nachfahre des Endosymbionten, aus dem die heutigen Chloroplasten der Algen und höheren Pflanzen hervorgingen. Weil die Mehrheit der Proteine kerncodiert ist, hat sich ein komplexer Translokationsapparat in der äußeren (TOC) und inneren (TIC) Membran der Chloroplasten entwickelt. Tic22 ist eine Komponente des TIC Komplexes, die im Intermembranraum liegt. Es wird zwar vermutet, dass es an der koordinierten Prä-Protein Übergabe zwischen dem TOC und TIC Komplex beteiligt ist, über die genaue Funktion ist jedoch kaum etwas bekannt. Die Beteiligung des cyanobakteriellen Homologes SynTic22 (Slr0924) an Protein-Verteilungsprozessen ist ein interessanter Gedanke, der auf zumindest zwei Fragen Aufschluss geben könnte. Zum einen müssen Bakterien, im Vergleich zu den Chloroplasten, keine Proteine importieren. Die biochemische und funktionelle Charakterisierung von SynTic22 könnte daher Informationen zur ursprünglichen Rolle in der Membranbiogenese liefern. Außerdem könnte sie dabei helfen die noch immer ungeklärte Frage zu beantworten, ob Plasmamembran und Thylakoidmembran in *Synechocystis* direkt miteinander verbunden sind oder nicht und wie Proteine zwischen ihnen verteilt werden. Das vollständige Ausschalten des Gens schlug unter den in dieser Arbeit angewendeten Wachstumsbedingungen fehl und bestätigt damit die Notwendigkeit des Proteins für den Erhalt der Lebensfähigkeit. Es konnte jedoch ein genetischer Austausch des endogenen Gens durch eine His<sub>6</sub> markierte Variante erreicht werden. Im Gegensatz zu bereits veröffentlichten Daten, deuten die Ergebnisse dieser Arbeit auf eine hauptsächliche Lokalisierung des Proteins im Periplasma und nicht im Thylakoidlumen hin. Darüber hinaus wurden in umfangreichen Pull-down Versuchen, gefolgt von massenspektrometrischen Analysen, mehrere vermeintliche SynTic22 Interaktionspartner identifiziert. Der darauffolgende Hefeinteraktionstest zeigte, dass SynTic22 weder mit sich selbst, noch mit dem möglichen Interaktionspartner Sll1784 Interaktionen eingeht.

Mit der Hilfe von Prata, einem an der PSII-Biogenese beteiligten Protein, sollte eine zeitlich aufgelöste Visualisierung von Prozessen der Membranbiogenese gezeigt werden. Dafür wurde in dieser Arbeit ein kompliziertes Konstrukt zur induzierbaren Expression von *pratA* entwickelt, zusammengefügt und in das endogene *pratA* Gen eingebaut. Es wurde damit beabsichtigt, den Einfluss von Prata auf die Reifung und Verteilung des extrachromosomal codierten eCFP-D1 Proteins zwischen Plasmamembran und Thylakoidmembran zu zeigen. Die Funktionalität des Konstruktes konnte *in vivo* gezeigt werden, jedoch hat die Neigung des eCFP-D1 codierenden Vektors homolog zu Rekombinieren die eigentliche mikroskopische Untersuchung verhindert.

Deshalb wurde ein neues Konstrukt zur stabilen Integration eines GFP-markierten D1 Proteins in die induzierbaren Stämme, für die zukünftige Verwendung, hergestellt.

# Table of Contents

<b>Summary</b> .....	<b>I</b>
<b>Zusammenfassung</b> .....	<b>II</b>
<b>Table of Contents</b> .....	<b>IV</b>
<b>Abbreviations</b> .....	<b>VII</b>
<b>1 Introduction</b> .....	<b>1</b>
1.1 Protein targeting in biological membranes .....	1
1.1.1 Protein sorting in gram-negative bacteria - <i>Escherichia coli</i> .....	2
1.1.2 Protein sorting in cyanobacteria - <i>Synechocystis</i> sp. PCC 6803.....	5
1.2 Tic22 in <i>Synechocystis</i> and chloroplasts of higher plants.....	8
1.3 PratA - a PSII assembly factor involved in membrane biogenesis .....	9
1.4 Aim of this work .....	14
<b>2 Materials</b> .....	<b>15</b>
2.1 Chemicals.....	15
2.2 Molecular weight markers and DNA standards.....	15
2.3 Antibodies .....	15
2.4 Kits.....	16
2.5 Enzymes .....	16
<b>3 Methods</b> .....	<b>17</b>
3.1 Microbiological methods .....	17
3.1.1 <i>Escherichia coli</i> .....	17
3.1.2 <i>Saccharomyces cerevisiae</i> .....	18
3.1.3 <i>Synechocystis</i> sp. PCC 6803 .....	22
3.2 Molecular biological methods.....	25
3.2.1 Isolation of plasmid DNA.....	25
3.2.2 Isolation of genomic DNA from <i>Synechocystis</i> .....	26

3.2.3	Determination of DNA concentration.....	26
3.2.4	PCR.....	27
3.2.5	Sequencing of DNA.....	27
3.3	Biochemical methods.....	27
3.3.1	Overexpression and purification of SynTic22 protein.....	27
3.3.2	Antibody production.....	28
3.3.3	Crude protein extraction from <i>Synechocystis</i> .....	29
3.3.4	Cellular sub-fractionation of <i>Synechocystis</i> .....	29
3.3.5	Protein concentration and buffer exchange.....	30
3.3.6	Determination of protein concentration.....	31
3.3.7	SDS-polyacrylamide gel-electrophoresis (PAGE).....	31
3.3.8	Protein staining procedures.....	31
3.3.9	Immunoblot analysis.....	32
3.3.10	Two dimensional blue native (BN) / SDS-PAGE.....	33
3.3.11	Mass-spectrometry.....	33
<b>4</b>	<b>Results</b> .....	<b>34</b>
4.1	SynTic22 (Slr0924) – a protein involved in sorting processes in <i>Synechocystis</i> .....	34
4.1.1	<i>In silico</i> characterization of SynTic22.....	34
4.1.2	Overexpression and purification of SynTic22.....	35
4.1.3	Localization of SynTic22.....	39
4.1.4	Generating <i>SynTic22</i> mutants.....	41
4.1.5	Two dimensional blue native (BN) / SDS-PAGE.....	44
4.1.6	Initial screening for SynTic22 interaction partners.....	46
4.1.7	Proving of potential SynTic22 interaction partners by using the split-ubiquitin system.....	49
4.1.8	Proving of potential SynTic22 interaction partners by yeast-two hybrid analysis.....	55
4.2	Visualization of membrane biogenesis processes via control of <i>prata</i> gene expression.....	58

---

4.2.1	Generating $\Delta prata$ mutants.....	58
4.2.2	Design and assembly of a <i>nirA::prata</i> inducible construct .....	60
4.2.3	The <i>nirA::prata</i> construct can be used for time-resolved studies of Prata protein expression .....	62
4.2.4	Analysis of extra-chromosomal expression of N-terminal tagged eCFP::D1 .....	65
4.2.5	Generating stable double mutants of $Big\Delta prata::nirAprata(2)//\Delta D1::GFP-D1$ ..	66
<b>5</b>	<b>Discussion</b> .....	<b>67</b>
5.1	The $\Delta synTic22$ strain.....	67
5.2	Localization of SynTic22.....	67
5.3	Initial screen for interaction partners of SynTic22 .....	70
5.4	Proving of potential SynTic22 interaction partners .....	74
5.5	Prata - visualization of membrane biogenesis processes .....	76
<b>6</b>	<b>References</b> .....	<b>78</b>
<b>7</b>	<b>Danksagung</b> .....	<b>91</b>
<b>8</b>	<b>Eidesstattliche Versicherung</b> .....	<b>92</b>
<b>9</b>	<b>Erklärung</b> .....	<b>92</b>



## Abbreviations

2D	two-dimensional
AA	amino acid
AD	activation domain
AP	alkaline phosphatase
At	<i>Arabidopsis thaliana</i>
BLAST	basic local alignment search tool
BN-PAGE	blue-native polyacrylamide gel electrophoresis
bp	base pair
BSA	bovine serum albumin
CBB	coomassie brilliant blue
CC	coiled-coil
CLSM	confocal laser scanning microscopy
Cm	chloramphenicol
CRP	cAMP-receptor protein
C-terminus	carboxy terminus
Da	Dalton
dNTP	deoxynucleotide-triphosphates
DoMa	n-dodecyl- $\beta$ -D-maltoside
DTT	dithiothreitol
E. coli	<i>Escherichia coli</i>
ECL	enhanced chemiluminescence
EDTA	ethylenediamine-tetraacetic acid
EtOH	ethanol
gDNA	genomic DNA
GFP	green fluorescent protein
Gm	gentamycin
HEPES	4-(2-hydroxyethyl)-1-piperazineethanesulfonic acid
His	histidine
HMW	high molecular weight
IEX	ion exchange chromatography
IMS	inter membrane space
IPTG	isopropyl $\beta$ -D-1-thiogalactopyranoside
k, K	kilo, times 1000
Km	kanamycin
LB	left border
MeOH	methanol
Met	methionine
mRNA	messenger-RNA
MS	mass spectrometry
Nt	amino terminus
N-terminus	amino terminus
OD	optical density
PAGE	polyacrylamide gel-electrophoresis
PCR	polymerase chain reaction
pD1	pre-D1 protein of PSII
PM	plasma membrane
PP	periplasma

---

PratA	processing associated TPR protein A
Ps	<i>Pisum sativum</i>
PSI, PSII	photosystem I, II
PVDF	polyvinylidene fluoride
RB	right border
rpm	revolutions per minute
RT	room temperature
SC	yeast selection medium
SDS	sodium dodecyl sulphate
SP	signal peptide
SSU	ribulose-1,5-bisphosphate carboxylase/oxygenase, small subunit
<i>syn, Synechocystis</i>	<i>Synechocystis</i> sp. PCC 6803
Tat	twin-arginine translocon
TIC	translocon at the inner envelope of chloroplasts
TM	thylakoid membrane
TOC	translocon at the outer envelope of chloroplasts
TPR	tetratricopeptide repeat
TX-100	triton X-100
v/v	volume per volume
w/v	weight per volume
WT	wild-type
x g	times the force of gravity
X-gal	5-bromo-4-chloro-3-indolyl beta-D-glucopyranoside
Y2H	yeast-two hybrid
$\beta$ -ME	$\beta$ -mercaptoethanol

# 1 Introduction

## 1.1 Protein targeting in biological membranes

Cells are the fundamental units of life, which are enclosed by a framework of biological membranes. Membranes serve as physical barriers that separate the interior from both the external environment and from specialized intracellular compartments, the organelles. Thereby, a controlled uptake and accumulation of molecules can occur, whereas others are prevented from entering. Using organelles, the biochemistry of the cell can be organized into different microenvironments for optimal performance of enzymatic reactions. Those are the basic characteristics of membranes but they are far from being empty shells. Since E. Overton's proposal in 1895 that biological membranes consist of lipid bilayers, many data has been gathered about composition, structure and function (Overton, 1895; Singer, 1974). According to the fluid-mosaic-model, all biological membranes share the same basic organization of proteins embedded in phospholipids or glycosylglycerides (Singer and Nicolson, 1972). However, membrane systems (e.g. plasma membranes, thylakoids or the endoplasmic reticulum) can be distinguished by their specific lipid and protein composition (Table 1). Thus, each membrane possesses unique functional characteristics (Pike, 2008). The essential role of membrane proteins for cell viability is especially illustrated by the fact that they make up to one third of proteins in sequenced genomes (Pollard and Earnshaw, 2007).

**Table 1: Structural lipids in chloroplast, mitochondrion and ER membranes.** Lipid composition in percentage of total lipids (according to Taiz, 2006). ER, endoplasmic reticulum.

Lipids	Chloroplasts	Mitochondria	ER
Phosphatidylcholine	4	43	47
Phosphatidylethanolamine	0	35	34
Phosphatidylinositol	1	6	17
Phosphatidylglycerol	7	3	2
Diphosphatidylglycerol	0	13	0
Monogalactosyldiacylglycerol	55	0	0
Digalagtosyldiacylglycerol	24	0	0
Sulfolipid	8	0	0

In order to maintain the specific membrane characteristics, insertion of membrane proteins in a random manner is not an option. For this reason, most proteins contain signal peptides, which

are address tags in their amino acid sequence that mediate the final protein localization (Mohoj and Degan, 2004). Furthermore, machines for accurate and efficient insertion have evolved in prokaryotic and eukaryotic cells (Pollard and Earnshaw, 2007).

### **1.1.1 Protein sorting in gram-negative bacteria - *Escherichia coli***

*E. coli*, a gram-negative proteobacterium, has been extremely useful in studies to establish the composition, structure and function of membranes (Filip et al., 1973; Osborn et al., 1972). The envelope of *E. coli* and other gram-negative bacteria is a complex structure that consists of an inner membrane and an outer membrane. The inner membrane (also plasma or cytoplasmic membrane; PM) is a common phospholipid bilayer. In contrast, the outer membrane (OM) consists of a phospholipid monolayer and a leaflet that contains almost all lipopolysaccharides (LPS) of the envelope (Filip et al., 1973; Osborn et al., 1972). Although the only known function is to serve as a protective barrier, *E. coli* cells die without an outer membrane (Silhavy et al., 2010). The periplasm (PP) is located between both membrane types. It contains a thin cell wall, an intermediate peptidoglycan layer, which is connected to the OM via lipoproteins to give the cell its shape and rigidity (Dalbey and Kuhn, 2012).

Apart from their structural differences, both inner and outer membranes contain a substantial amount of proteins. The plasma membrane, for instance, is known to contain more than thousand integral membrane proteins, corresponding to 20-30 % of the proteome (Xie and Dalbey, 2008; Dalbey and Kuhn, 2012). Plasma membrane proteins belong to a multitude of protein classes, whereas the outer membrane proteins can be divided in more or less two. The first class are lipoproteins. Lipoproteins are not transmembrane proteins as they are embedded only in the inner phospholipid leaflet of the OM. At the N-terminus, they have lipid moieties attached to cysteine residues (Sankaran and Wu, 1994; Miyadai, 2004). The second class are  $\beta$ -barrel proteins, integral membrane proteins that are made of  $\beta$  sheets, which are wrapped into cylinders. They function in the passive or specific diffusion of small molecules like sugars and ions or in the transport of large ligands like Fe-chelates (Silhavy et al., 2010). Altogether, approximately 2 % of the proteome are outer membrane proteins (Xie and Dalbey, 2008).

In order to insert or translocate those proteins into the OM, PP or PM, several machineries have evolved in *E. coli* (reviewed in Xie and Dalbey, 2008; Dalbey et al., 2011; Dalbey and Kuhn, 2012).

#### 1.1.1.1 Insertion into the plasma membrane

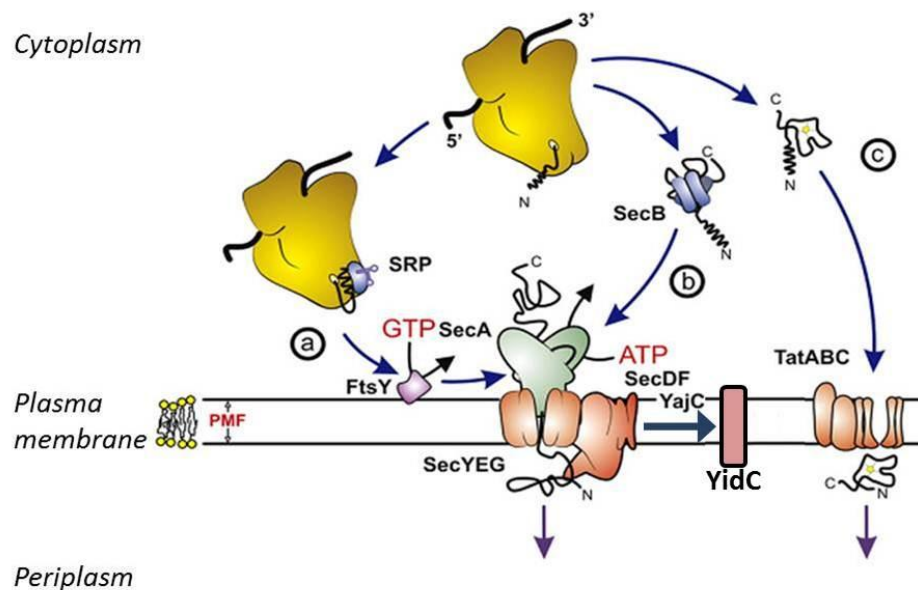
Most proteins of the plasma membrane (PM) in *E. coli* are inserted via the Sec-pathway. In an energy consuming process, hydrophilic segments are translocated into the periplasm, whereas the hydrophobic segments of the protein are transferred into the lipid bilayer (Xie and Dalbey, 2008; Dalbey and Kuhn, 2012; Dalbey et al., 2011). First, the signal-recognition particle (SRP), which is comprised of the Ffh peptide and 4.5S RNA, binds to a hydrophobic region on a nascent polypeptide chain at the ribosomal exit site, in a GTP-dependent manner. SRP delivers the complex to the membrane, where it binds the SRP receptor FtsY (Luirink and Sinning, 2004). FtsY, again, needs GTP to bind the SRP-ribosome complex, plasma membrane lipids and the SecYEG translocase. Transfer of the polypeptide-ribosome complex to SecYEG, which forms the translocation pore, occurs via hydrolysis of the GTPs in the SRP and SRP receptor, allowing both to dissociate from each other. Therefore, the targeting via SRP is a co-translational process (Xie and Dalbey, 2008). The actual membrane insertion seems to be determined by the hydrophobic character of the transmembrane segments. Those segments interact with the membrane lipids, leading to a stop of the transfer. Finally, YidC, which is another insertase in the plasma membrane, is used to laterally shift the transmembrane helices into the bilayer (Stiegler et al., 2011; Dalbey and Kuhn, 2012). It has been suggested that YidC acts as a chaperone that supports the transfer and stabilizes the transmembrane segments (Figure 1; Kuhn et al., 2003).

Interestingly, YidC has also been shown to function in a Sec-independent manner (Serek et al., 2004). The YidC-only pathway is evolutionary conserved and present in the plasma membrane, the inner membrane of mitochondria as well as in the thylakoid membrane of chloroplasts (Benz et al., 2009; Dalbey and Kuhn, 2012; Stiegler et al., 2011). The structure of YidC homologs is conserved and predicted to comprise five transmembrane segments, although the *E. coli* protein has an additional N-terminal transmembrane segment (Xie and Dalbey, 2008). YidC also possesses a large C-terminal periplasmic domain that is not conserved. YidC has been shown to be sufficient for Sec-independent insertion of Pf3, the major coat protein of the Pf3 phage, and the endogenous membrane protein F<sub>1</sub>F<sub>0</sub>-ATP synthase subunit c (Serek et al., 2004; Yi et al., 2003).

#### 1.1.1.2 Translocation into the periplasm

In *E. coli*, the Sec-pathway is also the major pathway for translocation of proteins into the periplasm (PP). An N-terminal signal sequence is required, which is composed of a positively charged region, a central hydrophobic domain and a polar C-terminal region (Dalbey and

Robinson, 1999). In contrast to Sec-dependent PM insertion, the targeting is post-translational and the SRP-pathway plays only a minor role. In this case, the homotetramer SecB, a chaperone that exerts anti-folding activity, steps in (Dalbey and Kuhn, 2012). It has been found to prevent pre-proteins from folding into stable conformations in the cytosol (Zhou and Xu, 2005). SecB interacts with the ATPase SecA. SecA uses energy released upon hydrolyzation of ATP to catalyze a stepwise translocation of up to 30 amino acids of the export pre-protein at a time through the SecYEG channel. After translocation into the periplasm, the signal peptide is removed by either signal peptidase I or signal peptidase II in the case of lipoproteins (Figure 1; Dalbey and Robinson, 1999).



**Figure 1: Insertion and translocation processes into and across the plasma membrane in *E. coli*** (modified from Natale *et al.*, 2008). Proteins translated within the cytosol are targeted either co- or post-translationally in an energy dependent manner. (A) Co-translational insertion of proteins into the plasma membrane via the Sec-pathway affords energy in form of GTP. The YidC insertase interacts with the SecDFYajC component and transfers proteins into the lipid bilayer. (B) Post-translational translocation of proteins into the periplasm via the Sec-pathway. The SecB chaperone keeps newly synthesized proteins in an unfolded state. Translocation through the translocation pore (SecYEG) affords energy in form of ATP. (C) Post-translational translocation of proteins into the periplasm via the Tat-pathway. Note, proteins are already folded. Energy in form of a proton motive force (PMF) is needed for transfer. For further details, see text (1.1.1).

The twin-arginine (Tat) pathway is the second pathway for translocation of proteins into the periplasm that exists in *E. coli*. Like the Sec-pathway, it functions post-translationally and in an energy dependent manner (Figure 1). However, the main difference is its ability to translocate proteins that were folded prior to export. Moreover, energy is not required in form of GTP or ATP. Instead, the proton motive force (PMF) is required and approximately 30.000 protons are consumed per protein in the process (Bageshwar and Musser, 2007; Robinson and Bolhuis, 2004). The Tat pathway machinery consists of the TatA, TatB and TatC proteins. A complex of

TatBC has been shown to recognize the Tat signal peptide (Alami et al., 2003), which is illustrated by the twin-arginine motif. The consensus sequence comprises a hydrophilic amino acid residue, the two central arginine residues followed by a residue of any kind and two hydrophobic amino acid residues (Natale et al., 2008). Finally, the TatBC-export protein complex binds to TatA homooligomers, which form the channel of the translocation mediating TatABC complex (Figure 1; Dalbey and Kuhn, 2012).

#### 1.1.1.3 Insertion into the outer membrane

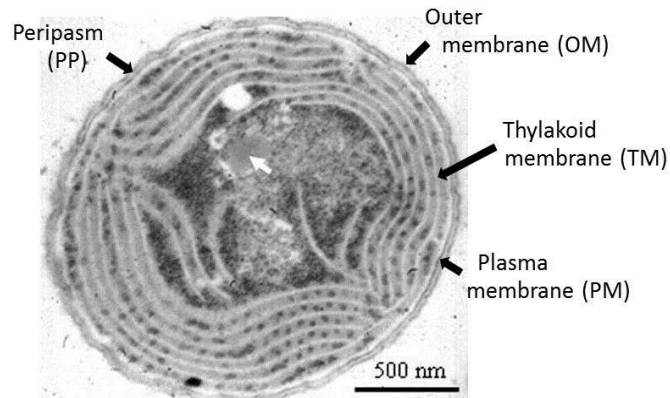
Two major pathways are used for insertion of proteins into the outer membrane (OM) in *E. coli*. First, all pre-proteins destined for the OM are translocated into the PP via Sec- or Tat-pathway and the signal sequence is subsequently removed by signal peptidases. The Lol-pathway consists of five proteins and is used for transports of lipoproteins to the OM. LolD, a peripheral PM protein in combination with the transmembrane proteins LolC and E, uses ATP to remove the exported lipoproteins from the periplasmic side of the plasma membrane. LolA, a periplasmic chaperon binds and transports the lipoproteins to the OM. Finally, the lipoproteins are transferred to LolB and inserted into the OM (Dalbey and Kuhn, 2012).

$\beta$ -barrel proteins are transported and inserted using the BAM machinery. Unfolded  $\beta$ -barrel pre-proteins are exported via the Sec-pathway and the signal sequence is cleaved off. Periplasmic chaperons like SurA, Skp or DegP guide the proteins to the OM. At the OM, BamA performs the insertion and folding process. It belongs to the evolutionary conserved Omp85 class of membrane proteins, which have been shown to perform a similar function in mitochondria and chloroplasts (Dalbey and Kuhn, 2012).

### 1.1.2 Protein sorting in cyanobacteria - *Synechocystis* sp. PCC 6803

*Synechocystis* sp. PCC 6803 is a unicellular freshwater cyanobacterium. Like *E. coli*, it belongs to gram-negative bacteria. It therefore possesses an inner and outer membrane system. However, like all organism that are able to perform oxygenic photosynthesis, it also possesses a specialized internal network, the thylakoid membranes (Figure 2).

In cyanobacteria, thylakoid membranes (TMs) organize in several concentric rings (Nevo et al., 2007) constituting most of the cellular membranes (van de Meene et al., 2006). The additional membrane system, together with the observation that TMs in *Synechocystis* merge at sites very close to the PM (van de Meene et al., 2006) (Figure 2), has led to an intensive debate about how membrane characteristics of PM and TM are established in cyanobacteria. Protein localization



**Figure 2: Transmission electron microscopic picture of non-dividing cell of *Synechocystis* wild-type** (modified from Marcus and Schleiff, 2010). Cyanobacteria have an additional membrane system, the thylakoid membrane, where oxygenic photosynthesis takes place. Note that the thylakoids are stacked in several layers and appear to merge close to or with the plasma membrane. White arrow marks a carboxysome.

studies as well as proteomic characterization of PM and TM protein composition have shown a unique distribution between both membrane types for most of the proteins investigated (Srivastava et al., 2005; Huang, 2002). For this reason, the key question is how this can be achieved, since *Synechocystis* uses sorting pathways similar to those that have been described for *E. coli*. One hypothesis has been proposed that sorting occurs prior to insertion/translocation processes (Barnett, 2011). That would mean that: (I) other pathways exist; (II) specialization of the pathways for one membrane system exists; (III) several isoforms of insertase/translocase subunits exist; (IV) different substrate specificity exists.

Although it cannot be excluded that other unidentified insertion/translocation pathways exist, no further mechanism have been identified so far (Kaneko, 1996; Nickelsen et al., 2011). A clear specialization for one membrane system, as observed in chloroplasts of higher plants (Figure 3; Jarvis, 2008), has not been demonstrated for insertion/translocation pathways in cyanobacteria. In contrary, subunits of the Sec-pathway, the major insertion/translocation pathway in *E. coli*, have been demonstrated to operate in TMs and PMs of *Synechococcus* PCC 7942 (Nakai et al., 1993). Furthermore, there is good evidence that also the Tat pathway is operating in both membrane types (Spence et al., 2003; Aldridge et al., 2008). A discrimination of protein substrates cannot be explained by a different subunit composition of the insertion/translocation complexes because there are only single copies of the encoding genes (Nakai et al., 1993; Kaneko, 1996). Recent data suggests that signal peptides function as allosteric activators of translocases (Gouridis et al., 2009). Binding to a lateral gate induces a conformational change thereby opening the channel (Dalbey and Kuhn, 2012). Using multivariate sequence analysis, signal peptides of experimentally verified proteins in *Synechocystis* have been demonstrated to possess distinguished chemical properties, corresponding to their cellular localization (Rajalahti



et al., 2007). Therefore, differences in membrane composition (e.g. accessory proteins or the kind of lipids) might modify the specificity of the same insertases/translocases for certain signal peptide types, in different membrane systems (Rajalahti et al., 2007). This idea was further supported by the observation that membrane properties seem to have a role in Tat mediated transport processes, too. In particular, signal peptides of some Tat substrates have been shown to interact with membranes prior to translocation (Barnett et al., 2011).

Another hypothesis is that proteins are sorted after insertion/translocation. Yet again, this raises the question how it is achieved (Nickelsen et al., 2011). Data supporting this hypothesis comes from a fractionation study where subunits and pre-complexes of photosystem I and II were found in the PM of *Synechocystis* (Smith and Howe, 1993; Zak, 2001; Jansén et al., 2002). Because the photosystems are functioning within the thylakoids, either a direct or an indirect connection has to exist. One possibility for an indirect connection could be vesicle transport between the PM and TM membranes as has been observed in chloroplasts (Westphal et al., 2001) and proposed as mechanism in *Microcoleus* sp. (Nevo et al., 2007). In *Synechocystis*, knockdown of the vesicle-inducing protein in plastid 1 (VIPP1), leads to a severely disrupted TM formation (Westphal, 2001) similar to that observed in *Arabidopsis thaliana* (Kroll, 2001). That would propose vesicle formation as an important mechanism for TM maintenance in *Synechocystis*. However, a complex vesicle transport system has not been observed in prokaryotes so far (Liberton et al., 2006). Furthermore, the chloroplast vesicle system is thought to have originated from the eukaryotic host (Westphal et al., 2003), thus vesicle transport might not be responsible for the majority of protein sorting processes in cyanobacteria (Pisareva et al., 2011). Thereby, in spite of the fact that periplasmic and luminal protein composition differs (Fulda et al., 2000; Pisareva et al., 2011) and experiments using membrane permeable and impermeable stains on living cells disagree with a stable connection (Schneider et al., 2007), a plain separation of PMs and TMs is highly unlikely. Electron-microscopic techniques, followed by computer-aided image processing, have led to contradictory results concerning PM-TM interaction (Liberton et al., 2006; van de Meene et al., 2006). Recently, characterization of the membrane biogenesis factor PratA (Klinkert, 2004; Schottkowski et al., 2008) as well as a combination of proteomics and multivariate sequence analysis favor a dynamical interaction between PM and TMs (Pisareva et al., 2011), most likely in specialized TM regions (Rengstl et al., 2011). This model shares some similarity to a mechanism that has recently been proposed for *Microcoleus* (Nevo et al., 2007). Like in other cyanobacteria, the TMs are densely packed with phycobilisomes (van de Meene et al., 2006). Therefore, restricted TM areas have been proposed, where protein insertion/translocation might occur (Nevo et al., 2007).

## 1.2 Tic22 in *Synechocystis* and chloroplasts of higher plants

In plants, multitudes of proteins are implicated in the general import pathway at the inner or outer envelope of chloroplasts (Oreb et al., 2008). In addition, several proteins were proposed to participate in translocation of proteins through the intermembrane space (IMS), however, for most of them such a function was put into question in recent studies (Aronsson et al., 2007; Chiu et al., 2010; Flores-Pérez and Jarvis, 2012). For example, *imsHsp70* is an ATP consuming outer membrane chaperone that might function as a pre-protein driving motor (Gross and Bhattacharya, 2009). Its existence and participation is still under debate and needs further examination (Flores-Pérez and Jarvis, 2012; Schwenkert et al., 2011). Tic22 was the first protein demonstrated to be localized within the IMS and up to now the only known soluble component of the IMS translocation complex (Kouranov et al., 1998; Schwenkert et al., 2011). Tic22 is a nuclear-encoded protein, represented by two major isoforms in *Arabidopsis thaliana* (Tic22-III and Tic22-IV; Moghadam and Schleiff, 2005). The protein is imported into the IMS via the general import pathway, although the exact mechanism and components involved have been under controversial debate (Kouranov et al., 1999; Vojta et al., 2007). So far, no functional domains have been identified within the amino acid sequence. However, in biochemical studies Tic22 was shown to build a ternary complex with TOC components Toc12, Toc34, Toc64 and the chaperone *imsHsp70* in an ATP-dependent manner (Kouranov et al., 1999; Becker, 2004; Qbadou et al., 2006). In addition, interaction was observed with translocating pre-proteins (Kouranov and Schnell, 1997) and TIC components Tic20, Tic32 and Tic110 (Kouranov et al., 1998; Hörmann et al., 2004). Based on these findings, Tic22 has been proposed to function as a connector that facilitates pre-protein routing between TOC and TIC complexes (Kouranov et al., 1998; Schwenkert et al., 2011). Although further supported by the observation that the majority of TIC translocon components do not permanently align but rather associate in a TOC complex mediated manner (Kouranov et al., 1998), there has been no direct test yet. Therefore, its exact role in translocation is still elusive (Gross and Bhattacharya, 2009). Intriguingly, Gross and colleagues (2009) reasoned that most of the TIC translocon subunits have more than one function. They speculate that a general characteristic of TIC complex evolution might have been the incorporation of functional proteins into simple translocon complexes. Consequently, those proteins obtained new functions in import but, at the same time, have not lost their ancestral assignment (Gross and Bhattacharya, 2009).

*Synechocystis* Tic22 (SynTic22) might be an interesting example in this respect (Gross and Bhattacharya, 2009) as it is one of a few chloroplast TOC-TIC subunit homologs, existing in cyanobacteria (e.g. Toc75; Bölter et al., 1998). It had first been identified in the periplasm of salt

treated cells (Fulda et al., 1999), but was later shown to be mainly localized within the thylakoid lumen (> 98 %; Fulda et al., 2002). In contrast to plants, there is only one isoform encoded in the genome of *Synechocystis* sp. PCC 6803 (Kaneko, 1996). The SynTic22 protein was demonstrated to be essential for cell viability, because attempts to knockout the monocistronically expressed gene failed. Nevertheless, a merodiploid knockdown strain was obtained under the conditions tested, showing an 80 % reduced protein content. Noticed phenotypes were mortality after glucose treatment and a reduced photosynthetic activity (Fulda et al., 2002). Moreover, the protein expression levels in wild-type cells have been found to correlate with light intensity and glucose concentration. Therefore, its connection to electron transfer processes in thylakoids was speculated (Fulda et al., 2002). Since cyanobacteria are the ancestors of today's chloroplasts the dual localization of SynTic22 was speculated to represent an intermediate stage where the dual functionality, in this case, sorting in PP versus putative involvement in electron transfer processes in TM, is still observable (Fulda et al., 2002; Gross and Bhattacharya, 2009). Although it is an attractive hypothesis, a putative role of SynTic22 as a membrane biogenesis factor is still elusive.

### **1.3 PrataA - a PSII assembly factor involved in membrane biogenesis**

Although some membrane proteins function as single proteins, most are only functional or stable in complexes. Protein complex formation seems to be an ordered process, which, if not properly executed, can have dramatic effects on the cells viability (Daley, 2008). However, even for extraordinarily well characterized complexes like the photosystems, comparatively little is known about their biogenesis. Only recently, substantial progress has been made in studying PSII assembly, repair and in identification of factors involved in those processes (Nixon et al., 2010).

Probably one of the most exciting factors involved in membrane biogenesis is the PrataA protein. It had first been identified in a screen for tetratricopeptide repeat (TPR) proteins in *Synechocystis* sp. PCC 6803 and was ever since the initial point for providing extraordinary useful experimental data on spatiotemporal organization of membrane biogenesis processes (Klinkert, 2004; Schottkowski et al., 2008; Rengstl et al., 2011; Stengel et al., 2012).

The TPR motif is a degenerated protein-protein interaction motif that consists of amphipathic  $\alpha$ -helical regions. Sikorski et al. first described it in 1990 as a multiple repeat of 34 amino acids in proteins of *S. cerevisiae*, which is involved in mitosis and RNA synthesis (Sikorski et al., 1990). In following years, the first structural model was published (Das, 1998) and more family members had been identified in numerous organisms ranging from bacteria to humans, showing

the apparent general usability. Moreover, a multitude of new functions of TPR proteins have been suggested like regulation of cell cycle and protein folding processes, transcriptional control and protein transport into mitochondria and peroxisomes (Blatch and Lässle, 1999; D'Andrea, 2003). In photosynthetic organism, TPR proteins like Nac2 and Hcf107 are known to be involved in mRNA stabilization of photosystem II subunits (Boudreau, 2000; Felder et al., 2001). Other factors in turn, like Ycf37 and LPA1, are involved in assembly of photosystems I and II, respectively (Stockel, 2006; Peng, 2006).

Using the screening approach, twenty-two putative TPR-protein encoding open reading frames had been identified in *Synechocystis* and the *prata* gene (*slr2048*) was subsequently analyzed in more detail (Klinkert, 2004). It turned out to be a protein of about 35 kDa that comprises nine TPR repeats within its 398 amino acids long polypeptide chain. Sequence similarity searches did not propose any obvious eukaryotic homologs. PrataA is encoded by a single copy of the *prata* gene on the chromosome of *Synechocystis*. However, it was possible to create a *prata* knockout strain by introduction of a kanamycin resistance gene into the endogenous locus, demonstrating the non-essentialness for its gene product. Nevertheless, when the physiological properties of the mutant strain had been tested, it turned out that the autotrophic growth, the chlorophyll emission peaks from PSII and the oxygen production were drastically decreased. Taken together, data suggested an impaired photosystem II in the mutant (Klinkert, 2004).

The photosystem II is the light-driven water:plastoquinone oxidoreductase, a multisubunit membrane protein complex integrated in thylakoids of cyanobacteria and chloroplasts (Allen et al., 2011). It functions in oxidizing water to molecular oxygen and in reducing plastoquinone (Zouni et al., 2001). Thereby, protons are released and an electron flow is initiated, which leads to a translocation of additional protons into the lumen. Altogether, a transmembrane proton motive force is created ( $\Delta p$ ). Eventually, the stored energy in  $\Delta p$  is used to drive an ATP synthase, thereby generating ATP (Allen et al., 2011). Recently, detailed structural data for PSII sub-unit organization has been published for the thermophilic cyanobacterium *Thermosynechococcus elongatus* (Guskov et al., 2009). In *T. elongatus*, a PSII monomer consists of 17 intrinsic factors, e.g. D1 (*psbA*), D2 (*psbD*), CP43 (*psbC*), CP47 (*psbB*), Cytochrome b559 $\alpha$  and  $\beta$  subunit (*psbE* and *psbF*) and 3 extrinsic factors PsbO, PsbU and PsbV (see Allen et al., 2011 for a complete list). In addition, the monomer contains 35 chlorophyll *a* pigments, twelve carotenoids, two pheophytin *a*, two haem and three plastoquinones, one non-haem iron, two Ca<sup>2+</sup>-ions, one or two Cl<sup>-</sup> ions, a few tens of lipid molecules, and a CaMn<sub>4</sub> metal cluster (Guskov et al., 2009, Guskov et al., 2009).

In the *pratA* knockout mutant, Klinkert and co-workers could observe a reduction in CP47 (PsbB), PsbO and D1 (PsbA) proteins of PSII (Klinkert, 2004). They could also show that this effect was not due to an altered RNA stabilization process as reported for other TPR proteins (Boudreau, 2000; Felder et al., 2001), since the gene-specific RNA levels were equal in wild-type and mutant (Klinkert, 2004). *In vivo* pulse labeling of proteins in combination with 2D-Blue native/SDS-PAGE analysis specifically pointed to an involvement of Prata in the processing of the precursor-D1 protein (pD1) to its mature form (D1) (Klinkert, 2004).

The D1 protein has been shown to be composed of five membrane-spanning  $\alpha$ -helices (Salih and Jansson, 1997). D1 together with the transmembrane protein D2 forms the reaction center core complex (RC) of PSII, which is an enzyme that uses light energy to reduce molecules. The RC complex is able to bind all co-factors involved in light-induced charge separation. These are the chlorophyll *a* molecules, the pheophytin, which is an electron carrier that takes the electrons from the reaction center, and the plastoquinone, a membrane protein that accepts the electrons from pheophytin, transfers them to the cytochrome  $b_6f$  complex and in the process shuttles protons into the lumen (Rappaport and Diner, 2008). The CP43 and CP47 antenna proteins add additional chlorophyll *a* and  $\beta$ -carotene molecules to the complex and pass on excitation energy to the reaction center. Importantly, CP43 and D1 ligate the  $CaMn_4$  cluster involved in water oxidation (Ferreira et al., 2004). As mentioned above, in virtually all photoautotrophic organisms the D1 protein is synthesized in a precursor form with a C-terminal extension of varying length (Marder et al., 1984; Nixon et al., 2010). For the proper assembly of the water-oxidizing cluster, the 16 amino acid C-terminal extension of *Synechocystis* needs to be cleaved off by the C-terminal endoprotease A (CtpA Anbudurai et al., 1994). This is performed in a two-step process via iD1, an eight amino acid intermediate form (Inagaki et al., 2001; Komenda et al., 2007). Since it is not necessary for the formation of the cluster, the reason for the C-terminal extension in the first place is not completely understood (Sato and Yamamoto, 2007). However, some data indicates it might have a photo-protective function (Kuviková et al., 2005). The Prata protein has first been shown to directly interact with the 68 amino acid C-terminus of pD1 protein suggesting specificity for the precursor (Klinkert, 2004). However, following yeast two-hybrid experiments revealed an affinity for the mature D1 protein as well (Schottkowski et al., 2008). Intriguingly, when Prata protein localization had been analyzed, it was found to be a soluble periplasmic protein, which agrees to the predicted N-terminal Sec signal sequence, though it raises the question of how a periplasmic protein could possibly interact with a protein that is supposed to be a thylakoid membrane protein (Klinkert, 2004; Salih and Jansson, 1997). Therefore, at first glance, this finding seemed implausible but it is actually in agreement with

previous data from *Synechocystis* suggesting the initial steps of biogenesis of photosystems to occur in the plasma membrane, thereby supporting a connection of plasma and thylakoid membrane (Zak, 2001). For instance, the CtpA endoprotease is solely found in the PM (Zak, 2001). In addition, following experiments strengthened a possible Prata-D1 interaction. First, Prata was shown to reside in two different complexes of which a 70 kDa, membrane-associated complex was dependent on the availability of D1 protein as shown in the TD41 triple *psbA* deletion strain. In contrast, a soluble ~ 200 kDa Prata complex was also observed and shown to be not affected by the availability of D1 protein (Schottkowski et al., 2008). Second, pD1 and D1 were able to pull-down Prata from native periplasmic extracts (Stengel et al., 2012). A two-step sucrose gradient (a step-gradient followed by a linear gradient) was used to find out whether the Prata-D1 complex is part of the plasma or thylakoid membrane system. In wild-type samples, Prata accumulated within the lower density fractions. The mature D1 protein and thylakoid marker proteins accumulated almost exclusively within the higher density fractions of the gradient, whereas pD1 did not considerably accumulate in any wild-type fraction. Consistent with the assigned defect in processing of the D1 protein, pD1 did accumulate in the *prata* knockout mutant, but surprisingly, in fractions of the gradient defined by the presence of Prata in wild-type (Schottkowski et al., 2008). The authors reasoned a specialized membrane subfraction where the early steps of *de novo* PSII assembly occur. They named it Prata-defined membrane (PDM), as it was shown to be biochemically different from the thylakoid membranes (Schottkowski et al., 2008).

PDMs, where early steps of PSII assembly take place, were first identified because of the presence of Prata (Schottkowski et al., 2008). However, since other assembly factors have been suggested to function during early assembly steps a comprehensive characterization was carried out leading to a better understanding of the spatial organization of the process (Rengstl et al., 2011). Of several assembly factors tested (Slr10933 Armbruster et al., 2010, Slr1471 Ossenbühl et al., 2006; Spence et al., 2004, and Ycf48 Komenda et al., 2008), the inactivation of Prata was found to have the most severe effect on spatial organization of PDMs. It has been suggested that the gradient fractions represent the assembly of PSII from lighter to denser membrane fractions, since D1 and D2 had been observed in PDMs and TMs, whereas the inner antenna protein CP47 and CP43 were almost exclusively in the denser TM fractions (Rengstl et al., 2011). This finding is in agreement with current models of PSII assembly (Nixon et al., 2010; Komenda et al., 2012). By analyzing the pigment distribution, chlorophyllide *a*, a precursor in chlorophyll *a* biosynthesis, was also found to accumulate in PDMs of wild-type (Rengstl et al., 2011). This finding and data derived from PDMs of early PSII assembly factor mutants suggests the

chlorophyll *a* synthesis and/or integration to correlate with the RC complex formation (Rengstl et al., 2011). Taken together, the characterization of the distribution of membrane-associated D1 assembly factors in PrtA defined membrane subfractions turned out to be a useful approach to study the early assembly steps of PSII in addition to the established 2D Blue native/ SDS-PAGE technique (Komenda, 2004; Komenda et al., 2005). In an approach to precisely determine the location of PDMs using immunogold labeling, semicircular-shaped structures of about 100 nm in diameter at the periphery of cells have been identified (Stengel et al., 2012). These structures were shown to surround the earlier described, rod-like thylakoid centers (Kunkel, 1982; van de Meene et al., 2006) in a PrtA-dependent manner, because PrtA was required for stability and/or fixation of the structures at the periphery. The structures seemed to coincide with pD1 localization and to connect PM and TM. Therefore, they were named biogenesis centers (thylakoid center + semicircular structure). Finally, the biogenesis centers might represent a further puzzle piece to solve the controversial PM-TM connection problem in cyanobacteria (Stengel et al., 2012).

Recently, yet another function for PrtA has been assigned underlining its immanent role as a central factor for initial steps of PSII *de novo* assembly (Stengel et al., 2012). Biophysical function and even the exact protein composition for proper coordination of the water oxidizing cluster of PSII is known in detail (Ferreira et al., 2004), but it is still not clear how the complex is loaded with manganese in the first place (Stengel et al., 2012). PrtA has now been demonstrated both to directly bind manganese in the periplasm and to transfer  $Mn^{2+}$  to the membrane where it is delivered to D1 protein of RC complexes (Stengel et al., 2012).

## 1.4 Aim of this work

This work aimed at the identification of molecular mechanisms underlying the biogenesis of the two principle membrane systems in the model organism *Synechocystis* sp. PCC 6803, the plasma and the thylakoid membrane. Especially, how proteins are sorted between those membrane systems is still an open question. Therefore, two proteins and their possible participation in membrane biogenesis were investigated.

Plant Tic22 functions in the import of proteins from the cytosol into the chloroplast via the general import pathway. Thus, as a homolog of Tic22 in higher plants, SynTic22 is an interesting but unconfirmed candidate for sorting processes in *Synechocystis*. The goals of the first part of this work were to examine its subcellular localization (I), to characterize it functionally by establishing a knockout strain (II) and to perform a screen for interaction partners using pull-down assays (III). The results could finally lead to a deeper insight into the evolution of membrane biogenesis from the original endosymbiont to modern chloroplasts.

PratA is a periplasmic protein that is involved in the processing of the pD1 protein to its mature form during photosystem II biogenesis. This has been shown in detail in preliminary experiments using different biochemical approaches *in vitro* as well as *in vivo* by localization of eCFP-tagged D1 protein. Since wild-type and *pratA* knockout strains had been used, only steady-state levels were visualized (Schottkowski et al., 2008).

Therefore, the second part of this work focused on the design, assembly and stable insertion of a complex construct for the inducible expression of the *pratA* gene to follow subcellular membrane flow via the eCFP-tagged D1 protein from the site of its assembly into PSII (plasma membrane) to the site of PSII function within the thylakoid membrane. Thereby, visualization of PratA-mediated biogenesis processes in a time-resolved manner will be possible.



## 2 Materials

### 2.1 Chemicals

All chemicals used were purchased in high purity from Sigma-Aldrich (Steinheim, Germany), Fluka (Buchs, CH), Roth (Karlsruhe, Germany), Roche (Penzberg, Germany), Merck (Darmstadt, Germany), AppliChem (Darmstadt, Germany) or Serva (Heidelberg, Germany). Radiolabeled amino acids ( $^{35}\text{S}$ Met) were obtained from Perkin Elmer (Dreieich, Germany).

### 2.2 Molecular weight markers and DNA standards

Agarose gel electrophoresis was performed using the *EcoRI* and *HindIII*  $\lambda$ -Phage DNA molecular size marker (MBI Fermentas).

For SDS-PAGE the MW-SDS-70L marker from Sigma-Aldrich (Steinheim, Germany) and the peqGOLD Protein Marker I from Peqlab (Erlangen, Germany) were used. For BN-PAGE the “HMW Native Marker Kit” from GE Healthcare (München, Germany) was used.

### 2.3 Antibodies

The following antibodies were used in this work:

**Table 2: Antibodies used in this work.** Additional information on type, Western analysis conditions and the source of the antibodies.

Name	Species	Immunoblot conditions	Source
$\alpha$ Tic22	rabbit, polyclonal	1:500; 3 % milk	this work
$\alpha$ PratA	rabbit, polyclonal	1:625; 5 % milk	kind gift of Prof. Nickelsen, LMU München
$\alpha$ GFP	mouse, monoclonal	1:1000; 5 % milk	Roche (Mannheim, Germany)
$\alpha$ His	mouse, monoclonal	1:500; 1 % BSA	Roche (Mannheim, Germany)
$\alpha$ NrtA	rabbit, polyclonal	1:1000; 0.1 % BSA, 0.05 % Tween-20	available in the lab
$\alpha$ D1	rabbit, polyclonal	1:2000; 2 % milk	available in the lab
$\alpha$ Ycf48	rabbit; polyclonal	1:500; 5 % milk	kind gift of Prof. Nickelsen, LMU München

## 2.4 Kits

Agarose gel extraction and PCR clean-up was achieved by using the NucleoSpin Gel and PCR Clean-up Kit, formerly known as NucleoSpin Extract II Kit. For purification and concentration of DNA with low or high yield, the NucleoSpin Plasmid and NucleoBond Midi kits were used, respectively. All kits were purchased from Machery-Nagel (Düren, Germany) and utilized according to manufacturer.

Protein concentration was determined using the Pierce BCA Protein Assay Kit from Thermo Scientific (Bonn, Germany; see section 3.3.6).

## 2.5 Enzymes

Enzymes for restriction of DNA and T4-DNA Ligase were obtained from Fermentas (St. Leon-Rot, Germany). In PCR either Extender Polymerase from 5 Prime (Hamburg, Germany), DFS-Taq Polymerase from Bioron (Ludwigshafen, Germany) or Phusion DNA Polymerase from New England BioLabs (Frankfurt am Main, Germany) were used. RNase free DNaseI was from Roche (Mannheim, Germany) and DNase free RNase was from GE Healthcare (München, Germany). Lysozyme was ordered from Roth (Karlsruhe, Germany).

## 3 Methods

### 3.1 Microbiological methods

#### 3.1.1 *Escherichia coli*

##### 3.1.1.1 Strains

Subcloning in *E. coli* was performed in the following strains:

**Table 3: *E. coli* strains used for cloning.** Additional information on genotype and source of supply are given.

Strain	Genotype	Manufacturer
DH5 $\alpha$	F <sup>-</sup> $\phi$ 80lacZ $\Delta$ M15 $\Delta$ (lacZYA-argF)U169 recA1 endA1 hsdR17 (r <sub>k</sub> <sup>-</sup> , m <sub>k</sub> <sup>+</sup> ) phoA supE44 thi-1 gyrA96 relA1 $\lambda$ <sup>-</sup>	Invitrogen (Karlsruhe, Germany) now Life Technologies (Darmstadt, Germany)
TOP10	F <sup>-</sup> mcrA $\Delta$ (mrr-hsdRMS-mcrBC) $\phi$ 80lacZ $\Delta$ M15 $\Delta$ lacX74 recA1 araD139 $\Delta$ (ara-leu) 7697 galU galK rpsL (Str <sup>R</sup> ) endA1 nupG $\lambda$ <sup>-</sup>	Invitrogen (Karlsruhe, Germany) now Life Technologies (Darmstadt, Germany)
XL1B	recA1 endA1 gyrA96 thi-1 hsdR17 supE44 relA	Stratagene (Heidelberg, Germany) now Agilent Technologies (Böblingen, Germany)

Overexpression in *E. coli* was performed in the following strains:

**Table 4: *E. coli* strains used for heterologous expression of proteins.** Additional information on genotype and source of supply are given.

Strain	Genotype	Manufacturer
BL21	F <sup>-</sup> ompT hsdS <sub>B</sub> (r <sub>B</sub> <sup>-</sup> m <sub>B</sub> <sup>-</sup> ) gal dcm (DE3)	Novagen/Merck (Darmstadt, Germany)
Rosetta (DE3)	F <sup>-</sup> ompT hsdS <sub>B</sub> (r <sub>B</sub> <sup>-</sup> m <sub>B</sub> <sup>-</sup> ) gal dcm (DE3) pRARE (Cam <sup>R</sup> )	Novagen/Merck (Darmstadt, Germany)

##### 3.1.1.2 Growth conditions

Cultures were grown at 37 °C in liquid LB medium (1% (w/v) tryptone; 0.5% (w/v) yeast extract; 1% (w/v) NaCl) or on plates supplemented with 1.5 % (w/v) agar. Appropriate antibiotics were added according to the resistance of the strains at concentrations of 100  $\mu$ g/ml of ampicillin (Amp), 50  $\mu$ g/ml of kanamycin (Kan), 10  $\mu$ g/ml of chloramphenicol (Cm) or at

10 µg/ml of gentamycin (Gm). For overexpression M9ZB medium was used (500 ml: 5 g tryptone; 2.5 g NaCl; 1.5 g KH<sub>2</sub>PO<sub>4</sub>; 0.5 g NH<sub>4</sub>Cl; 5 ml 40 % (w/v) glucose; 500 µl MgSO<sub>4</sub>).

### 3.1.1.3 Competent cells

To produce *E. coli* cells chemically competent for transformation of DNA molecules the protocol from Hanahan (1983) was applied.

### 3.1.1.4 Transformation

Heat shock transformation was used to transfer plasmid DNA into *E. coli* cells according to instructions (Sambrook and Russel, 2001). Constructs based on the pCR2.1 vector from Invitrogen (Karlsruhe, Germany) were selected for the presence of inserts by blue-white screening. As substrate 40 µL X-gal (40 mg/ml) were directly added to LB-plates.

### 3.1.1.5 Frozen stocks

For long-term storage frozen stocks were prepared by mixing 0.5 ml culture (OD<sub>600</sub> ~0.8-1.0) with 0.5 ml sterile 30% (v/v) glycerol solution. Cultures were frozen in liquid nitrogen and stored at -80 °C until further use.

## 3.1.2 *Saccharomyces cerevisiae*

### 3.1.2.1 Strains

**Table 5: Yeast strains used in this work.** Additional information on genotype, reporter genes and intended use are given.

Strain	Genotype	Reporter	Purpose
EGY48 <sup>a</sup>	MAT $\alpha$ , <i>his3</i> , <i>trp1</i> , <i>ura3</i> , <i>LexA</i> <sub>op(x6)</sub> - <i>LEU2</i>	<i>LEU2</i>	yeast-two hybrid assay
NMY51	MAT $\alpha$ <i>his3</i> $\Delta$ 200 <i>trp1</i> -901 <i>leu2</i> -3,112 <i>ade2</i> <i>LYS2</i> ::( <i>lexAop</i> ) <sub>4</sub> - <i>HIS3</i> <i>ura3</i> ::( <i>lexAop</i> ) <sub>8</sub> - <i>lacZ</i> <i>ade2</i> ::( <i>lexAop</i> ) <sub>8</sub> - <i>ADE2</i> <i>GAL4</i>	<i>ADE2</i>	split-ubiquitin assay
H6	EGY48 with p8op- <i>lacZ</i> plasmid	<i>URA</i>	yeast-two hybrid assay with blue white screening

<sup>a</sup> The UAS of the *LEU2* promoter was replaced with 6 copies of the LexA operator sequence, resulting in *LEU2* gene expression controlled by LexA protein (Estojak et al., 1995).

### 3.1.2.2 Growth conditions

Cultures were grown at 30 °C in either liquid YPD medium (1 % (w/v) bacto yeast extract; 2 % (w/v) bacto-peptone; 2 % (w/v) glucose) or on plates supplemented with 2 % (w/v) agar. Selection medium (SC) in Y2H or split-ubiquitin experiments (3.1.2.5 and 3.1.2.6) was made of 0.7 % (w/v) yeast nitrogen base without amino acids, 0.2 % (w/v) drop-out mix (according to experiment) and 2 % (w/v) glucose or 2 % (w/v) galactose and 1 % (w/v) raffinose (both glucose-free). The drop-out mixes were made of 4.3 % (w/v) of the following amino acids: alanine, arginine, asparagine, aspartic acid, cysteine, glutamic acid, glutamine, glycine, histidine, isoleucine, lysine, methionine, myo-inositol, phenylalanine, proline, serine, threonine, tryptophan, tyrosine, uracil, valine, 1 % (w/v) adenine, 8.5 % (w/v) leucine and 0.4 % (w/v) para-amino benzoic acid. According to requirements, one or more of these amino acids were excluded.

### 3.1.2.3 Competent cells

To produce *S. cerevisiae* cells, chemically competent for transformation of DNA molecules, the protocol from Gietz and co-workers was applied with modifications (Gietz and Woods, 2002). An overnight culture was used to inoculate 50 ml YPD or a certain selection medium to OD<sub>600</sub> ~0.15. Cells were grown at 30 °C to OD<sub>600</sub> ~0.5-0.6 and pelleted (1100 x g; 4 °C for 3 min). Cells were washed in one volume of sterile H<sub>2</sub>O, pelleted again and resuspended in ¼ volume LiSorb solution (100 mM LiOAc; 10 mM Tris-HCl, pH 8; 1 mM EDTA; 1 M sorbitol). After centrifugation, cells were resuspended in 300 µl LiSorb and 48 µl (2 mg/ml) single stranded carrier DNA from Dualsystems Biotech (Schlieren, Switzerland). Aliquots of 50 µl were slowly frozen and stored at -80 °C until further use.

### 3.1.2.4 Transformation

Competent cells were thawed at room temperature. Plasmid DNA equivalent to 1-2 µg DNA and 300 µl sterile LiPEG (100 mM LiOAc; 10 mM Tris-HCl, pH 8; 1 mM EDTA; 40 % (w/v) PEG 4000) were added, mixed and incubated for 20 min at room temperature. Heat shock for 15 min at 42 °C in a water bath was followed by a short centrifugation step (2000 x g; 4 °C for 3 min). The pelleted, transformed cells were resuspended in a physiological 0.9 % (w/v) NaCl solution and streaked out on appropriate selection plates under sterile conditions (Gietz et al., 1992).

## 3.1.2.5 Split-ubiquitin assay

The split-ubiquitin system was designed to detect heterologously expressed proteins for interaction *in vivo* (Johnsson and Varshavsky, 1994). The advantage of this system compared to a general yeast-two hybrid assay is that it allows not only detecting interactions of soluble proteins but also of integral membrane proteins and membrane associated proteins. In this work, the Dual Membrane Kit 3 from Dualsystems Biotech (Schlieren, Switzerland) was used to test for interaction between SynTic22 (Slr0924), Slr1841 and SynToc75 (Slr1227). pBT3 is a bait expression vector that adds the cub-part of ubiquitin to either the N-terminus (-N) or C-terminus (-Suc) (Table 6). The Suc sequence in pBT3-Suc is a yeast signal sequence derived from *SUC2* invertase gene of *Saccharomyces cerevisiae* that is supposed to help in recognition of the expressed protein by the yeast translocation machinery. pPR3 is a prey expression vector that adds the nubG-part of ubiquitin (leucin mutated to glycine, therefore nubL to nubG) that has lost its high affinity for the cub-part to either the N-terminus (-N) or C-terminus (-C). Therefore, only when the cub- and nubG-fusion proteins interact with each other, both parts come together close enough for the UBPs (proteases) to recognize the ubiquitin. The LexA-VP16 transcription factor, which is attached to the cub-part, will then be released and induces expression of the reporter genes. Bait and prey vectors used in this assay (Table 6) were checked by PCR analysis and sequencing (see 3.2.4 and 3.2.5) for in-frame integration and sequence accuracy. Afterwards, a two-step consecutive transformation of bait and prey vectors into NMY51 strain was performed (see section 3.1.2.1 and 3.1.2.4). The strength of interaction was judged by calculating the number of colonies under selection conditions (-His and -Ade).

**Table 6: Primers used for cloning of genes into Dual membrane kit bait and prey vectors**

Destination vectors	Primer	Sequence (5'-3')
pBT3-N:: <i>cssynTic22</i> ; pBT3-Suc:: <i>cssynTic22</i> ; pPR3-N:: <i>cssynTic22</i>	IW_93 fw	TAGGCCATTACGGCCATGTTGCCACCGAAGAGGTAG
	IW_98 re	GGCCGAGGCGGCCTTACTTAGGTTGTTGGGCGGA
pBT3-N:: <i>synTic22</i> ; pBT3-Suc:: <i>synTic22</i> ; pPR3-N:: <i>synTic22</i>	IW_97 fw	TAGGCCATTACGGCCATGAAATCCTTACTCCGCATC
	IW_98 re	GGCCGAGGCGGCCTTACTTAGGTTGTTGGGCGGA
pBT3-N:: <i>synToc75</i> ; pBT3-Suc:: <i>synToc75</i> ; pPR3-N:: <i>synToc75</i>	IW_94 fw	TAGGCCATTACGGCCATGGTGTCAAACCAGAACAAAAG
	IW_95 re	GGCCGAGGCGGCCTAGAACTTCTCGCCAATACCGA
pBT3-N:: <i>slr1841</i> ; pBT3-Suc:: <i>slr1841</i> ; pPR3-N:: <i>slr1841</i>	IW_100 fw	TAGGCCATTACGGCCATGCTTAAACTATCTTGGAAAG
	IW_101 re	GGCCGAGGCGGCCTTAGAAAGTGAAGGTACCACG
pPR3-C:: <i>cssynTic22</i>	IW_97 fw	TAGGCCATTACGGCCATGAAATCCTTACTCCGCATC
	IW_99 re	GGCCGAGGCGGCATCTTAGGTTGTTGGGCGGA
pPR3-C:: <i>synTic22</i>	IW_93 fw	TAGGCCATTACGGCCATGTTGCCACCGAAGAGGTAG
	IW_99 re	GGCCGAGGCGGCATCTTAGGTTGTTGGGCGGA
pPR3-C:: <i>synToc75</i>	IW_94 fw	TAGGCCATTACGGCCATGGTGTCAAACCAGAACAAAAG
	IW_96 re	GGCCGAGGCGGCATGAACTTCTCGCCAATACCG
pPR3-C:: <i>slr1841</i>	IW_100 fw	TAGGCCATTACGGCCATGCTTAAACTATCTTGGAAAG
	IW_102 re	GGCCGAGGCGGCATGAAAGTGAAGGTACCACGG

### 3.1.2.6 Yeast-two hybrid assay

The yeast two-hybrid system was designed to detect heterologously expressed proteins for interaction *in vivo* (Golemis et al., 1996; Gyuris et al., 1993). It is especially suitable to detect for protein-protein interactions of soluble proteins. In this work, the “Matchmaker LexA Two-Hybrid System” from Clontech (Mountain view, USA) was used to test for interaction between Slr0924 (SynTic22) and Sll1784 of *Synechocystis*.

**Table 7: Primers used for cloning of genes into Matchmaker LexA Y2H kit bait and prey vectors**

Destination vectors	Primer	Sequence (5'-3')
pEG202:: <i>cssynTic22</i>	IW_120 fw	ATGAATTCTTGCCCACCGAAGAGGTAG
pJG4-5:: <i>cssynTic22</i>	IW_12 re	ATCTCGAGCTTAGGTTGTTGGGCGGATAAAG
pEG202:: <i>cssll1784</i>	IW_117 fw	ATGAATTCATTTCTACGTTGGATAATTTTC
pJG4-5:: <i>cssll1784</i>	IW_118 re	TACTCGAGAAAGCATTAAACAGTTGCATC
pEG202:: <i>synTic22</i>	IW_121 fw	ATGAATTCATGAAATCCTTACTCCGCATC
pJG4-5:: <i>synTic22</i>	IW_12 re	ATCTCGAGCTTAGGTTGTTGGGCGGATAAAG
pEG202:: <i>sll1784</i>	IW_118 re	TACTCGAGAAAGCATTAAACAGTTGCATC
pJG4-5:: <i>sll1784</i>	IW_119 fw	ATGAATTCATGAAAACCTTTACGTTTATC

The pEG202 (alias pLexA, see manufacturer manual) is a bait vector used to generate fusions of the DNA-binding domain of the LexA protein with a bait proteins N-terminus. The pJG4-5 (alias pB42AD, see manufacturer manual) is a prey vector that generates a fusion of the activation domain (AD) of B42 and a SV40 nuclear localization domain to the N-terminus of a prey protein. Bait and prey vector also add nuclear localization signals to the expressed proteins. The bait protein binds via the LexA DNA binding domain to the LexA operator sequence of marker gens. When bait and prey interact with each other, the SV40 activation domain induces expression of the marker gene, allowing yeast cells to grow on SD-Ura-Trp-His-Leu. Bait and prey vectors were checked by PCR analysis and sequencing (see section 3.2.4 and 3.2.5) for in-frame integration and sequence accuracy. Afterwards a co-transformation of bait and prey vectors was performed into H6 cells (see 3.1.2.1 and 3.1.2.4). H6 cells contain the p8op-*lacZ* plasmid that confers the ability to grow on SD-Ura and blue-white screening for protein-protein interaction. The pEG202 vector allows growth on SD-His plates, whereas pJG4-5 allows growth on SD-Trp. After transformation, cells were streaked out on SD-Ura-Trp-His to select for transformants. All colonies that had been obtained were further kept on SD-Ura-Trp-His plates but also checked for growth on SD-Ura-Trp-His-Leu+glucose plates. As glucose prevents prey protein expression from pJG4-5, no interaction, and thus no growth on –Leu was expected. Therefore, only colonies that were not able to grow on –Leu under these conditions were chosen for further experiments.

### 3.1.3 *Synechocystis* sp. PCC 6803

#### 3.1.3.1 Strains

**Table 8: *Synechocystis* strains used in this work.** Additional information on origin, antibiotic resistances and reference source are given.

Strains	Origin	Resistance gene	Purpose	Source	
1	Wild-type strain Japan (J)	-	none	-	kindly provided by Kazusa DNA research institute
2	Wild-type strain Warwick (alias Big)	-	none	-	kindly provided by Prof. C. Mullineaux
3	Wild-type strain HP	-	none	-	kindly provided by Prof. J. Nickelsen
4	HP $\Delta$ <i>prata</i>	(3)	Km <sup>R</sup>	knockout	kindly provided by Prof. J. Nickelsen
5	Big $\Delta$ <i>prata</i>	(2)	Km <sup>R</sup>	knockout	this work
6	Big $\Delta$ <i>prata</i> :: <i>nirAprata</i> (1)	(2)	Cm <sup>R</sup>	inducible <i>prata</i>	this work
7	Big $\Delta$ <i>prata</i> :: <i>nirAprata</i> (2)	(5)	Km <sup>R</sup> , Cm <sup>R</sup>	inducible <i>prata</i>	this work
8	Big $\Delta$ <i>prata</i> $\Delta$ <i>slr0415</i> :: <i>nirAprata</i>	(5)	Km <sup>R</sup> , Cm <sup>R</sup>	inducible <i>prata</i>	this work
9	Big $\Delta$ <i>prata</i> :: <i>nirAprata</i> (2) + <i>pVZ322</i> :: <i>N-eCFP-D1</i>	(7)	Km <sup>R</sup> , Cm <sup>R</sup> , Gm <sup>R</sup>	inducible <i>prata</i> and extra-chromosomal fluorescent D1	this work + (Schottkowski et al., 2008)
10	Big $\Delta$ <i>prata</i> :: <i>nirAprata</i> (2)// $\Delta$ <i>D1</i> :: <i>D1-internal-GFP</i>	(7)	Km <sup>R</sup> , Cm <sup>R</sup> , Gm <sup>R</sup>	inducible <i>prata</i> and stably integrated fluorescent D1	this work
11	<i>JsynTic22</i> // $\Delta$ <i>JsynTic22</i> (merodiploid)	(1)	Km <sup>R</sup>	knockout/ knockdown	this work
12	$\Delta$ <i>JsynTic22</i> :: <i>synTic22-His</i>	(1)	Gm <sup>R</sup>	tagged <i>SynTic22</i>	this work

#### 3.1.3.2 BG11 medium

Solution 1	(200 ml)	0,6 g citric acid; 0,6 g ferric ammonium citrate; 0,1 g EDTA
Solution 2	(200 ml)	37,5 g NaNO <sub>3</sub> ; 0,975 g K <sub>2</sub> HPO <sub>4</sub>
Solution 2b	(200 ml)	1,5 g MgSO <sub>4</sub> x 7 H <sub>2</sub> O
Solution 3	(200 ml)	3,8 g CaCl <sub>2</sub> x 2 H <sub>2</sub> O
Solution 4	(200 ml)	4 g Na <sub>2</sub> CO <sub>3</sub>
Solution 5	(1000 ml)	2,86 g H <sub>3</sub> BO <sub>3</sub> ; 1,42 MgCl <sub>2</sub> ; 0,222 g ZnSO <sub>4</sub> ; 0,391 g NaMoO <sub>4</sub> ; 0,079 g CuSO <sub>4</sub> ; 0,049 Co(NO <sub>3</sub> ) <sub>2</sub>
Solution 6	(1000 ml)	119,16 g HEPES pH 8
2 M glucose	(200 ml)	79,27 g $\alpha$ -D(+) glucose monohydrate

Mix for 1L medium: 2 ml solution 1 + 50 ml solution 2 + 2 ml solution 2b + 2 ml solution 3 + 1 ml solution 4 + 1 ml solution 5 + 40 ml solution 6 + 2,4 ml 2 M glucose



### 3.1.3.3 BG11<sub>0</sub> medium

This medium is similar to BG11, but all nitrogen containing substances were substituted by similar compounds in an equal molar ratio (shown in bold). Nitrogen was supplemented by adding sterile solutions of NaNO<sub>3</sub> or NH<sub>4</sub>Cl to the medium.

Solution 1	(200 ml)	0,6 g citric acid; <b>0,5 g ferric citrate</b> ; 0,1 g EDTA
Solution 2	(200 ml)	<b>25,7 g NaCl</b> ; 0,975 g K <sub>2</sub> HPO <sub>4</sub>
Solution 2b	(200 ml)	1,5 g MgSO <sub>4</sub> x 7 H <sub>2</sub> O
Solution 3	(200 ml)	3,8 g CaCl <sub>2</sub> x 2 H <sub>2</sub> O
Solution 4	(200 ml)	4 g Na <sub>2</sub> CO <sub>3</sub>
Solution 5	(1000 ml)	2,86 g H <sub>3</sub> BO <sub>3</sub> ; 1,42 MgCl <sub>2</sub> ; 0,222 g ZnSO <sub>4</sub> ; 0,391 g NaMoO <sub>4</sub> ; 0,079 g CuSO <sub>4</sub> ; <b>0,0218 CoCl<sub>2</sub></b>
Solution 6	(1000 ml)	119,16 g HEPES pH 8
2 M glucose	(200 ml)	79,27 g α-D(+) glucose monohydrate

Mix for 1 l: 2 ml solution 1 + 50 ml solution 2 + 2 ml solution 2b + 2 ml solution 3 + 1 ml solution 4 + 1 ml solution 5 + 40 ml solution 6 + 2,4 ml 2 M glucose

### 3.1.3.4 Growth conditions

Cultures of *Synechocystis* sp. PCC 6803 wild-type and mutant strains were grown photoheterotrophically (5 mM glucose) in liquid BG11 medium (Stanier et al., 1971; Rippka et al., 1979) (see 3.1.3.2) in agitated Erlenmeyer flasks at 30 °C under continuous light (Innova® 44 from New Brunswick Scientific; 120 rpm; 47 μmol photons m<sup>-2</sup>s<sup>-1</sup>).

For the attempt to segregate the  $\Delta$ *synTic22* knockout strain a system was used to grow cells under different environmental conditions *e.g.* temperatures (27 °C, 30 °C and 32 °C), with or without CO<sub>2</sub>-enriched air (5 % (v/v)).

In induction experiments, standard BG11 medium was adjusted to BG11<sub>0</sub>, as the expression of *pratA* under control of the *nirA* promoter is regulated by either ammonium or nitrate. In BG11<sub>0</sub>, similar chemicals in an equal molar ratio exchanged all sources of nitrogen. Ferric ammonium citrate was exchanged by ferric citrate, sodium nitrate by sodium chloride and cobalt(II) nitrate by cobalt chloride.

### 3.1.3.5 Stable transformation of *Synechocystis* strains

Transformation of *Synechocystis* was performed similar to methods described elsewhere (Ermakova et al., 1993; Zang et al., 2007) using the following steps. Cultures were grown to OD<sub>730</sub> ~0.8-1 at 30 °C in agitated Erlenmeyer flasks. An aliquot of 10 ml was then centrifuged (4000 x g; RT for 10 min), washed twice using 10 ml of BG11 medium and resuspended finally in a volume of 2 ml BG11. A volume of 300 μl was supplemented with 1-3 μg of plasmid DNA

in a microtube, mixed and incubated in the light for 5 h. Cells were then spread on BG11 plates without any antibiotic but covered with a Immobilon-NC 0.45 µm filter membrane from Millipore (Schwalbach/TS, Germany) and kept in the dark overnight. On the next day, filters were transferred to BG11 plates supplemented with the appropriate antibiotics at low concentrations (*e.g.* Km at 20 µg/ml; Cm and Gm at 5 µg/ml) and incubated in the light at 30 °C. After that, filters were continuously transferred to new BG11 plates that contained increasing concentration of antibiotics. During this process, cells without introduced resistance genes died and transformed strains were segregated.

#### 3.1.3.6 Conjugation of *Synechocystis* strains by using autonomously replicating vectors

The autonomously replicating vectors pVZ321 and pVZ322 were used to stably introduce and express genes in *Synechocystis* cells without homologous recombination of these genes into the genome (Zinchenko et al., 1999). The vectors are different in the resistances they confer. The pVZ321 contains the genes *aphA* and *cat* that confer resistance to Km and Cm, respectively. The pVZ322 vector contains the genes *aphA* and *aacC1* that confer resistance to Km and Gm, respectively. Genes can be introduced in any of these resistance genes making it possible to screen for the loss of function.

Conjugational transfer was performed as described (Zinchenko et al., 1999). In a first step the pVZ vector that contained the inserted gene was transformed into *E. coli* XL1B strain (see 3.1.1.4). Overnight cultures of transformed XL1B cells and XL1B-pSI906 that contained a transfer gene were inoculated in 20 ml fresh LB medium, grown to OD<sub>600</sub> ~1, centrifuged, and resuspended in 1 ml BG11 without supplementation of glucose. Cultures of *Synechocystis* were grown to OD<sub>730</sub> ~0.7-1, centrifuged (4000 x g; 4 °C for 5 min), and resuspended in 2 ml BG11. For conjugation 100 µl of *Synechocystis* and 50 µl per *E. coli* strain were mixed carefully and dropped on BG11 plates without any antibiotics but covered with an Immobilon-NC 0.45 µm filter membrane from Millipore (Schwalbach/TS, Germany). After two days, filters were transferred to BG11 plates that contained appropriate antibiotics and incubated in the light for two weeks.

#### 3.1.3.7 *NirA* promoter controlled expression of *PratA* in *Synechocystis*

Induction of *prata* gene expression under control of the *nirA* promoter was carried out according to Qi and co-workers using slight modifications (Qi et al., 2005). Fresh 50 ml liquid cultures of *Synechocystis* wild-type strain Big, BigΔ*prata* and BigΔ*prata*::*nirAprata*(2) strains (see Table 8) were inoculated in BG11 medium. Cultures were grown at 30 °C to OD<sub>730</sub> ~1-1.5.

After centrifugation (4000 x g; 4 °C for 10 min) cells were resuspended in 250 ml BG11<sub>0</sub> supplemented with NH<sub>4</sub>Cl (17.6 mM) to OD<sub>730</sub> ~0.2. Under these conditions, expression of *nirA* promoter is inhibited. Cultures were pelleted (4000 x g; 4 °C for 10 min) after they had reached OD<sub>730</sub> ~0.8-1 and washed two times with 30 ml BG11<sub>0</sub> (without NH<sub>4</sub>Cl or NaNO<sub>3</sub>) to remove any residual ammonium chloride. Pellets were then resuspended in 250 ml BG11<sub>0</sub> supplemented with NaNO<sub>3</sub> (17.6 mM). Under these conditions, expression of *nirA* promoter is activated. At certain time points samples of 50 ml culture were taken, centrifuged (4000 x g; 4 °C for 10 min), the pellets frozen in liquid nitrogen, and stored at -80 °C until further use (see 3.3.3).

#### 3.1.3.8 Frozen stocks and cell recovery

To prepare frozen stock cultures of *Synechocystis* the method of Jerry J. Brand (Cryopreservation of Cyanobacteria, Botany Department, University of Texas at Austin, URL: <http://www-cyanosite.bio.purdue.edu/protocols/cryo.html>, 26.03.2012) was used. A logarithmic growing culture was pelleted five times in a 2 ml cryo-microtube. Pellet was resuspended in a cryoprotective solution (460 µl BG11, 460 µl H<sub>2</sub>O and 80 µl DMSO (8 % (v/v) final concentration) and frozen continuously at -80 °C. To avoid severe damage, cells were protected from bright light during freezing process.

Recovery of cells was achieved by thawing them rapidly at room temperature. Cells were pelleted (minimum speed that facilitates pelleting; RT for 1 min) and suspended in 1 ml of fresh BG11 medium. A volume of 100 µl was dropped on two BG11 plates, one supplemented with appropriate antibiotics and one without. The rest was used to inoculate 25 ml BG11 liquid cultures in Erlenmeyer flasks also with and without supplementation of antibiotics. After cells were incubated overnight at RT without any agitation they were transferred to 30 °C and shaken at 120 rpm. Cells recovered usually within one week of incubation.

## 3.2 Molecular biological methods

General molecular biological methods were performed according to (Sambrook and Russel, 2001) without or slight modifications.

### 3.2.1 Isolation of plasmid DNA

Crude plasmid DNA, for control of subcloning steps, was isolated according to Zhou and coworkers with slight modifications (Zhou et al., 1990). A volume of 1.5 ml per overnight culture was pelleted (14,000 x g; 4 °C for 1 min) and resuspended in 300 µL P1 buffer (50 mM

Tris-HCl, pH 8; 10 mM EDTA; RNase). To lyse the cells, 300 µl P2 buffer (0.2 M NaOH; 1 % (w/v) SDS) was added, followed by 300 µL P3 (3 M KAc, pH 5.5) to neutralize the solution. After 10 min of incubation on ice, the cell debris was removed by centrifugation (14.000 x g; 4 °C for 15 min). The supernatant was transferred into a new microtube and DNA precipitation was achieved by adding 1 volume of -20 °C cold isopropanol. DNA was pelleted (14.000 x g; 4 °C for 15 min) and washed once with 70 % (v/v) ethanol. Supernatant was removed and the pellet dried at room temperature. Finally, plasmid DNA was dissolved in DNase-free Tris-buffer (10 mM Tris-HCl, pH 7.5), frozen in liquid nitrogen, and stored at -20 °C until further use.

### **3.2.2 Isolation of genomic DNA from *Synechocystis***

Genomic DNA from *Synechocystis* cultures growing in logarithmic phase was isolated according to Tilett (Tilett and Neilan, 2000). Xanthogenate is a polysaccharide dissolving chemical and allows the break down of prokaryotic cells, plants and animals without mechanical or enzymatic means. A volume of 1-2 ml culture was pelleted at maximum speed, the supernatant was removed and 50 µl TER-buffer added (10 mM Tris-HCl, pH 7.4; 1 mM EDTA; 100 µg/ml RNase A). Cell lyses was achieved by adding 750 µl XS-buffer (1 % (w/v) potassium ethyl xanthogenate; 100 mM Tris-HCl, pH 7.4; 20 mM EDTA; 1 % (w/v) SDS; 800 mM ammonium acetate) followed by incubation for 2 h at 70 °C and 10 s of vortexing. After 30 min incubation on ice the cell debris was removed by centrifugation (14.000 x g; 4 °C for 10 min). The supernatant was transferred into a new microtube. Precipitation of genomic DNA was achieved by adding one volume of isopropanol followed by an incubation step (room temperature for 10 min). Genomic DNA was pelleted (14.000 x g; 4 °C for 15 min) and washed once with 70 % (v/v) ethanol. Supernatant was removed and the pellet dried at room temperature. Finally, the isolated genomic DNA was dissolved in DNase-free Tris-buffer (10 mM Tris-HCl, pH 7.5), frozen in liquid nitrogen and stored at -20 °C until further use.

### **3.2.3 Determination of DNA concentration**

DNA concentration was determined using the NanoPhotometer® P300 from Implen GmbH (München, Germany). Up to 1 µl of isolated plasmid or genomic DNA solution (see 3.2.1 and 3.2.2) was used in the procedure without prior treatment and measured according to manufacturer.

### 3.2.4 PCR

The Mastercycler ep Gradient S thermal cycler in 96-well format from Eppendorf (Hamburg, Germany) was used to amplify DNA fragments, to introduce restriction sites and to perform genotyping of transformed cultures. The following standard protocols were used:

**Table 9: PCR master-mixes and programs used.** Three different polymerases were used to amplify DNA for cloning or screening.

Polymerase	Master-Mix (30 µl)	PCR Program	Cycles
Phusion	1 µl DNA, 0.25 µl dNTP, 0.2µl Polymerase, 1 µl Primer fw 1 µl Primer re, (3 µl 50 mM MgCl <sub>2</sub> ), 6 µl HF buffer add H <sub>2</sub> O to 30 µl	30 s, 98 °C	30 x
		10 s, 98 °C	
		15 s, 62 °C	
		up to 90 s, 72 °C	
		3 min, 72 °C	
		hold at 15 °C	
Extender	1 µl DNA, 0.25 µl dNTP, 0.2 µl Polymerase, 1 µl Primer fw, 1 µl Primer re, (3 µl 50 mM MgCl <sub>2</sub> ), 3 µl buffer add H <sub>2</sub> O to 30 µl	30 s, 98 °C	30 x
		10 s, 98 °C	
		15 s, 62 °C	
		up to 90 s, 72 °C	
		3 min, 72 °C	
		hold at 15 °C	
Bioron	see Extender	see Extender	

### 3.2.5 Sequencing of DNA

Sequencing of DNA was performed by the “Genomics Service Unit” of the LMU (group of Dr. Andreas Brachmann). In general, the standard primers for subcloning or vector specific were used.

## 3.3 Biochemical methods

### 3.3.1 Overexpression and purification of SynTic22 protein

For overexpression of the *Synechocystis* sp. PCC 6803 Slr0924 (SynTic22) protein the full-length sequence of the gene was amplified from chromosomal DNA by PCR using the Tic22fw 5'-AGAGGATCCATGAAATCCTTACTCCGCATCG-3' and Tic22re 5'-ATCTCGAGCTTAGGTTGTTGGGCGGATAA-AG-3' custom primers from Metabion (München, Germany). The PCR fragments were cleaned-up and subcloned into the pCR2.1 vector from Invitrogen (Karlsruhe, Germany). Restriction digestion with enzymes *Bam*HI and *Xho*I

(sequences underlined) was used to clone the fragment into the pET21a overexpression vector from Novagen/Merck (Darmstadt, Germany) that adds a C-terminal His-tag to the protein when expressed. Correct in frame insertion was checked by both restriction analysis and sequencing of the plasmid. Chemically competent cells of *E. coli* strain Rosetta (DE3) were transformed with the plasmid and were selected on LB plates that contained ampicillin. Cells were cultured in M9ZB minimal medium at 37 °C to an OD<sub>600</sub> ~0.6-0.8 and pre-chilled at 4 °C for a few minutes. Expression was induced by 1 mM IPTG and the culture grown at 12 °C overnight to maximize soluble content of the overexpressed protein. The culture was pelleted (6000 x g; 4 °C for 10 min), resuspended in NaPi-buffer (20 mM, pH 8; 500 mM NaCl; 1 mM PMSF; 10 mM imidazole) and lysed by two times passage through the French® press cell disruptor. Nucleic acid molecules were broken by sonication or by addition of DNaseI. After centrifugation (30000 x g; 4 °C for 15 min), the cleared supernatant was used for Ni<sup>2+</sup>-affinity purification using Ni<sup>2+</sup>-NTA-sepharose from GE Healthcare (München, Germany). SynTic22 protein was bound to sepharose beads at 4 °C for 2 h. Beads were washed three times with 50 bead volumes of 20 mM NaPi-buffer (pH 8; 500 mM NaCl; 1 mM PMSF; 40 mM imidazole) and eluted with 10 bead volumes of 20 mM NaPi-buffer (pH 8; 150 mM NaCl; 1 mM PMSF; 500 mM imidazole). If required, imidazole was removed and/or protein concentrated (see 3.3.5). Finally, protein concentration was determined (see 3.3.6).

### 3.3.2 Antibody production

To raise an antibody specific against *Synechocystis* Slr0924 (SynTic22) protein, overexpressed protein from inclusion bodies was used. Overexpression was carried out as described (see 3.3.1). After cell disruption by French® press and subsequent centrifugation, the pellet was dissolved in resuspension buffer (50 mM Tris-HCl, pH 8; 200 mM NaCl) and sonified. Detergents in several subsequent wash steps were used to remove membrane lipids. First, the inclusion bodies were dissolved repeatedly in detergent buffer (20 mM Tris-HCl, pH 7.5; 200 mM NaCl; 1 % (w/v) deoxycholic acid; 1 % (w/v) Nonidet P-40; 10 mM β-mercaptoethanol) and pelleted (12000 x g; 4 °C for 10 min) until the pellet color was almost white. Then, a Triton buffer (20 mM Tris-HCl, pH 7.5; 0.5 % (w/v) Triton-X-100; 5 mM β-mercaptoethanol) was used in two consecutive washing steps and two washing steps with Tris buffer (20 mM Tris-HCl, pH 8; 10 mM DTT) finally removed the detergents. The cleaned inclusion bodies were dissolved in 1.5-3 ml buffer A (50 mM NaPi, pH 8; 300 mM NaCl; 2 mM β-mercaptoethanol; 6 M urea). For further cleaning, proteins were separated by SDS-PAGE (15 % (w/v); 4 M urea) according to Lämmli (Laemmli, 1970). SynTic22 protein (~3 mg) was cut out and the gel slice sent to

BioGenes (Berlin, Germany). Serum protein was harvested after 203 days (final bleeding after 231 days) and used without further purification.

### 3.3.3 Crude protein extraction from *Synechocystis*

Proteins were isolated using the following method. Cultures were grown in 50 ml BG11 to  $OD_{730} \sim 1-1.5$ , centrifuged ( $4000 \times g$ ;  $4^\circ C$  for 10 min) and resuspended in 200  $\mu$ l of cold extraction buffer (50 mM Tris-HCl, pH 7; 20 mM  $MgCl_2$ ; 20 mM KCl; 1 mM PMSF). Glass beads from Roth (Karlsruhe, Germany;  $\phi$  0.5 mm) were added to the sample tube so that only 1-2 mm solution was left above the beads. Cells were broken by shaking them (3 times; 90 s) in the “Tissue Lyser” from Qiagen (Hilden, Germany) with 1 min intervals on ice. A short, low speed centrifugation step was used to collect the solution on top of the beads and was then transferred to a new microtube. Unbroken cells were removed ( $1500 \times g$ ,  $4^\circ C$  for 2 min) and supernatant again transferred to a new microtube. To separate samples into soluble proteins and membranes, the solution was centrifuged for 10 min ( $20000 \times g$ ;  $4^\circ C$ ). The bluish green supernatant contained the soluble fraction. The pellet that contained the membranes was washed once with breaking buffer, solubilized using 100  $\mu$ l breaking buffer which was supplemented with Triton-X-100 (2 % (v/v)), incubated on ice for 5 min, and unsolved material was pelleted ( $40000 \times g$ ;  $4^\circ C$  for 10 min). The supernatant contained the solubilized membrane proteins.

### 3.3.4 Cellular sub-fractionation of *Synechocystis*

#### 3.3.4.1 Periplasm

Isolation of periplasmic proteins (PP) was achieved by cold osmotic shock (Fulda et al., 1999). A two liter culture of *Synechocystis* ( $OD_{730} \sim 1-1.5$ ) was centrifuged ( $4000 \times g$ ; RT for 5 min), the pellet washed twice in 100 ml cold buffer A (10 mM Tris-HCl, pH 7.6; 2 mM NaCl) and dissolved in 100 ml buffer B (10 mM Tris-HCl, pH 7.6; 2 mM NaCl; 0.5 M sorbitol; 1 mM EDTA). The Suspension was incubated under soft agitation at room temperature for 10 min and then pelleted again. Ice-cold, deionized water was used to resuspend the cells to a maximum volume of 50 ml and the suspension was agitated softly in an ice-bath for 10 min. By this, the cells were supposed to swell and the outer membrane to disrupt, thereby releasing the periplasmic proteins. Undisrupted cells and spheroplasts were removed by centrifugation ( $10000 \times g$ ;  $4^\circ C$  for 10 min) and kept for preparation of plasma and thylakoid membranes by sucrose gradient centrifugation. Supernatant was transferred carefully into a centrifugation tube suitable for T-647.5 rotor from Thermo Scientific (Bonn, Germany) and Tris buffer stock

solution added (10 mM Tris-HCl, pH 8 (for affinity chromatography) or pH 6.8 (for localization and BN-PAGE; 150 mM NaCl; 1 mM PMSF). To remove any membranes, the solution was centrifuged at 150000 x g at 4 °C for 1 h. Finally, soluble periplasmic proteins were concentrated (see 3.3.5).

#### 3.3.4.2 Plasma membrane and thylakoid proteins

To separate plasma membranes from thylakoid membranes a sucrose step-gradient was used (Schottkowski et al., 2008). Spheroplasts (see 3.3.4.1) were washed once with 75 ml buffer II (20 mM Tris-HCl, pH 6.8; 1 mM PMSF; 600 mM sucrose). After resuspending in 35 ml buffer II, the spheroplasts were lysed by two times passage through the French® press disruptor. To digest DNA, 20 µl DNaseI was added following 10 min incubation on ice. Cell debris was sedimented by centrifugation (4500 x g; 4 °C for 10 min) and the supernatant mixed with 0.83 volume of a sucrose solution (80 % (w/v) sucrose; 100 mM Tris-HCl, pH 6.8) to a final concentration of 50 % (w/v) sucrose. Each step gradient was made using the following steps and starting from the bottom. Sample (10 ml), 8 ml 39 % (w/v) sucrose in Tris-buffer, 6 ml 30 % (w/v) sucrose in Tris-buffer and 8 ml 10 % (w/v) sucrose in Tris-buffer on top. Membranes were separated by ultracentrifugation at 4 °C for 17 h at 135000 x g. After centrifugation, sucrose was removed by diluting plasma membrane and thylakoid membrane fractions 1:5 with 20 mM NaPi (pH 8) and centrifuged at 4 °C for 1 h at 150000 x g. Supernatant was discarded and membranes dissolved in a minimal volume of 20 mM NaPi (pH 8). For solubilization of membrane proteins, 2 % (v/v) Triton-X-100 was added and the mixture incubated on ice for 10 min. Insolubilized membranes were removed in a final centrifugation step at 4 °C for 15 min at 40000 x g and protein concentration of the supernatant was determined (see 3.3.6).

### 3.3.5 Protein concentration and buffer exchange

Liquid samples of soluble proteins were concentrated by centrifugation (4000 x g; 4 °C) using Amicon Ultra-15 (10 kDa) centrifugal filter units from Millipore (Schwalbach/TS, Germany). During centrifugation a filter membrane prevented proteins with a molecular weight higher than 10 kDa from crossing, whereas smaller proteins and buffers were able to pass. The centrifugal filter units were also used for buffer exchange *e.g.* to dilute imidazole from buffers after protein purification.



### 3.3.6 Determination of protein concentration

Protein concentration was determined using the “Pierce BCA Protein Assay Kit” from Thermo Scientific (Bonn, Germany). This assay was chosen, because it is unaffected by typical concentrations of most ionic and nonionic detergents.

Water was added to 1-5  $\mu$ l sample (final volume 50  $\mu$ l). Then 1 mL reagent A and 20  $\mu$ l reagent B were added and mixed shortly. After samples were incubated at 37 °C, OD<sub>562</sub> was measured at OD<sub>562</sub> using the Shimadzu UV-2401PC spectrophotometer (Columbia, USA) and calculated using the following equation:  $\mu\text{g}/\mu\text{l}=(\text{OD}_{562} * 32)/\text{sample volume}$ .

### 3.3.7 SDS-polyacrylamide gel-electrophoresis (PAGE)

For separation of proteins in a denatured form sodium-dodecyl-sulfate polyacrylamide gel-electrophoresis was applied (Laemmli, 1970). A ratio of acrylamide to N,N'-methylene-bisacrylamide of 30:0,8 was used. The concentrations of acrylamide were 10 %, 12.5 % or 15 % for the separation gel and 5 % for stacking gel, respectively. Protein samples were incubated in sample buffer (250 mM Tris-HCl, pH 6.8; 40 % glycerol; 9 % SDS; 20 %  $\beta$ -mercaptoethanol and bromphenol blue) at 40 °C for 30 min or at 95 °C for 3 min. Electrophoretic separation was performed at 25 mA/mini gel or 35 mA/big gel.

### 3.3.8 Protein staining procedures

#### 3.3.8.1 Coomassie

After electrophoretic separation, proteins were incubated in Coomassie staining solution (50 % (v/v) methanol; 7 % (v/v) acetic acid; 0.18 % (w/v) Coomassie Brilliant Blue-R250) for 30 min at room temperature. Unspecific staining was removed by repeated incubation in destain solution (40 % (v/v) methanol; 7 % (v/v) acetic acid; 3 % (v/v) glycerol).

#### 3.3.8.2 Silver staining

For a more sensitive staining of proteins, the silver staining method according to Blum (Blum et al., 1987) was used with modifications. After electrophoresis gels were incubated for 1 h in destain solution to fix the proteins. Gels were then incubated in solution A (50 % MeOH; 20 % TCA; 2 % CuCl<sub>2</sub> + 0.1 % formaldehyde for 15 min), solution B (10 % EtOH; 5 % acetic acid for 10 min) and solution D (0.01% KMnO<sub>4</sub> +0.01 % KOH for 10 min. Next, incubation in solution B (for 10 min), solution C (10 % EtOH for 5 min), ddH<sub>2</sub>O (for 10 min) and solution F (0.2 %

AgNO<sub>3</sub> for 10 min) was performed. Gels were rinsed in ddH<sub>2</sub>O shortly and developed by using solution G (2 % NaCO<sub>3</sub> + 27 µl per 100 ml formaldehyde). Staining was stopped by adding destain for at least 30 min.

### 3.3.9 Immunoblot analysis

After electrophoretic separation, proteins were transferred to Immobilon®-P PVDF membrane from Millipore (Schwalbach/TS, Germany) using the Trans Blot Cell from BioRad (München, Germany). PVDF membrane was activated in 100 % methanol for 20 s, rinsed with deionized water and incubated together with the gel in Towbin blotting buffer (25 mM Tris-HCl, pH 8.2-8.4; 192 mM glycine; 10-20 % (v/v) methanol; 0.025 % SDS) for 5 min as previously described by Towbin (1979). The semi-dry transfer was performed at 0.8 mA/cm<sup>2</sup> for 75 min. After the transfer, the marker lane was cut and stained in amido black solution (0.1 % (w/v) amido black; 40 % (v/v) methanol; 10 % (v/v) acetic acid) for 5 min. Unspecific staining was removed using destain solution (40 % (v/v) methanol; 10 % (v/v) acetic acid).

To saturate residual protein binding sites, the membranes were incubated for 30-60 min in blocking buffer containing BSA or skimmed milk powder in 1 x PBST (137 NaCl; 10 mM Phosphate; 2.7 mM KCl; 0.05 % Tween 20; pH 7.4) in different concentrations, dependent on the requirements of the antibodies used (see Table 2).

Immunodetection was performed by incubation with the primary antibody that was diluted 1:250 to 1:2000 in blocking buffer (see Table 2) for 2-3 h at room temperature or at 4 °C overnight. Membranes were washed three times for 5 min in 1 x PBST to remove any loose or unspecifically bound antibodies. The membranes were incubated with the secondary antibody at room temperature for 1 h and then washed three times for 5 min in PBST to remove any unbound antibodies.

A 1:8000 dilution of HRP-conjugated secondary goat anti-rabbit antibody in 1 x PBST was used for chemiluminescent detection of proteins (ECL). A mixture of solution A (100 mM Tris-HCl, pH 8.5; 1 % (w/v) luminol; 0.44 % (w/v) coomarcic acid) and B (100 mM Tris-HCl, pH 8.5; 0.018 % (v/v) H<sub>2</sub>O<sub>2</sub>) in a one to one ratio was applied as substrate for the enzyme. Luminescence was detected by a light sensitive Biomax film from Kodak (Stuttgart, Germany) after 30 s to 15 min of incubation in the dark.

A 1:10000 dilution of an alkaline phosphatase conjugated secondary goat anti-rabbit antibody from Sigma-Aldrich (Steinheim, Germany) was used for colorimetric detection of proteins directly on the membrane. In contrast to ECL, a final wash step in Western developer (105.7 mM Tris-HCl, pH 9.5; 100 mM NaCl; 50 mM MgCl<sub>2</sub>) was performed after washing.

A mixture of 66  $\mu$ l NBT (4-nitro blue tetrazolium chloride; 50 mg/ml in 100 % dimethylformamide) and 66  $\mu$ l BCIP (5-bromo-4-chloro-3-indolye-phosphate in 100 % dimethylformamide) per 10 ml Western developer solution was used as substrate for the enzyme.

### **3.3.10 Two dimensional blue native (BN) / SDS-PAGE**

Blue native gel electrophoresis (BN-Page) was performed essentially according to Schagger (1991). Periplasmic samples (300  $\mu$ g protein; see 3.3.4.1) were supplemented with 0.1 volume of a Coomassie buffer (5 % Coomassie Brilliant Blue G-250; 750 mM 6-aminocaproic acid) and loaded on a 6-15 % Bis-Tris polyacrylamide gel. Electrophoresis was performed at 4 °C, 12 mA/500 V max using a cathode buffer that contained 0.02 % Coomassie. The cathode buffer was exchanged by a cathode buffer without Coomassie after 80 min (~ one-third of the run) and the electrophoresis continued for 3 more hours. For second dimension, lanes were cut from the gel and incubated first in buffer containing 1 % SDS and 1 mM  $\beta$ -mercaptoethanol for 10 min followed by a 10 min incubation step in a 1 % SDS buffer without  $\beta$ -mercaptoethanol. Single lanes were placed on top of a 14 % polyacrylamide gel containing 4 % urea and electrophoresis was carried out at room temperature using 35 mA/12 x 14 cm gel. Immunoblot analysis was performed as described (see 3.3.9).

### **3.3.11 Mass-spectrometry**

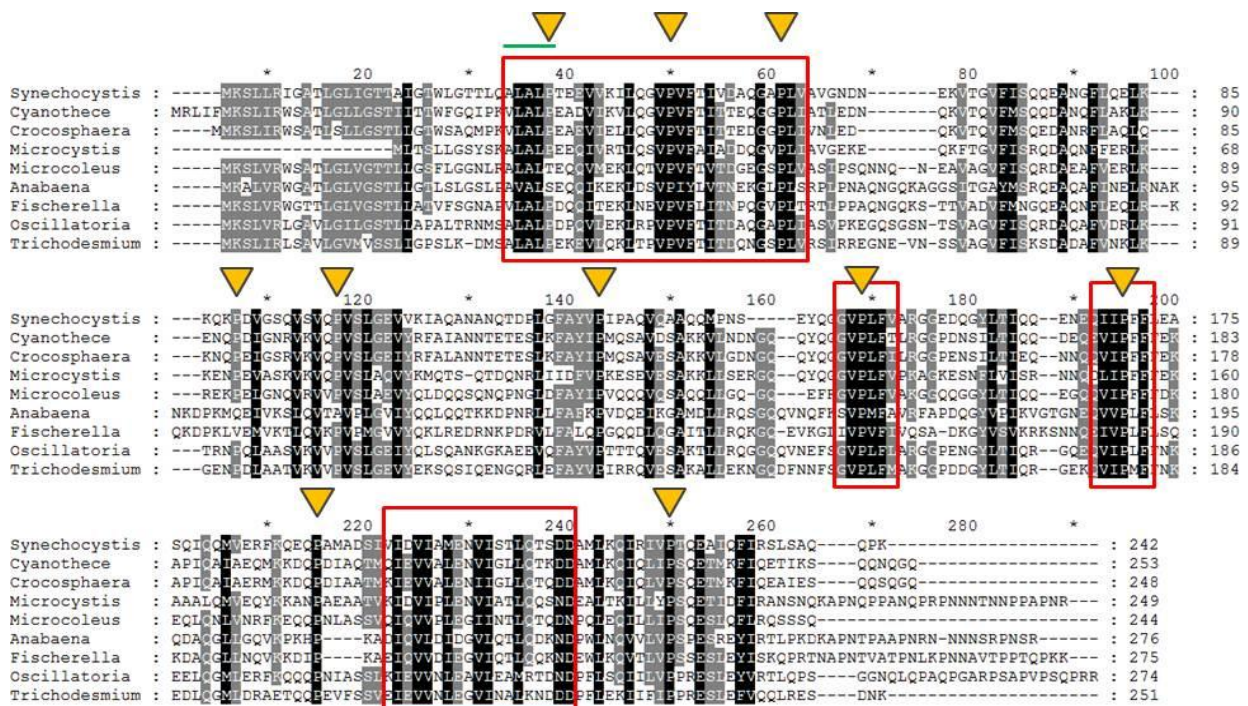
For protein identification Coomassie- or silver-stained protein bands were cut from SDS-PAGE gels and sent to Dr. Ulrike Oster at Biozentrum (Department Biologie I, LMU München) for further experimental procedures.

## 4 Results

### 4.1 SynTic22 (Slr0924) – a protein involved in sorting processes in *Synechocystis* sp. strain PCC 6803?

#### 4.1.1 *In silico* characterization of SynTic22

SynTic22 was initially identified in a screen for periplasmic proteins expressed under high salt conditions. At that time, the protein sequence showed no significant match to any protein or motif of known function (Fulda et al., 1999). Three years later, it was shown to be a homolog of Tic22 of higher plants (Fulda et al., 2002). Since then almost ten years have past in which new protein motifs were identified and more genes sequenced. Therefore, an integration of *synTic22* in the context of new database knowledge was performed using bioinformatics tools. The *Synechocystis* Tic22 protein sequence was aligned with Tic22-like proteins from other cyanobacteria. Most of the sequences were very similar in their N-terminal amino acids, whereas the C-terminal amino acids revealed the highest dissimilarity of the whole protein sequence (Figure 3). In addition, several conserved blocks were found that mainly contained hydrophobic amino acids (Figure 3, red boxes).



**Figure 3: Protein sequence alignment of Tic22 family members in cyanobacteria.** Black boxes indicate identical or conserved residues in all sequences. Grey boxes indicate similar or less conserved residues. Comparisons were performed using VectorNTI and alignments were plotted using the GENEDOC program. The thick green bar indicates a possible signal peptidase cleavage site. Orange triangles mark position of conserved proline residues. Red boxes indicate regions of highly conserved hydrophobic amino acids.

In particular, proline was found to be highly conserved at several positions within the amino acid sequences (Figure 3, orange triangles).

In a next step, homologs in higher organism were obtained by using the amino acid sequence of SynTic22 (Figure 4) in PSI-BLAST searches (blastp) on NCBI (<http://www.ncbi.nlm.nih.gov/>). Analysis using the default threshold of PSI-BLAST revealed that the closest relative to SynTic22 is the putative Tic22-like protein in *Cyanothece* sp. ATCC 51142 (54 % identity, 75 % similarity, E-value  $7e^{-89}$ ) followed by putative Tic22-like proteins of other cyanobacteria (*Crocospaera Watsonii* WH-8501, 51 %, 75 %,  $4e^{-75}$ ; *Microcystis aeruginosa* NIES-843, 47 %, 69 %,  $3e^{-66}$  and *Anabaena variabilis* ATCC 29413, 32 %, 54 %,  $3e^{-28}$ ). Similarity searches with the green algae *Chlamydomonas reinhardtii* (24 %, 48 %,  $2e^{-6}$ ), the moss *Physcomitrella patens* (25 %, 48 %,  $1e^{-16}$ ) and higher plants (*Zea mays*, 23 %, 47 %,  $1e^{-11}$ ; *Arabidopsis thaliana* Tic22-III, 20 %, 49 %,  $8e^{-8}$  and *Pisum sativum*, 20 %, 46 %,  $2e^{-9}$ ) showed the expected decrease in similarity during evolution to higher plants.

The SynTic22 amino acid sequence was also searched against protein databases (InterProScan; Hunter et al., 2011). Apart from the Tic22 motif, no other protein motif could be identified.

```

1  MPWLQTFSFRRSPFSLARRHLKNKIFVKIKSIFLLSLLFEATATMKSLLRIGATLGLIGTTAIGTWL
68  GTTLQALALPTEEVVKILQGVPVFTIVDAQGAPLVAVGNDNEKVTGVFISQQEANGFLQELKK
131 QKPDVGSQVSVQPVS1LG2EVV3KIAQANANQTDPLGFAYVPIPAQVQAAQQMPNSEYQGGVP
191 L4FVARGGEDQGYLTIQQENEQIIPFFLEASQIQQMVERFKQE5Q6PAMADSIDVIAMENVISTL
254 QTSDDAMLKQIRIVPTQEAIQFIRLSAQPK

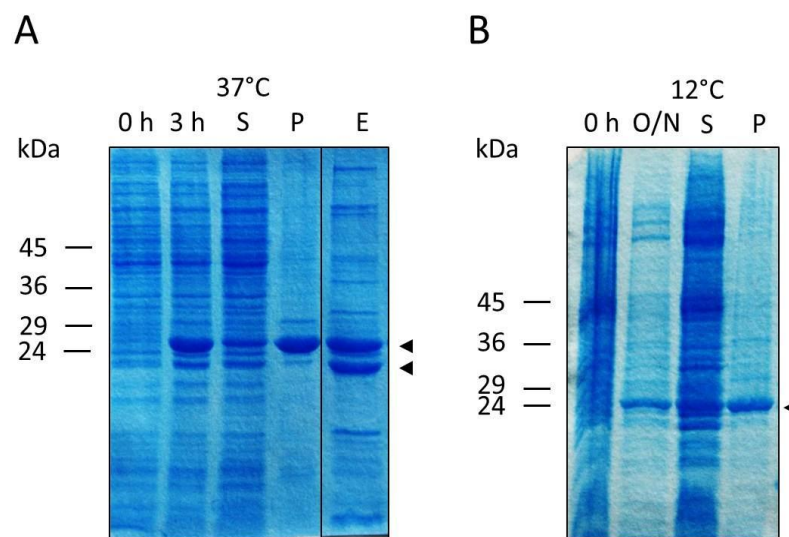
```

**Figure 4: Putative protein sequences of SynTic22.** Overbars mark methionine's of two possible start points, leading to a 32 kDa and 26 kDa protein, respectively. Underline indicates a putative Sec signal peptide as predicted by PRED-TAT algorithm (Bagos et al., 2010)). Processing of the putative Sec signal sequence gives a 23 kDa form of SynTic22 (according to Fulda et al., 2002).

#### 4.1.2 Overexpression and purification of SynTic22

The SynTic22 protein was overexpressed and purified for use in further biochemical experiments. At that time, no structural data of any Tic22 homolog were available. *In silico* predictions proposed that SynTic22 might possess an N-terminal signal peptide and/or an N-terminal transmembrane segment, when the second methionine is used as translational start (Figure 4). In order to consider a potential role of this part of the protein for its proper function and localization, primers were designed to amplify the sequence of 729 bp from chromosomal DNA (see 3.3.1). After cloning into the pET21a expression vector, overexpression of a Coomassie-stainable amount of the protein (26 kDa) was achieved at 37 °C without any obviously toxic effects for the *E. coli* host strain (Figure 5A, lane 3h). Since most of the protein was accumulated in inclusion bodies (Figure 5A, lane P), temperature used during

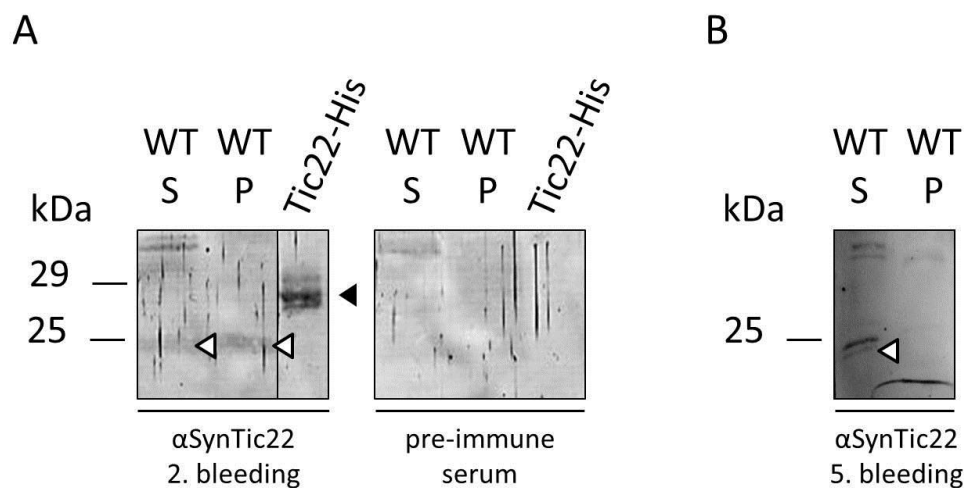
overexpression was lowered to 12 °C and the time of incubation extended to overnight (Figure 5B). Fifty percent of SynTic22 was expressed in a soluble form under those conditions and a total of about 10 mg per 3 L culture was obtained (Figure 5B, lane S and P). In addition, no detergent or urea was used during the procedure, making a proper folding of the protein most likely. Interestingly, when affinity chromatography was used to bind the protein via its His<sub>6</sub>-tag to a Ni<sup>2+</sup>-sepharose matrix a second, lower band was obtained after elution. The molecular weight of about 23 kDa indicated to a processed form of SynTic22 in which the putative signal sequence might have cut off (Figure 5A, lane E, lower arrowhead). Neither working under cold conditions (4 °C), application of diverse protease inhibitors like PMSF or cOmplete Mini from Roche (Mannheim, Germany) nor more stringent conditions during the purification procedure could prevent the lower band from appearing. In order to determine their identity, both bands were cut out and characterized by mass spectrometric analysis. The upper band was unambiguously identified as the expected SynTic22 protein (Figure 5A, lane E, upper arrowhead). In contrast, the lower band turned out to be a mixture of two proteins. The first protein was a shorter form of SynTic22 protein starting from 1-QALALPTEEVVKI-13, thus 4 AA ahead of the predicted signal peptide end. The second protein was identified as the 210 AA, 23.6 kDa *E. coli* cAMP-receptor protein (UniProtKB/ Swiss-Prot: P0ACJ8.1).



**Figure 5: Overexpression and purification of SynTic22 protein.** (A) Expression of SynTic22 in Rosetta (DE3) cells at 37 °C. Total cell lysates (10 µl) taken before (0 h) and 3 hours (3 h) after induction are compared. Samples taken after 3 h were lysed and separated into soluble proteins (S) and total membrane fraction (P). Soluble proteins were applied to Ni<sup>2+</sup>-affinity chromatography, washed, and eluted as described in “methods”. E, elution fraction (B) Expression of SynTic22 at 12 °C. Total cell lysates (10 µl) taken before (0 h) induction and after overnight incubation (O/N) are compared. Black arrowheads indicate the overexpressed protein.

To test whether the cAMP-receptor protein is unspecifically bound to the sepharose matrix, a control experiment was performed. *E. coli* cells were transformed with the empty pET21a vector and treated as before. No accumulation of the cAMP receptor protein was observed after separation of the elution fraction in a SDS-polyacrylamide gel (data not shown). To further test if the accumulation is caused by the SynTic22 protein expression, *E. coli* cells were transformed with pET21a-*synTic22stop* that encodes for SynTic22 with a Stop-codon and thus has no C-terminal His<sub>6</sub>-tag. Again, no accumulation of the cAMP receptor protein was observed after separation of the elution fraction in a SDS-polyacrylamide gel (data not shown). Since the negative controls did not show unspecific binding of the cAMP receptor protein to the sepharose matrix, it was possible that co-purification by interacting with SynTic22 had occurred.

To generate a SynTic22 specific antibody for further experiments, the protein with putative signal peptide but without a His<sub>6</sub>-tag was heterologously expressed in *E. coli* and subsequently separated on a preparative 14 % polyacrylamide gel containing 4 % urea. The protein band was cut from the gel and sent for generation of an antibody by immunization of a rabbit. First tests using the serum of the second bleeding detected the protein as a weak signal of about 23 kDa in both the wild-type soluble and membrane protein fraction, which corresponds to the molecular weight of the predicted processed SynTic22 (Figure 6A, lane S and P, white arrowheads).

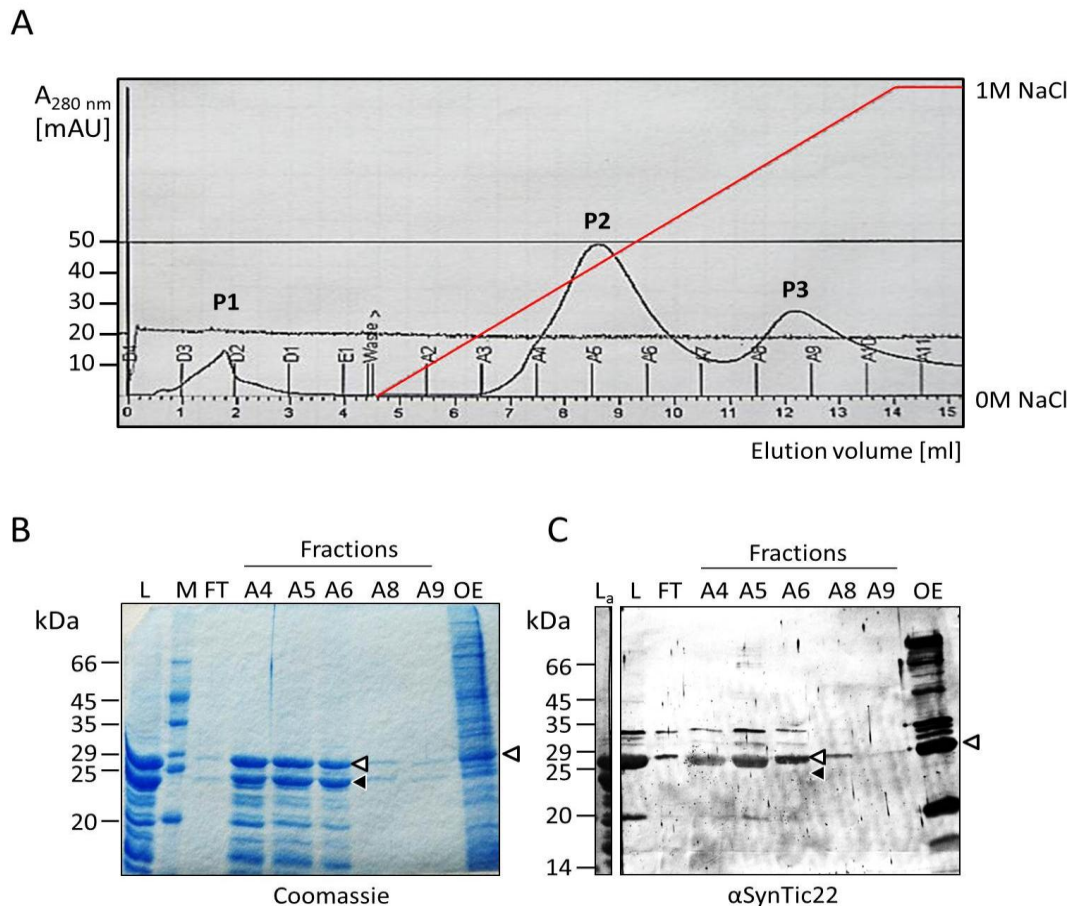


**Figure 6: Immunoblotting analysis of new SynTic22 antiserum.** (A) Crude protein extract from *Synechocystis* wild-type cells was separated into soluble proteins (S) and membrane fraction (P). Proteins samples (20 μg each) were fractionated by SDS-PAGE, and blot was probed with SynTic22 antiserum of the second bleeding (lanes 1-3). Metal affinity chromatography purified recombinant SynTic22-His protein was loaded as positive control (lane 3; 2 μl of a 1:100 dilution). As negative control, the samples were also probed with the corresponding pre-immune serum (lanes 4-6). White arrowheads mark SynTic22 protein. Black arrowhead marks SynTic22 recombinant protein (26 kDa) (B) Wild-type crude protein extract was separated into soluble proteins (S) and membrane fraction (P), fractionated by SDS-PAGE, and blot was probed with the SynTic22 antiserum of the fifth bleeding. White arrowhead marks a third putative SynTic22 form.

A strong signal at 26 kDa was detected for the recombinant SynTic22 protein sample, which was used as a positive control (Figure 6A, lane 3, black arrowhead). In contrast, the pre-immune serum, which was used as negative control, did not detect any proteins of that size in the wild-type or in recombinant protein samples, thereby demonstrating the specificity of the antibody (Figure 6A, lanes S and P). However, further refinements of the extraction method indicated a distribution solely in the soluble fraction (Figure 6B). Even with antiserum of later bleedings, which are supposed to have a higher SynTic22 antibody titer, it was not possible to detect the putative 32 kDa or 26 kDa forms of SynTic22 in wild-type samples. This was judged by comparison with the running behavior of the recombinant SynTic22 protein, which has a molecular weight of 26 kDa (data not shown). Instead, a faint and slightly smaller second band appeared sometimes when total soluble proteins were used (Figure 6B, lane S, white arrowhead).

As the recombinant SynTic22 protein was important for further biochemical experiments ion exchange chromatography (IEX) was performed in an attempt to separate it from the 23 kDa *E. coli* cAMP receptor protein. IEX allows separation of proteins with differences in their surface charge. This method was very promising as the isoelectric points of the SynTic22 (pI 5.08) and the cAMP receptor protein (pI 8.38) were predicted to be rather different. A positively charged HiTrap Q FF anion column from GE Healthcare (München, Germany) was used to bind the negatively charged SynTic22 protein under low salt conditions (0 M NaCl). Proteins were eluted using a linear gradient of up to 1 M NaCl and detected by measuring the absorbance at 280 nm. On the chromatogram three peaks were observed (Figure 7A, black curve, P1, P2 and P3). The first peak corresponded to low amounts of unbound protein (Figure 7B, lane FT). Peak 2 contained the highest amount of protein and eluted after application of about 250-600 mM NaCl. Peak 3 eluted after application of about 700-850 mM NaCl. However, although proteins eluted in different peaks, SDS-PAGE analysis showed that IEX was not successful to separate the proteins. Both elution peaks consisted of a similar protein composition when compared with each other and the load (compare Figure 7B, lane L and lanes A4-9). To investigate the SynTic22 distribution between both protein bands, Western analysis was performed using SynTic22 antiserum (Figure 7C). Interestingly, only one of the protein bands was detectable using the antiserum (Figure 7C, lanes L and A4-8). Comparing the amido black stained load control with the immune signal showed that the 23 kDa protein band was not detectable (Figure 7C, lane L<sub>a</sub> in comparison to lane A6, black arrowhead).





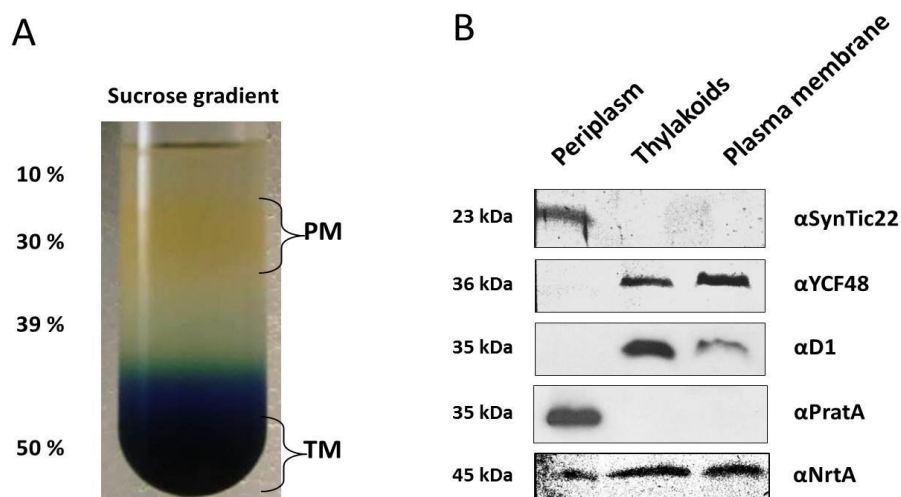
**Figure 7: Ion Exchange Chromatography (IEX).** Anion exchange chromatography was used to separate recombinant SynTic22 (pI 5.08) and 23 kDa *E. coli* cAMP receptor protein (pI 8.38). **(A)** About 10 mg of overexpressed SynTic22 protein obtained from metal affinity chromatography was applied to IEX. Proteins were eluted by a linear increasing salt gradient (red line). Samples of 500  $\mu$ l were collected (A1-A12). Protein elution was detected measuring the optical density at 280 nm (black curve) **(B)** Aliquots of load (L), flow through (FT), elutions (A4-9) and overexpressed SynTic22 were compared by SDS-PAGE. **(C)** SDS-PAGE was applied as in B and proteins blotted onto PVDF membrane for immunoblotting analysis using antiserum against SynTic22. Load lane (L) of the PVDF membrane was cut and stained with amido black ( $L_a$ ). White arrowheads, SynTic22 protein; Black arrowheads, putative 23 kDa cAMP receptor protein; M, marker lane.

Therefore, no SynTic22 is present in the lower band. It was further tried to separate both proteins by hydrophobic interaction chromatography (HIC), which led to a similar result (data not shown).

### 4.1.3 Localization of SynTic22

Initial immunoblot analysis of wild-type soluble and membrane protein fractions indicated SynTic22 to be a soluble protein. To determine the precise subcellular location cell fractionation was performed. Cell fractionation should also answer the question if SynTic22 is attached to underrepresented membranes like the plasma membrane or the PrtA-defined membranes (PDM; Schottkowski et al., 2008).

Periplasmic proteins were extracted from *Synechocystis* wild-type cells by method of cold osmotic shock (Fulda et al., 1999). During the procedure the outer membrane, but not the plasma membrane is supposed to burst. Soluble proteins released were separated by centrifugation from disrupted outer membranes and remaining spheroplasts. After disrupting the spheroplasts, a five-step sucrose gradient was used to separate plasma membrane and thylakoid membrane systems (Figure 8A). The sucrose fractions were then subjected to Western analysis (Figure 8B). SynTic22 was detectable solely within the periplasmic fraction, as judged by the immunodetection of the periplasmic marker protein PrtA (Figure 10B, lane 1). This result confirmed the previous data that suggested SynTic22 to be a soluble protein (Figure 6B). However, in contrast to crude cell lysates, only one signal was observed in periplasm samples at about 23 kDa.



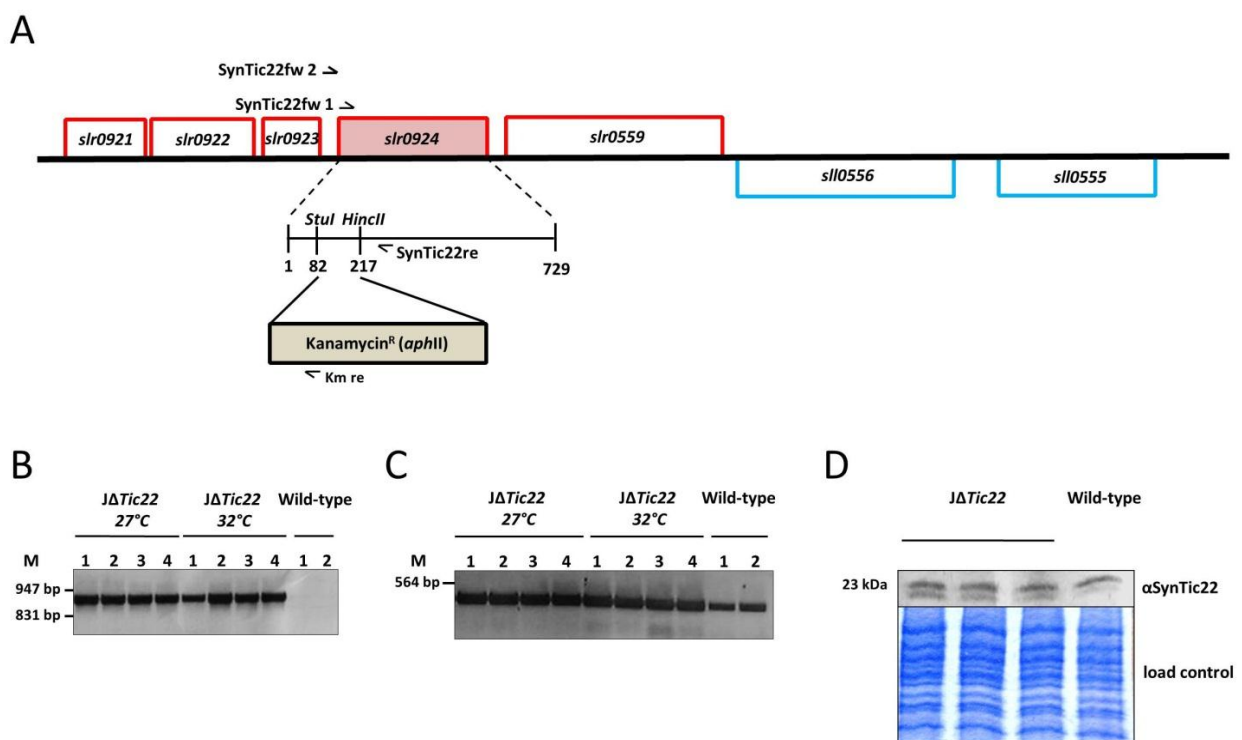
**Figure 8: Localization of Tic22 protein in *Synechocystis* sub-compartments.** (A) Periplasm was isolated from *Synechocystis* wild-type cells by cold osmotic shock. Remaining spheroplasts were disrupted and applied to a five-step sucrose density gradient that separated the lighter plasma membranes (yellow) from denser thylakoid membranes (dark green) (B) Plasma- and thylakoid fractions were subsequently washed, concentrated, solubilized and fractionated together with samples of periplasm by SDS-PAGE (30  $\mu$ g per sample). Blots were probed with antibodies against SynTic22 and against marker proteins for thylakoid lumen (YCF48), thylakoid membrane (D1), periplasm (PrtA) and plasma membrane (NrtA).

Purity of the periplasmic fraction was demonstrated by immunodetection of marker proteins for plasma membrane (NrtA), thylakoid lumen (YCF48) and thylakoid membrane (D1) (Figure 8B, row 2-5). YCF48 is supposed to be a luminal marker protein, although it might also be attached to the membrane to some extent. Signals for YCF48 were observed in thylakoid and plasma membrane fraction (Figure 8B, row 2). D1 protein was only detected within thylakoids and to some extent within the plasma membrane fraction but not within the periplasm. This suggests that periplasm was free of contamination by thylakoid proteins (Figure 8B, row 3). In contrast, immunodetection of the NrtA protein suggests that the periplasmic and thylakoid fractions are contaminated with plasma membrane material.

#### 4.1.4 Generating *SynTic22* mutants

##### 4.1.4.1 The $\Delta$ *synTic22* strain

To obtain insight into the role of *SynTic22* function, a construct was designed which should result in the disruption of the reading frame and generate knockout strains. First, the *synTic22* gene was PCR amplified from wild-type genomic DNA and cloned into the pCR2.1 vector. In a second step, a kanamycin resistance gene ( $Km^R$ ) was ligated into the *StuI-HincII* sites of pCR2.1\_*synTic22*, thereby adding *synTic22* flanking regions to the  $Km^R$  gene. The assembled construct was then used for transformation into *Synechocystis* wild-type strain Japan. The *synTic22* flanking regions were necessary for the subsequent introduction of the resistance cassette into the endogenous *slr0924* gene by homologous recombination (Zang et al., 2007) (Figure 9A). After two weeks of strong selection on plates supplemented with kanamycin, dozens of green colonies were obtained, which were not discriminable from wild-type cells (data not shown).



**Figure 9: *SynTic22* knockout construct.** (A) The *synTic22* locus on genomic DNA is illustrated. Neighboring genes are shown in upper red boxes (transcription 5'-3') or lower blue boxes (transcription in opposite direction). A kanamycin resistance gene was inserted into the *synTic22* locus (*slr0924*) by homologous recombination. The primers for genotyping and their corresponding binding sites (arrowheads) are illustrated. (B) Genotyping of mutant and wild-type strains grown at 27 °C and 32 °C. Primers SynTic22fw 2 and Km re were used. Expected size: 919 bp in mutants, no signal in wild-type. M, DNA marker. (C) Complete segregation of the resistance gene was determined with primers SynTic22fw 1 and SynTic22 re. Expected size: 419 bp in wild-type, no signal in completely segregated knockout mutants. M, DNA marker. (D) Crude protein extracts (30 μg) of three representative merodiploid  $\Delta$ *synTic22* strains and one wild-type were fractionated by SDS-PAGE, and blots probed with antibody against *SynTic22*.

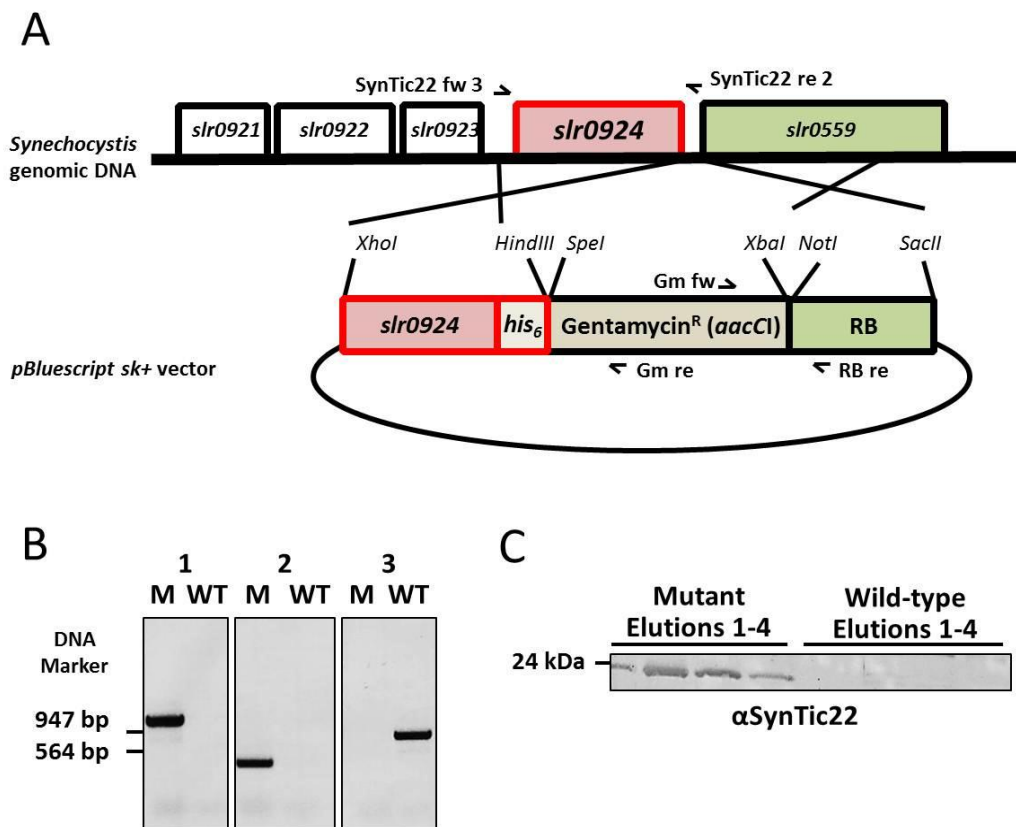
Genotyping was performed by PCR analysis using the primers SynTic22fw 2 and Km re (Figure 9A). SynTic22fw 2 binds upstream of the *synTic22* part that was used for homologous recombination and Km re within the kanamycin resistance gene. This primer combination was expected to confirm the site-specific integration of the kanamycin resistance gene into the *synTic22* locus of *Synechocystis* (Figure 9A). Indeed, site-specific integration of the resistance gene was demonstrated for several mutant strains grown at 27 °C and 32 °C (Figure 9B, lanes 1-8). As control, wild-type genomic DNA was used as template. As expected, no signal was obtained in this reaction (Figure 9B, lanes 9-10). *Synechocystis* is not a haploid organism. It possesses several copies of its genome per cell. Therefore, in a second PCR reaction using the primers SynTic22 fw 1 and SynTic22 re, the segregation state of the mutant strains was analyzed. A short extension time was chosen in which only 419 bp of the wild-type *synTic22* gene could be amplified. In completely segregated mutant strains, no signal was expected since the kanamycin gene interrupts all copies of *synTic22* in their genomes (Figure 9A). However, although the concentration of antibiotic applied was increased slowly up to 400 µg/ml agar for several weeks, the endogenous *synTic22* gene was still detectable in all strains (data not shown). This suggested that the gene is essential for cell survival under the conditions applied and cannot be knocked-out. In some cases, changing the growth conditions can circumvent such restrictions. Therefore, two different temperatures 27 °C and 32 °C were tested but the wild-type *synTic22* gene was still detectable (Figure 9C, lane 1-8). All strains were merodiploid, that is, they have the endogenous gene and the one with the kanamycin gene (Figure 9C). Although not all copies of *synTic22* can be disrupted in merodiploid strains, it might still be possible that the overall gene copy number is lower than in the wild-type. Ultimately, this could lead to a moderate phenotype because of reduced expression of SynTic22 proteins (knockdown). To determine whether the merodiploid strains are knockdown strains, Western blot analysis was performed using antiserum against SynTic22 (Figure 9D). As in previous experiments on crude soluble proteins, two signals at about 23 kDa were detected. Comparison of the signal intensities obtained from merodiploid strains with the wild-type strain showed no reduction of SynTic22 protein level and was confirmed by the corresponding loading control (Figure 9D).

#### 4.1.4.2 The $J\Delta_{synTic22}::synTic22-His$ strain

A second construct was designed that did not aim at producing a knockout or knockdown of the endogenous *synTic22* gene but to replace it with a version that encodes for SynTic22 with a C-terminally added His<sub>6</sub>-tag. The construct was assembled and transformed into *Synechocystis* wild-type strain Japan by using the *synTic22* gene sequence as left border and part of the

downstream *slr0559* gene sequence as right border for stable integration into the genomic DNA by homologous recombination (Figure 10A).

After two weeks of strong selection on plates supplemented with gentamycin, dozens of green colonies were obtained, which were not discriminable from wild-type cells (data not shown). The genotype of the new transgenic  $J\Delta_{synTic22}::synTic22-His$  strain was analyzed by PCR (Figure 10B). Using the primer combination SynTic22 fw 3 with Gm re and Gm fw with SynTic22 re 2 confirmed the correct integration into the genomic DNA since only signals in the mutant strain were obtained (Figure 10B, block 1 and 2). More interestingly, when  $J\Delta_{synTic22}::synTic22-His$  strain was tested for segregation, no wild-type *synTic22* gene was detectable anymore (Figure 10B, block 3). This suggests that *synTic22-His* could completely replace the wild-type *synTic22* even though it adds a C-terminal His<sub>6</sub>-tag to the protein. Since SynTic22 seems to be an essential protein this suggests, that it is still functional.

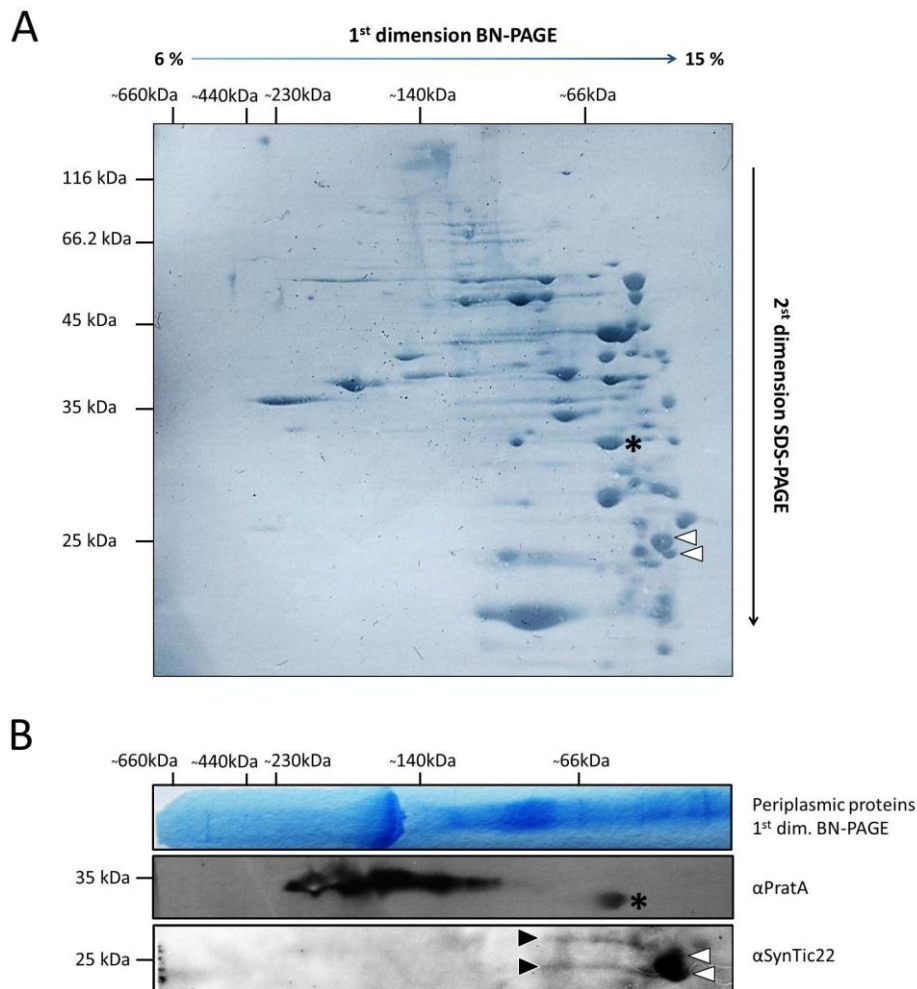


**Figure 10:** (A) The *synTic22* (*slr0924*) locus on *Synechocystis* genomic DNA with neighboring genes is illustrated. A construct containing *slr0924* as left border, *aacCI* as resistance gene, and part of *slr0559* as right border (RB) was cloned and transformed into *Synechocystis* wild-type strain Japan. Thereupon, insertion of *synTic22-His* into the *synTic22* locus occurred by homologous recombination. The primers for genotyping and their corresponding binding sites are shown (arrowheads). (B) Genotyping of mutant and wild-type strain by PCR analysis. M, mutant. WT, wild-type. Primer combinations and expected sizes in mutant (M) and wild-type (WT): 1) SynTic22 fw 3/Gm re, 1200 bp M, no signal WT; 2) Gm fw/RB re, 450 bp M, no signal WT; 3) SynTic22 fw 3/SynTic22 re 2, no signal fully segregated mutant (M), 899 bp WT. (C) Cultures of wild-type and mutant were grown at standard conditions. Crude soluble proteins were extracted and exposed to Ni<sup>2+</sup>-sepharose beads. Elutions were applied to SDS-PAGE, and blot probed with an antibody against SynTic22.

In order to test expression of the tagged protein on protein level, crude soluble proteins were extracted from wild-type and  $J\Delta_{synTic22}::synTic22-His$  strain, incubated with  $Ni^{2+}$ -sepharose, and elutions separated by SDS-PAGE. When the blot was probed with antiserum against SynTic22 a band at 24 kDa was detected in the mutant, which is consistent with a processed form of SynTic22 that has a His<sub>6</sub>-tag (0.8 kDa) added but lost its Sec signal sequence (Figure 10C). In contrast, no SynTic22-His protein was detected in elutions from the column that was exposed to crude soluble proteins from the wild-type control (Figure 10C). In this work, the  $J\Delta_{synTic22}::synTic22-His$  strain was used to screen for SynTic22 interaction partners in pull-down experiments (see 4.1.6).

#### 4.1.5 Two dimensional blue native (BN) / SDS-PAGE

A reverse genetically approach to investigate SynTic22 function was not possible because the *synTic22* gene could not be knocked-out. Furthermore, the available merodiploid strains did not even show reduced protein levels, thus making a scientific comparison with wild-type cells by physiological and biochemical approaches impossible. For this reason, the focus was on biochemical methods to investigate SynTic22 behavior and to find possible interaction partners. Two dimensional blue native/ SDS polyacrylamide gel electrophoresis (2D BN/SDS-PAGE) was used to determine, whether SynTic22 forms higher molecular complexes. As the protein was identified exclusively within the periplasmic fraction, only freshly isolated periplasmic proteins were used in this approach. They were isolated by method of cold osmotic shock, concentrated via membrane-based centrifugation in a gentle and native form, and applied to 2D-BN-PAGE. First, a linear polyacrylamide gradient gel was used to separate native periplasmic complexes. A single lane from the first dimension (Figure 11B, row 1) was then set on top of a second, denaturing polyacrylamide gel to separate each complex into its single subunits. Figure 11A gives an overview of the periplasmic protein composition of *Synechocystis* wild-type after 2D-BN-PAGE separation. In order to check the successful extraction of periplasmic complexes the second dimension was blotted and probed with an antibody against the periplasmic PrtA protein. PrtA had been demonstrated to form a soluble periplasmic complex of about 200 kDa (Schottkowski et al., 2008). Consistent with this result, a PrtA complex of similar size was found (Figure 11B, row 2). In addition, no monomeric PrtA sub-units were detectable (Figure 11B, row 2). The signal at approximately 45-50 kDa is most likely unspecific, because no corresponding PrtA proteins were visible on the amido black stained membrane when compared to the Western blot (Figure 11A and B, black asterisks). Together, both findings suggested that successful extraction of periplasmic complexes had occurred.



**Figure 11: Two forms of SynTic22 appear in BN-PAGE.** Wild-type cells were grown under standard conditions and periplasmic proteins isolated as described in Methods (3.3.4.1). **(A)** Protein composition of periplasmic fraction after 2D BN/SDS-PAGE loaded with 300  $\mu$ g protein. Gel was blotted on PVDF membrane and stained with amido black. White arrowheads mark SynTic22 protein. **(B)** Coomassie-stained first dimension of blue native PAGE (6-15 % acrylamide) and second dimensions (14 % acrylamide; 4 M urea) subjected to Western blotting analysis using the antibodies indicated on the right margin. Positions of the molecular weight marker bands for first and second dimension are given on top and left side, respectively. Black asterisk, putatively unspecific PrtA antibody signal.

In contrast to previous immunodetection of SynTic22 in periplasmic samples, two slightly shifted spots of almost similar molecular weight were found (Figure 11B, row 3, white arrowheads). This was surprising, because neither the faint, slightly smaller band beneath the SynTic22 protein detected in samples of total soluble protein (Figure 6B and Figure 9D) nor the putative unprocessed SynTic22 protein, which has an N-terminal signal sequence and a molecular weight of about 26 kDa had been detected in the periplasmic fraction before. In contrast to PrtA, the Western blot signal could be assigned to two spots on the amido black stained membrane suggesting SynTic22 to be a major protein within the periplasm (Figure 11A, white arrowheads). The molecular weight of the proteins could correspond to the unprocessed SynTic22 (26 kDa) and processed SynTic22 (23 kDa) or it could correspond to the two protein

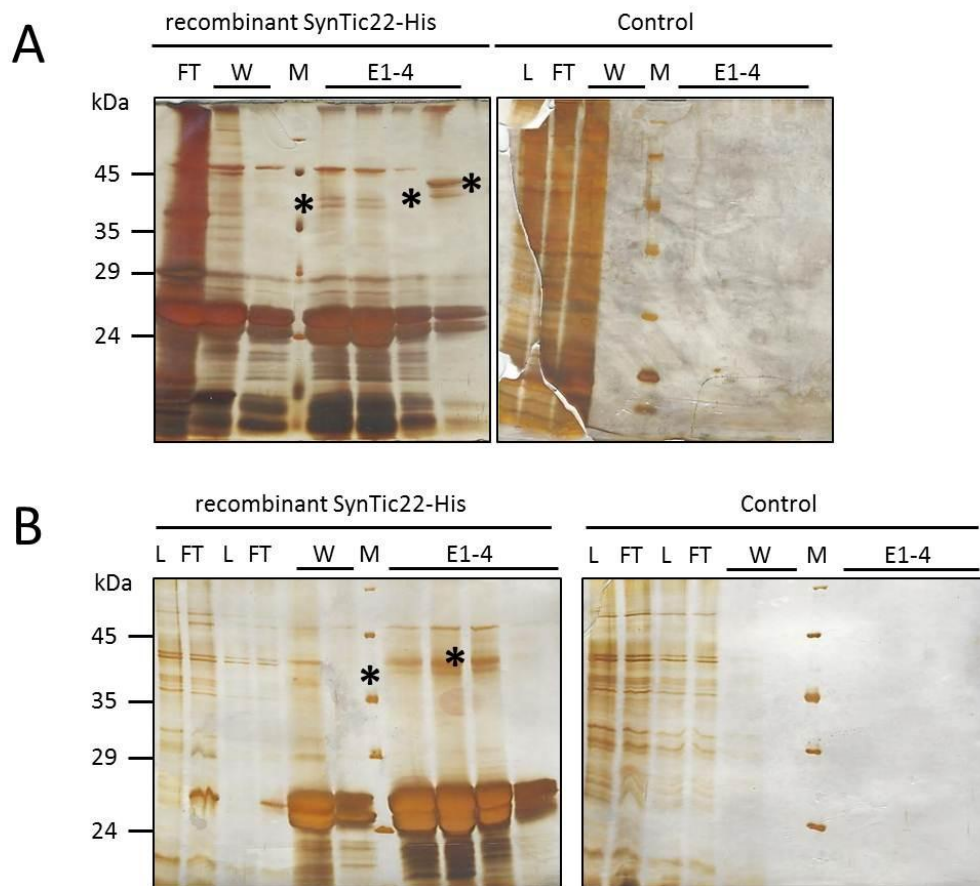
bands at 23 kDa that had been observed in crude soluble protein samples earlier (Figure 6B and Figure 9D). When both spots were compared, the higher mass protein was more prominent than the lower mass protein (Figure 11A, white arrowheads). In contrast to Prata, the majority of the protein was available as monomers; although small amounts of SynTic22 material of both molecular mass forms formed a faint smear towards higher molecular mass regions of about 90 kDa (Figure 11B, row 3, black arrowheads).

#### 4.1.6 Initial screening for SynTic22 interaction partners

The presented BN-PAGE data suggested that SynTic22 might form complexes of higher molecular mass. For this purpose, pull-down experiments were performed to determine the composition of these complexes and to screen for possible interaction partners. Two different approaches were applied.

In the first approach, SynTic22-His recombinant protein was expressed in *E. coli* cells and purified via metal affinity chromatography. It is important to note, that in *Synechocystis* a direct connection of plasma- and thylakoid membrane is still under debate. If those two membrane systems are connected, periplasm and thylakoid lumen could also be associated. Therefore, proteins of those compartments were considered as potential binding partners. Periplasmic proteins were isolated by cold osmotic shock. Remaining spheroplasts were used to isolate plasma membrane and thylakoid membranes via sucrose gradient centrifugation. SynTic22-His was re-bound to nickel sepharose matrix and incubated with periplasmic proteins and with solubilized plasma- and thylakoid membrane proteins. Plasma membranes constitute a minority of the total membranes in *Synechocystis*. The protein amount that was retrieved and used for the following interaction test was thus rather low. No potentially interacting proteins were observable in Coomassie stained gels. However, silver staining revealed several potentially interacting proteins (Figure 12A, lanes E1-4, black asterisks). Two bands of about 40 kDa eluted in E1 and E2, whereas two more bands of about 41-44 kDa eluted in a later elution step (Figure 12A, E4). Those bands did not occur in the first or final wash step indicating an interaction with the recombinant protein (Figure 12A, lanes W1 and W2). To determine the specific binding to SynTic22-His an empty Ni<sup>2+</sup>-sepharose matrix was incubated with plasma membrane proteins as control. As expected, no stainable amounts of protein were found in the final wash and the elution steps (Figure 12A, control). When thylakoid membrane and luminal proteins were incubated with recombinant SynTic22-His, two bands were identified at about 40 kDa in elutions 1-3 (Figure 12B, E1-3, black asterisks).





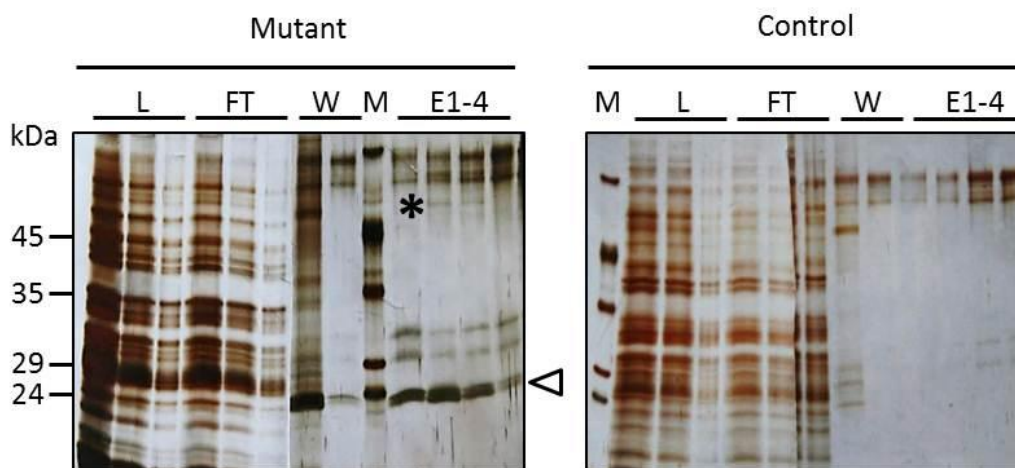
**Figure 12: Pull-down experiments using recombinant SynTic22-His.** SynTic22-His recombinant protein was expressed in *E. coli* and purified by affinity chromatography. **(A)** About 0.6 mg recombinant protein was incubated with ~100  $\mu$ g solubilized plasma membrane proteins (0.5 % DoMa) and Ni<sup>2+</sup>-sepharose. Eluted proteins (E1-4) were TCA precipitated and subjected to SDS-PAGE. L, load; FT, flow-through; W, first and final wash step. Black asterisks, potential SynTic22 interacting proteins. **(B)** As in (A), but recombinant protein was incubated with 2 mg solubilized thylakoid membrane proteins (0.5 % DoMa). In controls, solubilized thylakoid or plasma membrane proteins were incubated with Ni<sup>2+</sup>-sepharose but without recombinant protein. Black asterisks indicate some protein bands that were sent to mass spectrometric analysis.

Cross-reaction with the matrix was checked by incubation with an empty Ni<sup>2+</sup>-sepharose matrix (Figure 12B, control). For identification, protein bands were cut out and sent to mass spectrometric analysis (Figure 12A and B, black asterisks). Table 10 gives a summary of putative SynTic22 interacting proteins identified by mass spectrometric analysis using the recombinant SynTic22-His.

In the second approach, the  $J\Delta_{synTic22}::synTic22-His$  strain in which the endogenous *synTic22* gene was exchanged by *synTic22* with an additional C-terminal His<sub>6</sub>-tag was used (see 4.1.4). Thereby, two advantages compared to the first approach were expected. First, the SynTic22-His protein can function *in vivo* in its natural environment, which should increase the chance for identification of interaction partners. Second, overexpressed SynTic22-His protein could not be separated from the *E. coli* cAMP receptor protein, thus at least some of the interacting proteins found might be due to interaction with the latter one. The second approach does not only

circumvent this problem but delivers a possibility for relatives of the *E. coli* cAMP receptor protein in *Synechocystis* to bind to SynTic22 if such an interaction exists.

To look for interaction partners, periplasmic proteins were isolated from *Synechocystis* wild-type and  $J\Delta\text{synTic22}::\text{synTic22-His}$  mutant strains by cold osmotic shock. Afterwards, proteins were incubated with  $\text{Ni}^{2+}$ -sepharose matrix and after elution from the column separated by SDS-PAGE. Gels were then silver stained and checked for proteins that were co-purified with SynTic22-His. In the experiment shown, only a faint band at about 60 kDa was found (Figure 13, lane E2 and E3, black asterisk). In contrast to the two bands at about 31 and 33 kDa, this band was not found in the wild-type control, therefore might represent a SynTic22 interaction partner. Surprisingly, after pull-down a double band was obtained at 24 kDa (Figure 13, lane E1-4, arrowhead) that could represent two forms of SynTic22 (see discussion). The ratio of the two proteins varied strongly when the experiment was repeated, usually the upper band was much more pronounced (data not shown).



**Figure 13: Pull-down experiment using the  $J\Delta\text{synTic22}::\text{synTic22-His}$  strain.** Periplasm was isolated from 2 L cultures of  $J\Delta\text{synTic22}::\text{synTic22-His}$  strain and from wild-type strain Japan (negative control). Samples were incubated with  $\text{Ni}^{2+}$ -sepharose. Eluted proteins (E1-4) were TCA precipitated and subjected to SDS-PAGE. L, load; FT, flow-through; W, first and final wash step. Black asterisk, potentially SynTic22 interacting protein. White arrowhead, endogenously expressed SynTic22-His.

Table 11 gives a summary of putative SynTic22 interacting proteins identified by mass spectrometric analysis using the endogenously expressed SynTic22-His.

Taken together, almost all proteins identified belong to different classes. Slr0114 e.g. is a putative phosphatase of the PPM family, whereas Slr1841 is a probable outer membrane porin. Only PilT1, PilT2, CheY and McpA are supposed to have a common function in chemotaxis. No homologs of proteins like Tic20 or Toc75 were found, which had been shown in other organism to interact with Tic22 (Kouranov and Schnell, 1997).

**Table 10: Mass-spectrometrically identified, putative interaction partners obtained from pull-down experiments with recombinant SynTic22-His protein.** Overexpressed protein was bound to Ni<sup>2+</sup>-sepharose and incubated with either isolated periplasm or solubilized plasma- or thylakoid membrane proteins.

Gene	Name	Mass (kDa)	Identified in fraction
sll0109	AroH	14.4	plasma membrane proteins
slr0114	putative PP2C-type phosphatase	56.7	periplasmic proteins thylakoid membrane proteins
sll1951	HlyA	178.2	periplasmic proteins
sll1987	KatG	81.4	plasma membrane proteins thylakoid membrane proteins
slr0335	ApcE	100.3	thylakoid membrane proteins
slr1031	TyrS	44.9	periplasmic proteins
slr1044	McpA (PilJ)	93.2	plasma membrane proteins

**Table 11: Mass-spectrometrically identified, putative interaction partners obtained from pull-down experiments with endogenously expressed SynTic22-His protein.** Periplasm was isolated from JΔ<sub>synTic22::synTic22-His</sub> strain and putative SynTic22 interaction partners were obtained by co-purification via Ni<sup>2+</sup>-sepharose.

Gene	Name	Mass (kDa)	Identified in fraction
slr0114	putative PP2C-type phosphatase	56.7	periplasmic proteins
sll0947	IrtA	21.9	periplasmic proteins
sll1533	PilT2	47.9	periplasmic proteins
Sll1784	protein of unknown function	29.7	periplasmic proteins
sll1987	KatG	81.4	periplasmic proteins
slr0161	PilT1	40.6	periplasmic proteins
slr1325	SpotT	86.6	periplasmic proteins
slr1841	probable outer membrane porin	67.6	periplasmic proteins
slr1924	AmpH	44.3	periplasmic proteins
slr2024	CheY family protein	20.2	periplasmic proteins

#### 4.1.7 Proving of potential SynTic22 interaction partners by using the split-ubiquitin system

By performing pull-down experiments of *Synechocystis* cell fractions, several putative SynTic22 interaction partners were identified (Table 10 and Table 11). From this list, two proteins were of particular interest, the Sll1784 and the Slr1841 proteins. Sll1784 is a soluble protein and therefore was examined using yeast-two hybrid analysis (see 4.1.8). In contrast, the Slr1841 protein was found in a proteomic study of outer membrane proteins (Huang, 2002). It consists of 630 AA (67.6 kDa; pI 4.47) and represents a probable porin and S-layer protein. Porins are  $\beta$ -barrel proteins. *Pisum sativum* Tic22 was suggested to interact with proteins that possess  $\beta$ -barrel structures, e.g. it was shown to crosslink with PsToc75, which forms a  $\beta$ -barrel-type pore

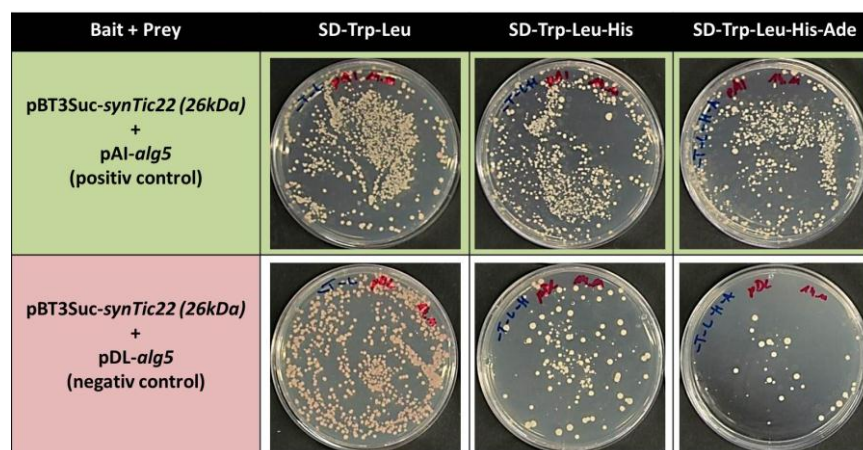
(Kouranov and Schnell, 1997). *Synechocystis* possesses a homolog of PsToc75 that was previously shown to function as a voltage-gated channel in liposomes (Bölter et al., 1998). It was thus very interesting to see whether Slr1841 and SynToc75 proteins can interact with Tic22 in *Synechocystis*.

Slr1841 and SynToc75 have multiple transmembrane domains and are extremely hydrophobic. To test for protein-protein interaction with SynTic22 the split-ubiquitin system was chosen, which is suitable for membrane proteins. Interaction of a bait protein, which is fused to the cub-part of ubiquitin, with a prey protein, fused to the mutated nubG-part of ubiquitin allows both parts to come into close proximity. Only then, a protease recognizes the complemented ubiquitin and cuts off the LexA-VP16 transcription factor, which is attached to the cub-part. Eventually, the transcription factor induces reporter gene expression. When the experiment was performed, no structural data of any Tic22-like protein was available. Since bioinformatics tools proposed the N-terminus of the protein to be either a signal peptide that could be processed by a signal peptidase or a transmembrane domain both forms were considered in the assay. First, the genes encoding for SynTic22 with (26 kDa) or without the putative N-terminal transmembrane domain (23 kDa), Slr1841 and SynToc75 were amplified by PCR from wild-type genomic DNA and ligated into the split-ubiquitin bait vector pBT3N, which adds the cub-part of split ubiquitin to the N-terminus of the bait protein. The in-frame integration and sequence accuracy was determined by sequencing of the constructs. A control assay was performed to test for proper expression and insertion of bait proteins into the membrane of yeast. This was achieved by co-expression with pAI-*Alg5* and pDL-*Alg5* control prey vectors. The vectors express an endoplasmic reticulum protein (*Alg5*) fused to either the mutated nub-part (nubG, pDL) or the wild-type nub-part (nubL, pAI) of ubiquitin. Due to the strong affinity of wild-type nubL to the cub-part, reporter genes will be induced and strong growth on dropout plates (-His and -His-Ade) is expected dependent on proper bait expression and exposition of cub-part into the cytosol but independent of bait-*Alg5* interaction (positive control). On the other hand, co-expression of the mutated nubG-part fused to *Alg5* should not allow growth on dropout plates because an interaction of bait and *Alg5* would be required (negative control). Table 12 gives a summary of the control experiment. It shows that no growth on SD-Trp-Leu-His and SD-Trp-Leu-His-Ade selection plates was observed for bait proteins that had the cub-part of ubiquitin fused to the N-terminus (Table 12, rows 5, 9, 13). The only exceptions were transformants of pBT3N-*synTic22* (23 kDa) that showed ability to grow on selection plates (Table 12, row 1). However, growth was also observed in the negative control, suggesting autonomous activation of the reporter genes by the bait protein (Table 12, row 2).

**Table 12: Verifying correct expression of bait proteins using the control assay.** If a bait protein is properly inserted into the membrane of yeast and has the cub-LexA-VP16 moiety within the cytosol can be tested by co-expression with pAI-*Alg5* and pDL-*Alg5* control prey vectors. SD-Trp-Leu plates select for yeast cells co-transformed with bait and prey vectors (vector combination). SD-Leu-Trp-His and SD-Leu-Trp-His-Ade plates select for interaction of bait and prey protein. The percentage of growth on SD-Leu-Trp-His and SD-Leu-Trp-His-Ade plates was calculated by setting the number of colonies on SD-Leu-Trp plates to one hundred percent. Percentage of growth should be above 20 % for use in further experiments.

	Vector combination	% growth on -Trp-Leu -His	% growth on -Trp-Leu -His-Ade		Vector combination	% growth on -Trp-Leu -His	% growth on -Trp-Leu -His-Ade
1	pBT3N- <i>synTic22</i> (23kDa) + pAI- <i>Alg5</i> (positive)	22	36	9	pBT3N- <i>slr1841</i> + pAI- <i>Alg5</i> (positive)	0	0
2	pBT3N- <i>synTic22</i> (23kDa) + pDL- <i>Alg5</i> (negative)	37	29	10	pBT3N- <i>slr1841</i> + pDL- <i>Alg5</i> (negative)	0	1
3	pBT3Suc- <i>synTic22</i> (23kDa) + pAI- <i>Alg5</i> (positive)	10	6	11	pBT3Suc- <i>slr1841</i> + pAI- <i>Alg5</i> (positive)	0	0
4	pBT3Suc- <i>synTic22</i> (23kDa) + pDL- <i>Alg5</i> (negative)	0	0	12	pBT3Suc- <i>slr1841</i> + pDL- <i>Alg5</i> (negative)	0	0
5	pBT3N- <i>synTic22</i> (26kDa) + pAI- <i>Alg5</i> (positive)	0	0	13	pBT3N- <i>synToc75</i> + pAI- <i>Alg5</i> (positive)	0	0
6	pBT3N- <i>synTic22</i> (26kDa) + pDL- <i>Alg5</i> (negative)	0	0	14	pBT3N- <i>synToc75</i> + pDL- <i>Alg5</i> (negative)	0	1
7	pBT3Suc- <i>synTic22</i> (26kDa) + pAI- <i>Alg5</i> (positive)	25	32	15	pBT3Suc- <i>synToc75</i> + pAI- <i>Alg5</i> (positive)	8	17
8	pBT3Suc- <i>synTic22</i> (26kDa) + pDL- <i>Alg5</i> (negative)	0	1	16	pBT3Suc- <i>synToc75</i> + pDL- <i>Alg5</i> (negative)	0	0

The absence of colonies on selection plates after co-transformation with the positive control vector suggested that Slr1841 and SynToc75 are either not expressed or do not have their N-terminus exposed within the cytosol. Since the cub-part must be exposed to the cytosol as a prerequisite of the system, a different bait vector (pBT3Suc) was used that added the cub-part of ubiquitin to the C-terminus of the bait proteins. Still no colonies were obtained for pBT3Suc-*slr1841* on dropout plates after co-transformation of the construct with the positive vector, indicating that Slr1841 might not be properly expressed or inserted into the yeast membrane (Table 12, row 11). In contrast, using pBT3Suc-*synToc75* co-expressed with the positive control led to growth of some colonies on the dropout plates. Nevertheless, the number of colonies compared to the number grown on SD-Trp-Leu was too low for use in further experiments (Table 12, row 15). However, yeast cells transformed with the pBT3Suc-*synTic22* (26 kDa) and with the positive control vector resulted in growth of colonies on SD-Trp-Leu-His and



**Figure 14: Verifying the correct expression of SynTic22 (26 kDa) bait protein using the control assay.** SD-Trp-Leu plates select for co-transformants that carry the bait and the prey vectors. Co-expression of the bait and the positive control pAI vector results in the ability to grow on selection plates SD-Trp-Leu-His and SD-Trp-Leu-His-Ade. Co-expression of the bait and the negative control pDL vector does not results in normal growth on selection plates SD-Trp-Leu-His and SD-Trp-Leu-His-Ade.

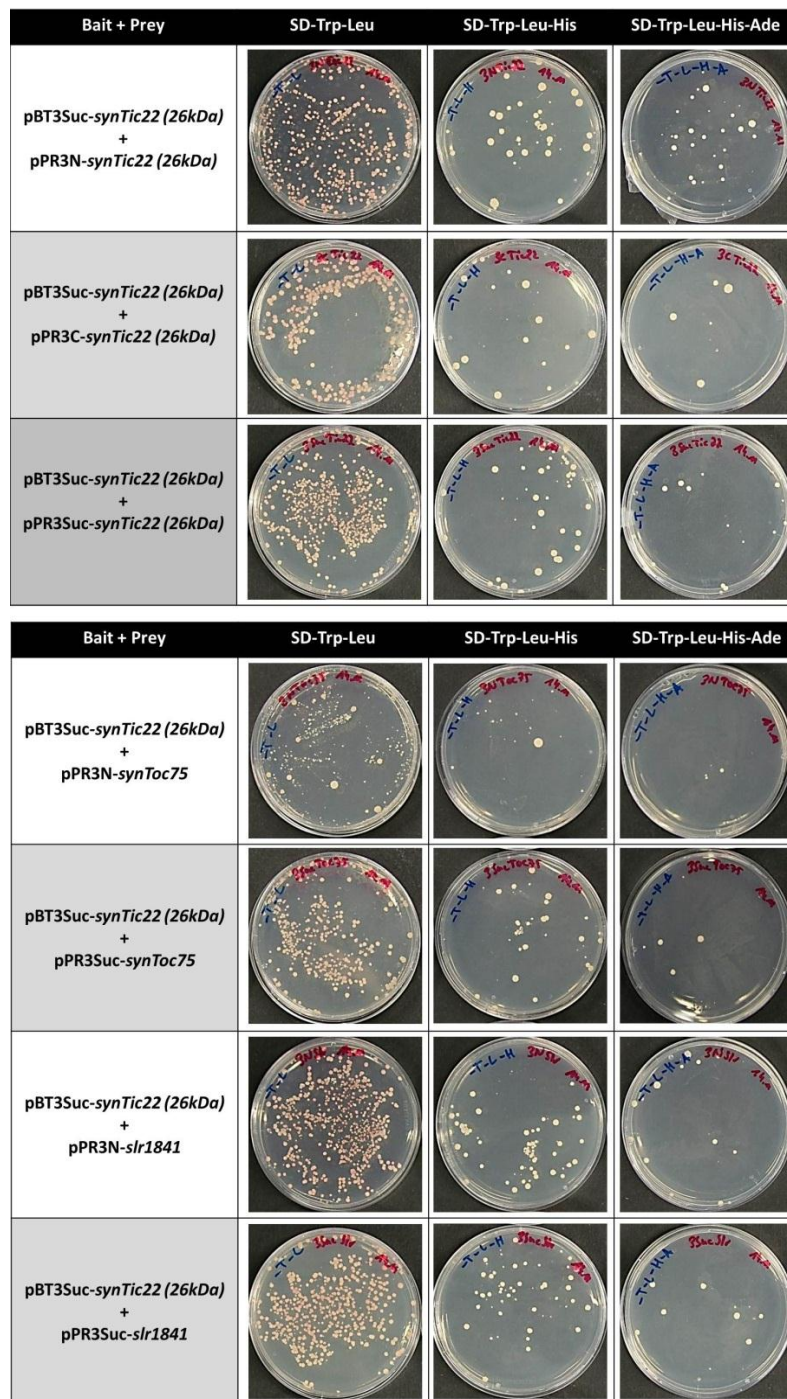
SD-Trp-Leu-His-Ade dropout plates (Table 12, row 7 and Figure 14). Since the number of colonies grown on those plates in comparison to the number of colonies grown on SD-Trp-Leu was high enough to be specific (>20 %), pBT3Suc-*synTic22*(26 kDa) was used as bait vector in further experiments.

In the subsequent experiments, *synTic22*(23 kDa), *synTic22* (26 kDa), *slr1841* and *synToc75* were ligated into the pPR3N vector that adds the mutated nubG-part of ubiquitin to the N-terminus of the protein. In-frame integration and sequence accuracy was determined by sequencing of the constructs. Co-transformation of the bait construct pBT3Suc-*synTic22*

---

(26 kDa) together with the pPR3N-*synTic22* (26 kDa) prey vector did not result in a number of colonies above background level (>20 %) on selection plates (Figure 15, row 1). Adding the nubG-part to the C-terminus of the prey protein via the pPR3C vector gave a similar result (Figure 15, row 2). The pPR3Suc vector was also tried as prey vector. This vector adds the nubG-part to the C-terminus and attaches the Suc signal sequence to the N-terminus of the SynTic22 (26 kDa) protein. Thereby, the recognition of prey proteins by the yeast insert machinery should be improved. Yet, no growth on selection plates was observed (Figure 15, row 3). Expression of *synTic22* (23 kDa) in those three prey vectors gave a similar result (data not shown). Therefore, SynTic22 seems not to interact with itself in yeast.

Previous experiments using the Slr1841 and SynToc75 proteins as bait proposed that either their expression or insertion into the membrane did not occur. Still, the pBT3Suc-*synTic22* (26 kDa) was co-transformed with either the pPR3N-*synToc75* or pPR3N-*slr1841* since a different expression vector can sometimes circumvent such problems. However, for both combinations,



**Figure 15: Split-ubiquitin assay.** Two microgram of plasmid DNA were used for each vector in co-transformation into NMY51 yeast cells. Transformants that had introduced the pBT3 bait (-Leu) and pPR3 prey (-Trp) vectors were selected by growth on appropriate dropout plates (SD-Trp-Leu). Bait-prey interaction was determined using reporter genes that mediated growth on dropout plates deficient of either histidin (SD-Trp-Leu-His) or histidin and adenin (SD-Trp-Leu-His-Ade).

a number of colonies above background level was not observed on selection plates (Figure 15, rows 4 and 6). Co-transformation of pBT3Suc-*synTic22* (26 kDa) with pPR3C-*synToc75* or pPR3C-*slr1841* showed that changing the nubG-part of ubiquitin from the N- to the C-terminus of the prey proteins could not demonstrate an interaction of bait and prey either (data not shown). To increase the chance of prey membrane insertion, *slr1841* and *synToc75* genes were


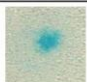
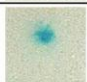
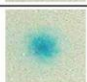
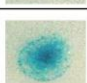


also cloned into the pPR3Suc vector and co-transformed with the pBT3Suc-*synTic22* (26 kDa) bait vector. Figure 15, rows 5 and 7 illustrate that even then an interaction between bait and prey was not observable.

Taken together, split-ubiquitin analysis suggested that *SynTic22* does not interact with itself in forming oligomers. Moreover, neither interaction of *SynTic22* with *Slr1841* nor *SynToc75* was observed. However, control experiments proposed that *Slr1841* as well as *SynToc75* might not be properly expressed or inserted into the yeast membrane and therefore seem to be incompatible to the split-ubiquitin system.

#### 4.1.8 Proving of potential *SynTic22* interaction partners by yeast-two hybrid analysis

*Sll1784* is one of the putative *SynTic22* interacting proteins that were identified in pull-down experiments (Table 11). In protein databases, it is annotated as a hypothetical protein, although it was found in a proteomic study of periplasmic proteins (Fulda et al., 2000). The *Sll1784* is a soluble protein of unknown function, has a theoretical molecular mass of 29.8 kDa (267 amino acids, pI 4.99) and like *SynTic22* was predicted to have a Sec signal sequence (1-33 AA; Bagos et al., 2010). Because 2D-BN-PAGE data suggested a soluble complex of *SynTic22* up to 90 kDa within the periplasm, the protein was chosen to be tested for interaction by yeast two-hybrid analysis. In contrast to the split-ubiquitin assay, yeast-two hybrid is a suitable system to test for interactions of soluble proteins (Gyuris et al., 1993; Golemis et al., 1996).

Bait + Prey	Strain	LacZ
pEG202_ <i>synTic22</i> + pJK101	1	
	2	
pEG202_ <i>sll1784</i> + pJK101	1	
	2	
pEG202 (empty) + pJK101		

**Figure 16: Repression assay.** EGY48 yeast cells were co-transformed with the bait and pJK101 control vector. Expression and transfer of the bait proteins into the nucleus is monitored by a reduced  $\beta$ -galactosidase activity.  $\beta$ -galactosidase activity results in development of blue colored cells when SD-Ura-His plates are supplemented with 80 mg/l X-gal. pEG202 empty vector is the negative control that shows full  $\beta$ -galactosidase activity. Two independent strains are shown for bait constructs and one for control.

Prerequisite for the assay to work is the transfer of the expressed bait and prey proteins into the nucleus. Nuclear localization signals encoded on the bait and prey vectors mediate the transfer.

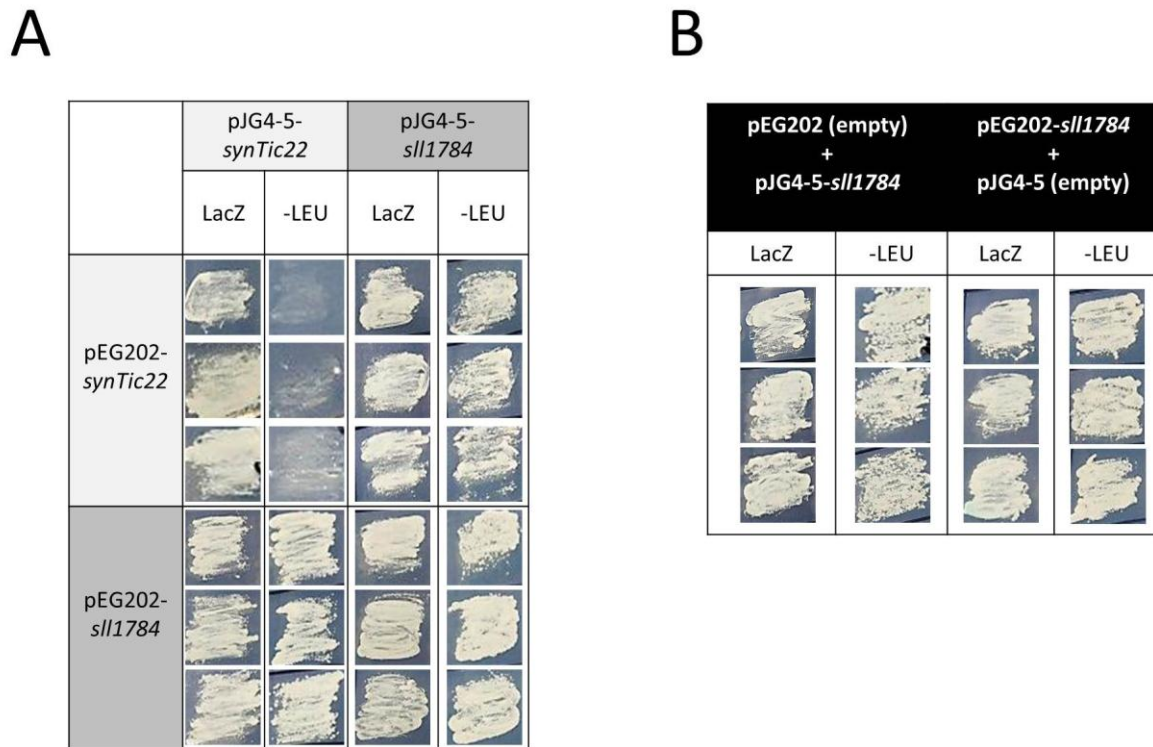
The putative Sec signal sequences of SynTic22 and Sll1784 were omitted, because each harbors putative hydrophobic transmembrane domain that could possibly interfere with the import of the protein into the nucleus (Sato et al., 1994). Moreover, a LexA-DNA binding domain is N-terminally fused to bait proteins in the Y2H system used in this work. Processing of the N-terminal signal peptide of SynTic22 could therefore result in loss of the LexA-DNA binding domain and thus give a false negative result in the assay. To check whether the bait proteins are expressed and transported into the nucleus, a repression assay was performed (Figure 16). EGY48 yeast cells were co-transformed with the bait vector, that constitutively expresses the gene of interest at high levels from the strong ADH1 promoter, and the pJK101 control vector. Selection for transgenic strains was performed on SD-Ura-His. The pJK101 encodes a  $\beta$ -galactosidase reporter gene, which is under control of a LexA-operator. When the bait-LexA fusion protein is properly expressed and transported into the nucleus, it will bind to the LexA-operator of the reporter gene. Thereby, reporter gene expression is inhibited or abolished. As expected, co-transformation of the pJK101 vector with pEG202-*synTic22* bait vector almost abolished  $\beta$ -galactosidase activity. This suggests that the protein is properly expressed and transferred into the nucleus (Figure 16, row 1). As a negative control, the empty pEG202 bait vector was used which was supposed to exert full  $\beta$ -galactosidase activity (Figure 16, row 3). For pEG202-*sll1784* as bait, reduction of  $\beta$ -galactosidase activity was lower but still clearly detectable. Therefore, the Sll1784 bait protein is expressed and transferred into the nucleus (Figure 16, row 2).

The Y2H system used in this work offers two reporter genes. First, the nutritional reporter gene *LEU2* was used to trace protein-protein interactions. As a negative control, all transformants were tested for growth on SD-Ura-Trp-His-Leu when glucose was added to the medium. No growth was observed for any strain under this condition. This finding was consistent with the galactose dependency of the *GALI* promoter, which is used to drive protein expression from the pJG4-5 prey vector. Glucose concentrations above 0.01 % (w/v) effectively prevent gene expression from the *GALI* promoter.

Co-expression of SynTic22 as bait and prey did not result in growth on SD-Ura-Trp-His-Leu plates that contained galactose (induces the *GALI* promoter). As in the split-ubiquitin analysis, this result indicates that the SynTic22 protein does not form homo-oligomers in yeast (Figure 17A).

When SynTic22 was used as bait and Sll1784 as prey, a strong growth on -Leu plates was observed, which suggested an interaction between both proteins (Figure 17A). However, control expression of the empty bait vector together with the Sll1784 encoding prey vector also resulted

in a strong growth on –Leu selection plates, indicating an autonomous activation of the system by the Sll1784 prey protein itself (Figure 17B, lane 2). Sometimes a simple switch of bait and prey vectors can solve the problem. Therefore, the combination of pEG202-*sll1784* as bait with the empty pJG4-5 prey vector was examined. Even as bait protein that is fused to the LexA-DNA binding domain instead of the SV40 activation domain resulted in autonomous



**Figure 17: Test for interaction of SynTic22 and Sll1784.** (A) Genes for periplasmic proteins SynTic22 and Sll1784 were cloned into pEG202 (bait, -His) and pJG4-5 (prey, -Trp) vectors. Co-transformation of the plasmids was performed into H6 yeast cells that contained the p8op-*lacZ* vector (-Ura). Transformants obtained on SD-His-Trp-Ura were streaked out on plates selecting for reporter gene expression (SD-His-Trp-Ura-Leu or SD-His-Trp-Ura+X-gal for *lacZ*). Three representative transformants are depicted for each bait and prey combination. (B) Test for autonomous activation of the two Y2H reporter genes by Sll1784. *Leu2* nutritional reporter mediates growth on plates without leucin. *LacZ* encodes the  $\beta$ -galactosidase enzyme that results in blue colored cells on plates supplemented with X-gal (80 mg/l).

reporter gene activation (Figure 17B, lane 4).

The yeast two-hybrid system used also offers a *lacZ* reporter gene via the p8op-*lacZ* plasmid of the H6 cells (-Ura). The promoters of the *LEU2* nutritional reporter gene and the *lacZ* reporter gene are under control of multiple LexA operators, but they differ in the sequences flanking those operators. As this dissimilarity can help to eliminate false positives, combined expression of all proteins was tested on SD-Ura-Trp-His plates supplemented with galactose and X-gal. Indeed,  $\beta$ -galactosidase activity was not observed in controls using Sll1784 as bait or prey (Figure 17B, lanes 1 and 3). However,  $\beta$ -galactosidase activity was also not observed in any bait to prey combination (Figure 17A, lanes 1 and 3) suggesting that no interaction between the proteins occurs.

## 4.2 Visualization of membrane biogenesis processes via control of *pratA* gene expression

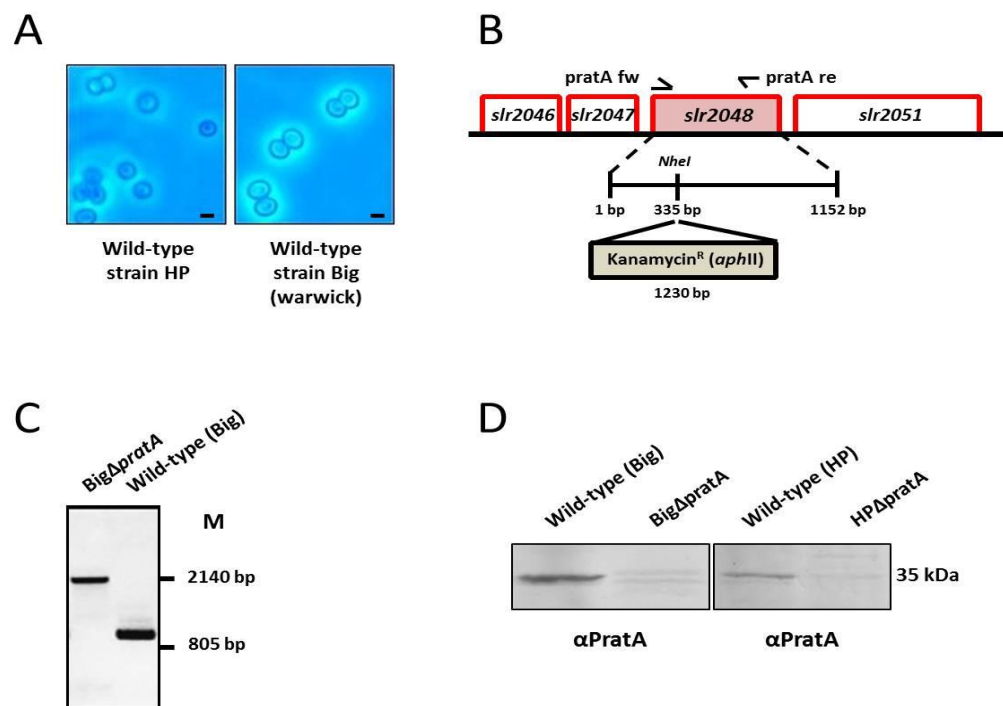
PratA (Slr2048) is a periplasmic protein in *Synechocystis* sp. PCC 6803 that has been shown, amongst others, to be involved in processing of pre-D1 protein of photosystem II to its mature form. Moreover, in the *pratA* knockout mutant it was shown that N-terminally eCFP-tagged D1 protein accumulation occurred in the plasma membrane or in its close proximity. In contrast, fluorescence in wild-type cells was detected primarily within the thylakoid membrane system (Schottkowski et al., 2008; Klinkert, 2004). The experiment confirmed the participation of PratA protein in pD1 processing. It also suggested an affected transfer of the D1 protein from its place of assembly into PSII at the plasma membrane or in its close proximity, to the place of function in the thylakoid membrane. The disadvantage of the comparison of wild-type and mutant was that only steady-state levels of eCFP-D1 were monitored. In order to also visualize the dynamic processes of membrane biogenesis *in vivo*, like the intracellular membrane flow by eCFP-D1, and in a time-resolved manner, an inducible *pratA* expression system was established.

### 4.2.1 Generating $\Delta$ *pratA* mutants

Light microscopes have a restricted resolution of approximately 0.2  $\mu\text{m}$ . To be able to discriminate subcellular compartments, the size of the investigated subject is of uttermost importance. In particular, in *Synechocystis* the thylakoid membranes arrange in circles that start very close to the plasma membrane, making discrimination difficult. Since the set up of this experiment was led out to finally follow the eCFP-D1 fusion protein by confocal laser scanning microscopy (CLSM) some changes to the preceding experiment were performed. To maximize the chance for a discrimination of plasma and thylakoid membrane in CLSM, *Synechocystis* sp. PCC 6803 wild-type strain Warwick (kind gift of Prof. Mullineaux) was used in subsequent experiments (herein after referred to as wild-type Big for easier distinction). The Big wild-type strain ( $\emptyset$  3  $\mu\text{m}$ ) is about one third bigger in size than the wild-type HP that had been used in the preliminary work (Schottkowski et al., 2008) (Figure 18A).

A construct was designed which should result in the disruption of the reading frame and generate knockout strains. First, the *pratA* (*slr2048*) gene was PCR amplified from wild-type genomic DNA and cloned into the pCR2.1 vector. In a second step, a kanamycin resistance gene ( $\text{Km}^{\text{R}}$ ) was ligated into the *NheI* site of pCR2.1\_ *pratA*, thereby adding *pratA* flanking regions to the  $\text{Km}^{\text{R}}$  gene. The assembled construct was then used for transformation into *Synechocystis* wild-type strain Big. The *pratA* flanking regions were necessary for the subsequent introduction

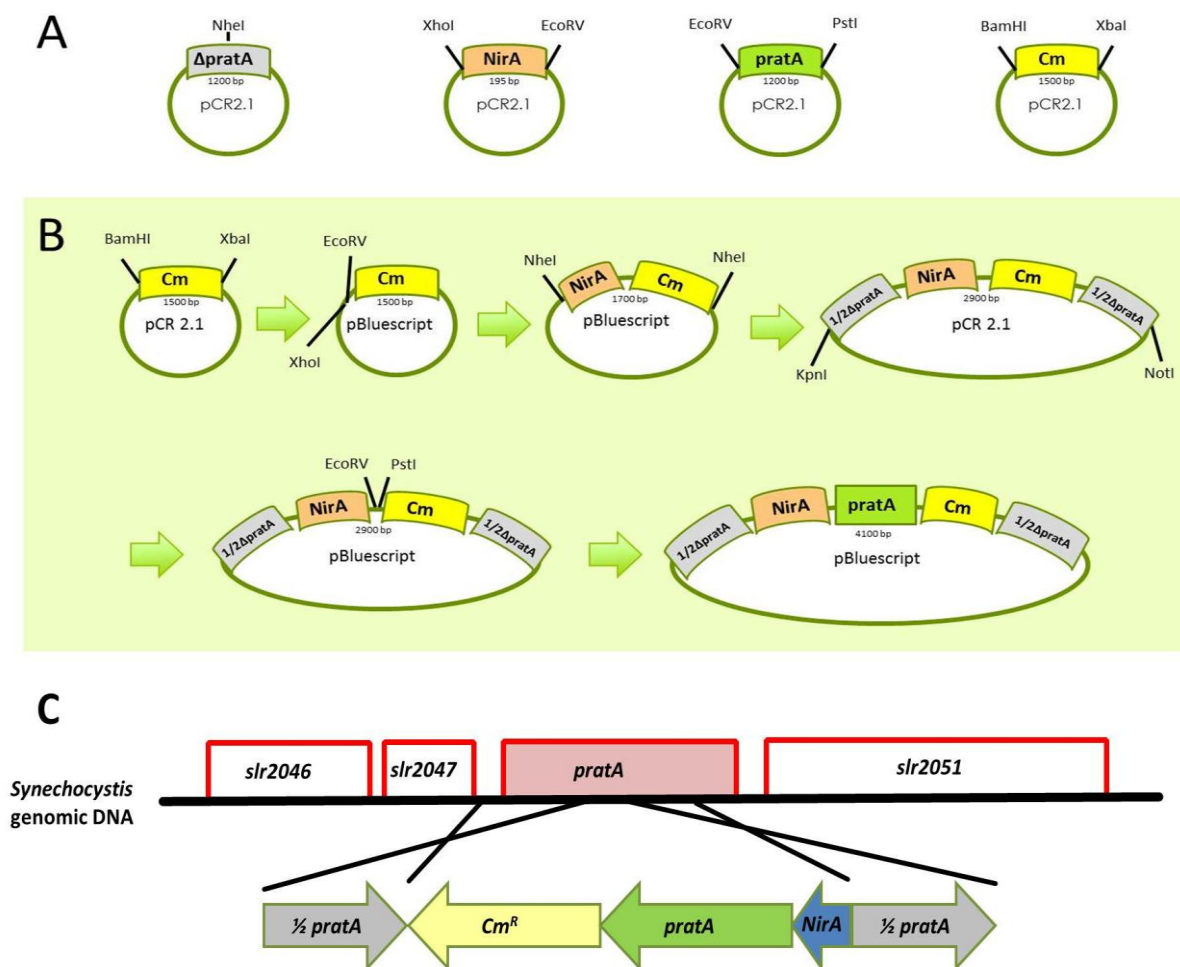
of the resistance cassette into the endogenous *slr2048* gene by homologous recombination (Zang et al., 2007) (Figure 18B). After two weeks of strong selection on plates supplemented with kanamycin, dozens of green colonies were obtained, which were not discriminable from wild-type cells (data not shown). In contrast to the *synTic22* gene, a complete knockout of the *prata* gene was possible. Genotyping was performed by PCR analysis using the primers *prata* fw and *prata* re (Figure 18B). This primer combination was expected to confirm the integration of the  $\text{Km}^{\text{R}}$  into the endogenous *prata* gene. Indeed, PCR analysis confirmed the integration of  $\text{Km}^{\text{R}}$ . Moreover, it showed that full segregation had occurred, since no wild-type *prata* gene was detectable anymore (Figure 18C, lanes 1 and 2). To determine the  $\Delta$ *prata* knockout on protein level crude soluble proteins of mutant and wild-type were fractionated by SDS-PAGE and blots probed with an antiserum against PrataA. No PrataA protein was detected in the mutant strains, confirming the complete knockout. Sometimes one or two faint bands appeared in immunoblots at a similar molecular weight as PrataA. Those bands can most likely be attributed to cross-reactions of the antiserum (Figure 18D, lanes 2 and 4). Taken together, a complete knockout of *prata* in *Synechocystis* strain Big was possible, which resulted in the  $\text{Big}\Delta$ *prata* strain.



**Figure 18: Introduction of a *prata* knockout in the wild-type Big strain.** (A) Comparison between sizes of *Synechocystis* sp. PCC 6803 wild-type strain HP and wild-type strain Big. The scale bar represents 2  $\mu\text{m}$ . (B) The *prata* locus on genomic DNA is illustrated. Neighboring genes are shown in upper red boxes (transcription 5' -3'). A kanamycin resistance gene was inserted into the *prata* locus (*slr2048*) by homologous recombination. The primers for genotyping and their corresponding binding sites are illustrated (arrowheads). (C) Genotyping of mutant and wild-type strain by PCR analysis. Primers *prata* fw and *prata* re were used. Expected size: 2110 bp in mutants, 880 bp in wild-type. M, DNA marker. (D)  $\text{Big}\Delta$ *prata* strain and wild-type Big strain as well as the HP $\Delta$ *prata* and wild-type HP strains used in preliminary work (Klinkert, 2004; Schottkowski et al., 2008) were compared by Western analysis. Crude soluble proteins were loaded (20  $\mu\text{g}$ ), fractionated by SDS-PAGE, and blots probed with antibody against PrataA.

#### 4.2.2 Design and assembly of a *nirA::pratA* inducible construct

In order to see differences in the distribution of the eCFP-D1 fusion protein similar to experiments, which had been performed with wild-type and knockout mutant strains (Schottkowski et al., 2008), a tight control of *pratA* gene expression was a prerequisite. For this purpose, the *nirA* promoter of the *nir* operon was chosen, which consists of several genes that are involved in nitrogen uptake in *Synechococcus* sp. strain PCC 7942 (Suzuki et al., 1993). The *nirA* promoter mediated gene expression is induced by nitrate ( $\text{NO}_3^-$ ) and tightly repressed by ammonium ( $\text{NH}_4^+$ ) in the growth medium, thus suitable for engineering of metabolic pathways in *Synechocystis* and other cyanobacteria (Desplancq et al., 2005; Qi et al., 2005).



**Figure 19: Assembly of a construct for the inducible expression of the *pratA* gene.** (A) Sequences for *pratA* gene, *pratA*-flanking regions, *NirA* promoter and the chloramphenicol resistance gene (Cm) were amplified by PCR and subcloned into pCR2.1 vectors. Restriction sites for further cloning steps were included within the primer sequences. (B) Summary of the inducible *pratA* construct cloning procedure. Restriction enzymes used for the next cloning step are indicated. Border fragments (grey) of the construct mediate homologous recombination into a specific site on the genomic DNA (here the *pratA* gene). (C) The *pratA* locus on genomic DNA is illustrated. Neighboring genes are shown in upper red boxes (transcription 5'-3'). Integration of the inducible cassette via *pratA*-flanking regions is indicated. A similar construct was established for homologous recombination of the inducible *pratA* gene into the *slr0415* gene by using *slr0415* instead of *pratA* flanking regions. bp= number of base pairs of insert.

Two strategies were followed for the introduction of the inducible *pratA* gene into the *Synechocystis* genome.

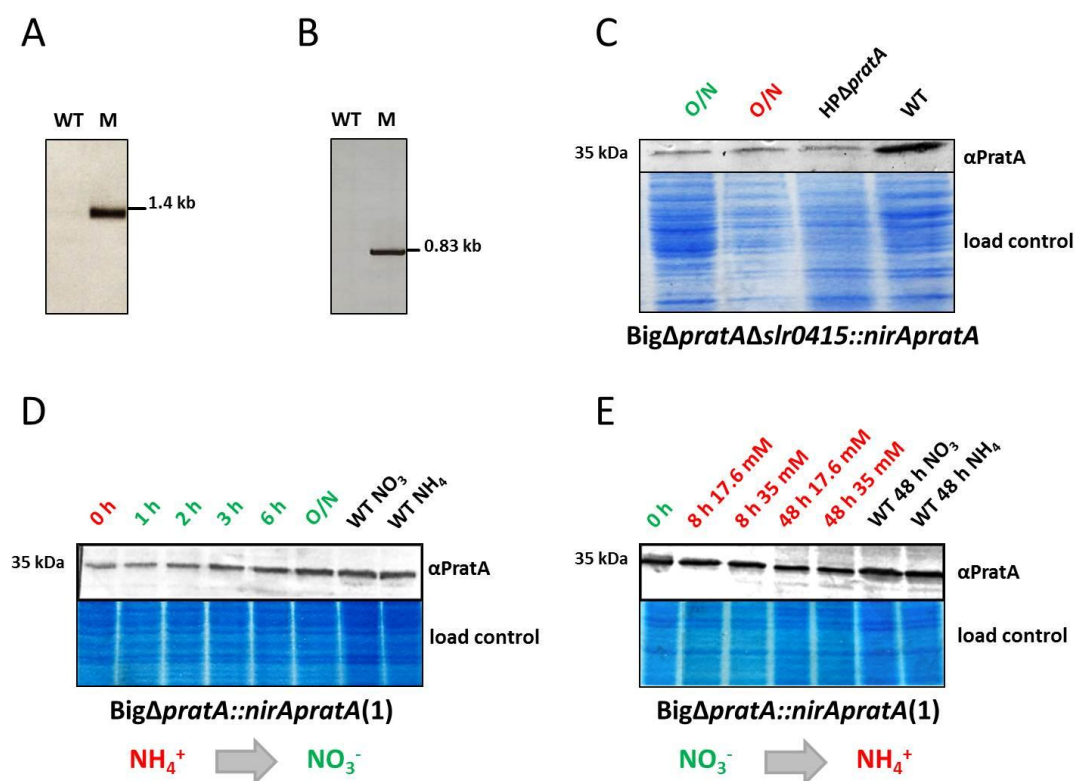
First, via substitution of the endogenous *pratA* gene by homologous recombination of the construct using *pratA*-flanking regions. The sequences for *pratA* gene and *pratA*-flanking regions were amplified by PCR from *Synechocystis* genomic DNA. The *nirA* promoter sequence and the chloramphenicol resistance gene ( $\text{Cm}^{\text{R}}$ ) were amplified from *Synechococcus* sp. PCC 7942 genomic DNA and pVZ321 vector, respectively. All fragments were subcloned into pCR2.1 and sequence accuracy was confirmed by sequencing (Figure 19A). The final inducible construct was assembled in a complex cloning procedure (Figure 19B). During the cloning procedure, the transfer of the *NheI* cut Nir\_Cm fragment into the cut pCR2.1\_Δ*pratA* vector could finally lead to transcription of the construct in the same or opposite direction of the targeted gene (Figure 19B). PCR analysis with specific primers showed that in the construct used for transformation, the transcription would be in opposite direction of the target gene (Figure 19C).

In a second approach, *slr0415* flanking regions were used for homologous recombination of the inducible construct into the *slr0415* gene, thereby creating a knockout of the *nhaS5* (*slr0415*) gene. This was done, because there is little space between genes in *Synechocystis* for homologous recombination. The gene encodes for one of five putative  $\text{Na}^+/\text{H}^+$  antiporters in *Synechocystis*. Although the *nhaS5* gene is expressed, a knockout has most likely no influence on the cells under the conditions used and was thus regarded as a silent site (Elanskaya et al., 2002). Both constructs were checked for correct assembly by PCR analysis (data not shown). Subsequently, the construct for homologous recombination into *pratA* was transformed into *Synechocystis* wild-type Big. In contrast, the construct for homologous recombination into *slr0415* was transformed into the BigΔ*pratA* knockout strain in order to have no endogenous Prata background. After two weeks of strong selection on plates supplemented with chloramphenicol, dozens of green colonies were obtained, which were not discriminable from wild-type cells (data not shown). This suggested that the integration of the inducible construct into the *slr0415* site did not cause any obviously toxic effects.

Taken together, two *pratA* inducible constructs have been assembled, verified and transformed into *Synechocystis* Big and BigΔ*pratA* stains resulting in the BigΔ*pratA*::*nirAprata(1)* and BigΔ*pratA*Δ*slr0415*::*nirAprata* mutant strains, respectively.

### 4.2.3 The *nirA::prata* construct can be used for time-resolved studies of PrataA protein expression

In a next step, the functionality of the *nirA* inducible systems of both strains had to be established. First, site-specific homologous recombination into the target genes was confirmed for both constructs by PCR analysis using isolated total DNA (Figure 20A and B). Cultures of transgenic strains were then grown under inducing ( $\text{NO}_3^-$ ) and repressing ( $\text{NH}_4^+$ ) conditions in BG11<sub>0</sub> medium. At certain time points, samples were taken and after centrifugation frozen in liquid nitrogen. After all samples from different time points had been collected,



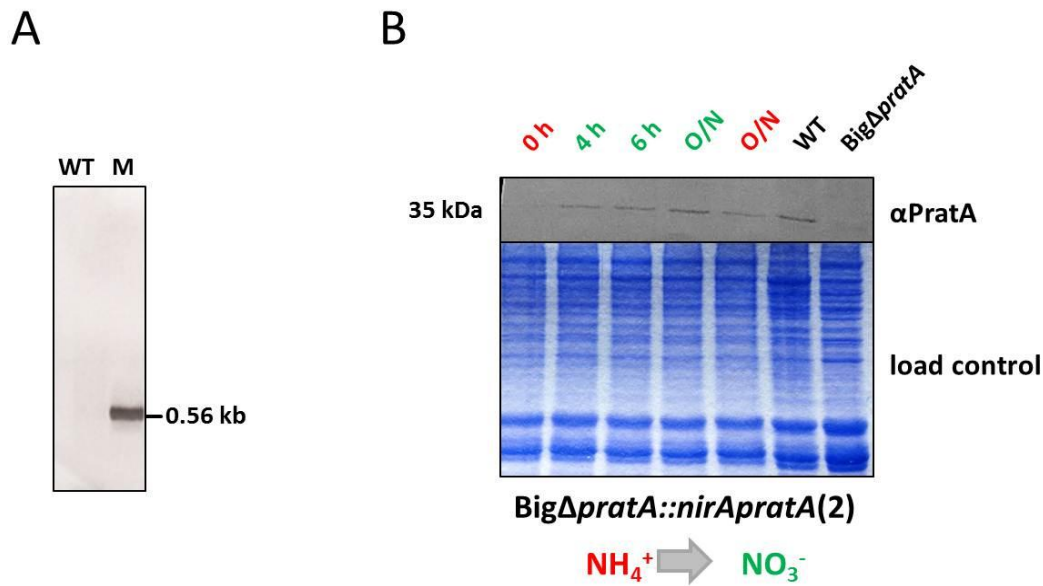
**Figure 20: NirA promoter controlled expression of *prataA*.** (A) Genotyping of *BigΔprataΔslr0415::nirAprata* (M) and wild-type Big strain (WT) by PCR analysis. Primers Slr0415 fw and PrataA re were used. Expected size: 1452 bp in mutant, no signal in wild-type. DNA marker is shown at the right. (B) Genotyping of *BigΔprata::nirAprata(1)* (M) and wild-type Big strain (WT) by PCR analysis. Primers NirA re and PrataA re were used. Expected size: 791 bp in mutant, no signal in wild-type. (C) Cultures of *Synechocystis* wild-type Big and *BigΔprataΔslr0415::nirAprata* strains were grown in BG11<sub>0</sub> medium supplemented with 17.6 mM NaNO<sub>3</sub> (O/N green) or NH<sub>4</sub>Cl (O/N red) and incubated overnight. Crude soluble proteins (20 μg) were fractionated by SDS-PAGE, and blots probed with antiserum against PrataA. (D) **Activation NH<sub>4</sub><sup>+</sup> to NO<sub>3</sub><sup>-</sup>.** Cultures of *Synechocystis* wild-type Big and *BigΔprata::nirAprata(1)* strains were grown in BG11<sub>0</sub> medium supplemented with 17.6 mM NH<sub>4</sub>Cl to OD<sub>730</sub> of 0.8-1 (0 h, red), washed and resuspended in BG11<sub>0</sub> supplemented with 17.6 mM NaNO<sub>3</sub> (green). Samples were taken at the time points indicated. The wild-type (WT) was incubated overnight either with NH<sub>4</sub>Cl or NaNO<sub>3</sub>. Crude soluble proteins (20 μg) were extracted, fractionated by SDS-PAGE, and probed with antiserum against PrataA. (E) **Inhibition NO<sub>3</sub><sup>-</sup> to NH<sub>4</sub><sup>+</sup>.** Cultures of wild-type Big (WT) and *BigΔprata::nirAprata(1)* strains were grown in BG11<sub>0</sub> medium supplemented with 17.6 mM NaNO<sub>3</sub> to OD<sub>730</sub> of 0.8-1 (0 h, green), washed and resuspended in BG11<sub>0</sub> supplemented with 17.6 or 35 mM NH<sub>4</sub>Cl (red). Samples were taken at the time points indicated and treated as in (D).



crude soluble proteins were extracted, fractionated by SDS-PAGE and accumulation of PrataA protein subsequently examined by Western analysis. Figure 20C shows the result of a representative *BigΔprataΔslr0415::nirAprata* strain. Cells treated with NaNO<sub>3</sub> did not accumulate PrataA when compared to wild-type (Figure 20C, lanes 1 and 2). Similar to the NH<sub>4</sub>Cl treated cells and the HPΔ*prata* knockout strain, only the cross-reacting signal of the PrataA antiserum was observed (Figure 20C, lanes 1, 2 and 3). In all strains of *BigΔprataΔslr0415::nirAprata* that had been tested, no accumulation of PrataA protein was detectable (data not shown). This indicated that the construct was not functional in these strains, although the correct assembly and integration had been confirmed.

In contrast, when *BigΔprata::nirAprata(1)* strain had been grown under inhibiting conditions (NH<sub>4</sub>Cl) and was then induced for several hours (NaNO<sub>3</sub>), a significant protein accumulation up to wild-type levels was achieved (Figure 20D, compare lane 1 and 7). Accumulation of PrataA was discernible from two hours after induction by nitrate (Figure 20D, compare lane 1 and 3). Taken together, these findings suggested that the *nirA* promoter could indeed induce PrataA expression, but did not cause overexpression.

As mentioned before, the tight repression of the *prata* gene would be crucial for visualization of the dynamic processes of membrane biogenesis *in vivo*, especially in a time-resolved manner. Instead, PrataA was detectable even under repressing conditions (Figure 20D, lane 1). Although not at wild-type level, the remaining PrataA molecules could severely interfere with the experiment. For this reason, additional experiments were performed that varied in the concentration of ammonium chloride used to repress the promoter (data not shown). Since PrataA was detectable regardless of the ammonium concentration used, a different approach was performed. It was assumed, that growth of the culture under inhibiting conditions for several days could somehow have caused a reactivation of the *nirA* regulated *prata* gene expression. Therefore, the *BigΔprata::nirAprata(1)* strain had been grown under inducing conditions and was then inhibited for several hours (Figure 20E). After 8 hours of repression, a slight reduction of PrataA protein level was observed (Figure 20E, lane 2), which was even more pronounced after 48 hours (Figure 20E, lane 4). Nevertheless, even by doubling the ammonium concentration to 35 mM for a short period, PrataA protein was still detectable (Figure 20E, lane 3 and 5).



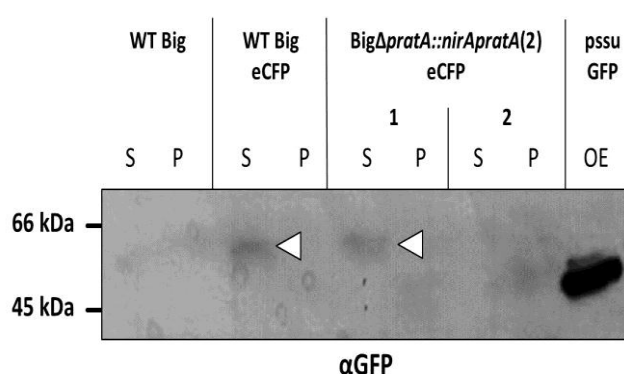
**Figure 21: *NirA* promoter controlled expression of *pratA* in *BigΔpratA* background.** (A) Genotyping of *BigΔpratA::nirApratA(2)* (M) and wild-type *Big* strain (WT) by PCR analysis. Primers *NirA* fw and *PratA* re were used. Expected size: 568 bp in mutant, no signal in wild-type. (B) Cultures of *Synechocystis* wild-type and *BigΔpratA::nirApratA(2)* strains were grown in BG11<sub>0</sub> medium supplemented with 17.6 mM NH<sub>4</sub>Cl to OD<sub>730</sub> of 0.8-1 (0 h red), washed and resuspended in BG11<sub>0</sub> supplemented with 17.6 mM NaNO<sub>3</sub> (green). Samples were taken at the time points indicated. After 24 h cells were washed again, resuspended in BG11<sub>0</sub> supplemented with 17.6 mM NH<sub>4</sub>Cl and incubated overnight (O/N red). Soluble proteins (15 μg) were subjected to SDS-PAGE, and blots probed with an antiserum against *PratA*.

The problem was finally solved by using the *pBS\_ΔpratA::nirApratA* construct that had previously been transformed into WT *Big*, for transformation into the *BigΔpratA* knockout strain. It was not clear whether homologous recombination into the *pratA* gene would work because it already contained the kanamycin resistance gene that had been used to create the knockout. However, after transformation dozens of colonies of *BigΔpratA::nirApratA(2)* strain were obtained. PCR analysis confirmed the integration of the inducible construct into the genomic DNA (Figure 21A). Further analysis suggested that in the new inducible strains, no *PratA* protein was present when cultures had been grown under repressing conditions (Figure 21B, lane 1). After changing to inducing conditions, protein accumulation was observed after 30 min (data not shown) with a maximum after overnight incubation (Figure 21B, lanes 2, 3 and 4). The *PratA* concentration could even be reduced again by changing to repressing conditions again, although some *PratA* protein was still available (Figure 21B, lane 5). A reason could be that the *PratA* stability is too high for the residual protein to have vanished completely after 12 hours.

Taken together, the *nirA* controlled expression of the *pratA* gene is functional and can be used in further experiments with the extrachromosomally expressed eCFP-D1 to follow membrane flow *in vivo*.

#### 4.2.4 Analysis of extra-chromosomal expression of N-terminal tagged eCFP::D1

For expression of the N-terminally labeled eCFP-D1 protein the pVZ322-*Nt-eCFP-D1* vector, which had been used in a previous work (Schottkowski et al., 2008), was conjugated into wild-type strain Big, Big $\Delta$ *prataA* and the inducible Big $\Delta$ *prataA::nirAprataA(2)* strains. The strains obtained after growth on selection plates were examined for eCFP fluorescence in confocal laser scanning microscopy (CLSM). No unambiguous eCFP signal was detectable in any of the strains tested (>30). This was surprising, since the construct is under control of the light induced, strong promoter of the *psbA2* gene and had been used before (Schottkowski et al., 2008). In order to test expression of eCFP-D1 on protein level, soluble and membrane protein fraction was isolated from wild-type and conjugated strains, separated by SDS-PAGE, and checked by Western analysis using a GFP specific antiserum. Whereas the recombinant pssu-GFP control was clearly detected by the antiserum (Figure 22, lane 9), only weak signals at about 62.9 kDa that could represent the eCFP-D1 fusion protein were observed in some of the conjugated strains tested (Figure 22, lanes 3 and 5). No signal was detected in the wild-type control (Figure 22, lanes 1 and 2) suggesting that the weak signals indeed represented a eCFP-fusion protein. Surprisingly though, the signals were observed in the soluble protein fraction, whereas the D1 protein was expected to be membrane localized. Higher light conditions to induce the *psbA2* promoter did not result in a stronger expression and when the concentration of antibiotic was increased, the cells finally died.

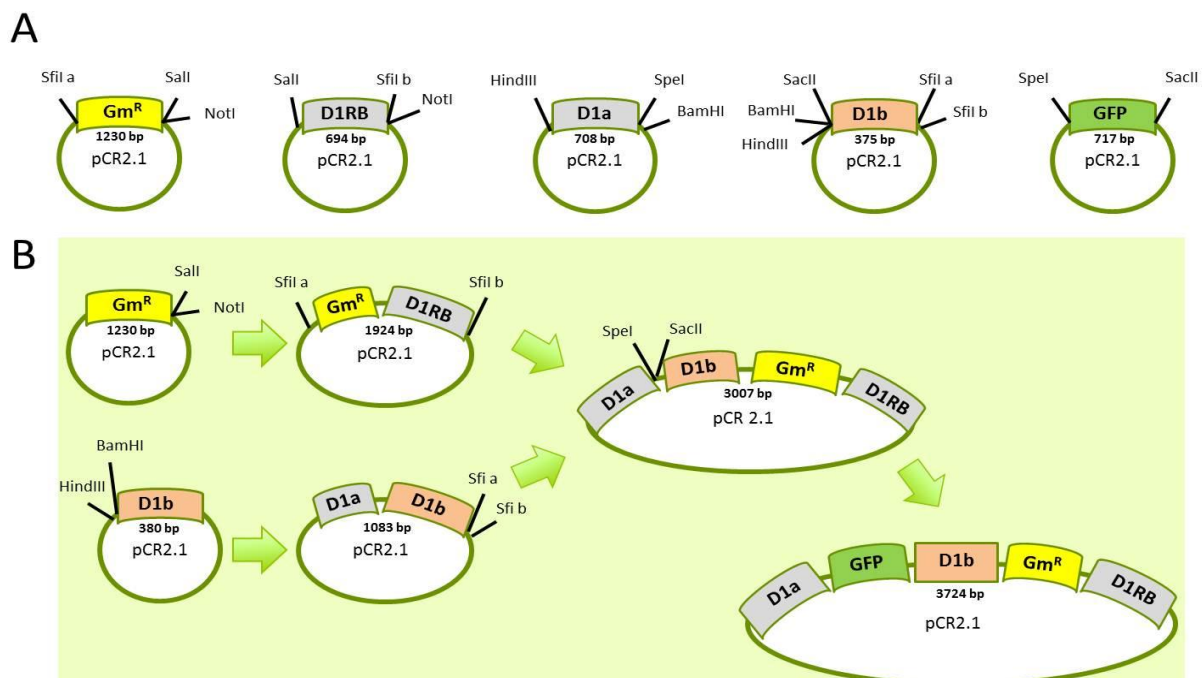


**Figure 22: Test of pVZ322-*Nt-eCFP::D1* transformants for expression of eCFP-D1.** Cultures of wild-type strain Big and Big $\Delta$ *prataA::nirAprataA(2)* were conjugated with the pVZ322-*Nt-eCFP-D1* extrachromosomal vector (Schottkowski et al., 2008). Crude soluble (S) and membrane proteins (P) were extracted, applied to SDS-PAGE (40  $\mu$ g), and blots probed with an antiserum raised against GFP. Putative eCFP-D1 signals are indicated by white arrowheads (62.9 kDa expected). As negative control, soluble and membrane proteins (40  $\mu$ g each) of a non-conjugated wild-type strain Big was used. As positive control, GFP labeled small subunit of rubisco was used (5  $\mu$ g; 48.9 kDa expected).

#### 4.2.5 Generating stable double mutants of

##### *Big* $\Delta$ *prataA::nirAprataA(2)// $\Delta$ *D1::GFP-D1**

To circumvent unintended homologous recombination or loss of the extrachromosomal D1 expressing pVZ322 vector, a construct was designed for stable integration of an internal GFP tagged *D1* gene into the endogenous *D1* gene. The sequences for the N-terminal part of D1 (D1a), which additionally functions as left border in homologous recombination and the C-terminal part of D1 (D1b) were amplified by PCR from *Synechocystis* genomic DNA and chosen for insertion of GFP between amino acid 236 and 237. The right border sequence for homologous recombination (D1RB) was comprised of the D1b sequence plus 320 bp downstream of the D1 gene and was also amplified by PCR. The *GFP* gene sequence and the gentamycin resistance gene (*Gm<sup>R</sup>*) were amplified from pBAD-GFP (promoterless) and pVZ322 vector, respectively. All fragments were subcloned into pCR2.1 and sequence accuracy was confirmed by sequencing (Figure 23A). Afterwards the construct was assembled as depicted in Figure 23B. Correct assembly was again checked by PCR analysis and sequencing and the construct subsequently used for transformation of wild-type strain *Big*, *Big* $\Delta$ *prataA* and *Big* $\Delta$ *prataA::nirAprataA(2)*. Transformants of *Big::D1-GFP*, *Big* $\Delta$ *prataA::D1-GFP* and *Big* $\Delta$ *prataA::nirAprataA(2)::D1-GFP* will be tested for expression, membrane integration and fluorescence of D1-GFP in future experiments.



**Figure 23: Assembly of a construct for stable expression of D1-GFP.** (A) Sequences for *D1a*, *D1b*, *D1RB*, *GFP* and *Gm<sup>R</sup>* were amplified by PCR and subcloned into pCR2.1 vectors. Restriction sites for further cloning steps were included within the primer sequences. (B) Summary of the internal GFP-D1 cloning procedure. Restriction enzymes used for the next cloning step are indicated. Border fragments (grey) of the construct mediate homologous recombination into a specific-site on the genomic DNA (here the *D1* gene).

## 5 Discussion

### 5.1 The $\Delta$ *synTic22* strain

Today, reverse genetic is an essential tool of modern biology. Instead of analyzing the genetic reason for a certain phenotype, a specific gene is affected by mutagenesis (Reski, 1998). Thereby, it is avoided that the phenotype is caused by more than a single factor. *Synechocystis* is an extraordinarily useful model organism in this respect. It is naturally competent for transformation and even more important it allows site-specific integration of foreign DNA by mechanism of homologous recombination (Zang et al., 2007).

To functionally characterize *SynTic22*, a kanamycin resistance gene was inserted into the gene locus. Different environmental conditions were used in an attempt to obtain completely segregated knockout strains. Those attempts failed, underlining the essentialness of the protein for cell survival, that has been reported for *Synechocystis* and other cyanobacteria (Fulda et al., 2002; Tripp et al., 2012). A previous work reported a reduction in *SynTic22* protein content to only 20 % of wild-type level in merodiploid strains (Fulda et al., 2002). Similar results have been obtained for the attempted knockout of *Tic22* in the multicellular, filamentous cyanobacterium *Anabaena* sp. PCC 7120 (Tripp et al., 2012). Interestingly, a reduction in gene dosage was not detected in the merodiploid strains that were created in this work (Figure 9), even though a similar knockout construct and the same resistance gene were used. Moreover, the reported loss of glucose tolerance in the merodiploid strains, which eventually led to cell death after a few days (Fulda et al., 2002), was also not observed. Generally, the discrepancy might have been due to differences in the growth conditions used, especially because *SynTic22* protein content was shown to be regulated by irradiance levels and the addition of glucose (Fulda et al., 2002). The protein amount was found to increase with higher irradiance and glucose levels (Fulda et al., 2002). However, the glucose concentration we used in our approach was the same (0.1 %). Furthermore, the irradiance level used to grow cultures in the present work was  $47 \mu\text{mol photons m}^{-2} \text{s}^{-1}$  compared to  $60 \mu\text{mol photons m}^{-2} \text{s}^{-1}$  used by Fulda. Therefore, even less *SynTic22* protein would have been expected. Ultimately, differences in the laboratory strains of *Synechocystis* sp. PCC 6803 that were used could account for the observed differences in *SynTic22* expression levels.

### 5.2 Localization of *SynTic22*

Knowledge about the cellular localization of a protein provides important information about the functional processes it might be involved in. In *Pisum sativum*, *Tic22* is involved in the general

import pathway that translocates nuclear encoded preproteins into the chloroplast. Therefore, the protein is exclusively localized in the intermembrane space of chloroplasts, peripherally associated to the inner envelope membrane (Kouranov et al., 1998). Parallels in localization were found for *Plasmodium falciparum* apicoplasts where Tic22 was shown to be an insoluble membrane-associated protein (Kalanon et al., 2009). In contrast to those data, *Synechocystis* Tic22 was reported to be mainly localized as a soluble protein within the thylakoid lumen and to a lower extent within the periplasm (Fulda et al., 2002). It has been suggested that Tic22 of cyanobacteria, the progenitors of today's chloroplasts, might still possess a dual function, whereas Tic22 function in chloroplast thylakoids is supposed to have lost or replaced by other proteins (Fulda et al., 2002). Because the reported SynTic22 localization did not resemble the localization of other organisms, it was a major goal in the present work to answer the question if SynTic22 is localized in both compartments or not and if it could be involved in membrane biogenesis processes.

Present data highly favor direct connections between plasma and thylakoid membranes in *Synechocystis* even though those might occur transiently (Pisareva et al., 2011). Therefore, it is crucial to consider the fractionation method used for the interpretation of localization results. In the present work, sucrose gradient centrifugation was used that is supposed to separate membranes according to their density (Peschek et al., 2004). Separation results in a low-density membrane fraction (at the border of 10 % and 30 % (w/v) sucrose) which has been suggested to represent those minor parts of the plasma membrane (PM) that are in direct contact with the thylakoid membrane (Pisareva et al., 2011). The majority of plasma membranes (PM2) and thylakoid membranes have the same, higher density thus accumulate at the bottom of the sucrose gradient (at the border of 39 % and 50 % (w/v) sucrose). Two-phase partitioning separates membranes according to surface properties and needs to be applied to get pure PM2 and thylakoid membranes (Norling et al., 1998). Notice that two-phase partitioning was not used in this work, thus a mixture of thylakoid membranes (TMs) with PM2 had to be considered. Consistently, NrtA, a plasma membrane protein was detected within the TM fraction (Figure 8). In addition to its occurrence in TM, low amounts of the thylakoid membrane marker protein D1 were also found in the plasma membrane fraction (PM). This is in agreement with the hypothesis that photosystem II biogenesis starts within the plasma membrane (Zak, 2001). Interestingly, YCF48 was also found in the PM fraction of the gradient (Figure 8), which is consistent with available proteomics data (Pisareva et al., 2011). YCF48 is a PSII biogenesis factor in cyanobacteria and chloroplasts that is supposed to be a luminal protein, which transiently interacts with PSII subunits during the assembly process (Meurer et al., 1998;

Komenda et al., 2008). Localization of YCF48 in PM supports both that PSII assembly already starts within the plasma membrane and that this gradient fraction represents putative PM–TM contact sites (Pisareva et al., 2011). Because YCF48 and other PSII factors are part of the PM fraction (Pisareva et al., 2011) it is tempting to speculate that it might represent some sort of counterpart to the recently identified PrtA-defined membranes (PDM) subfraction (Schottkowski et al., 2008; Rengstl et al., 2011).

Antiserum against SynTic22 showed an exclusive localization within the periplasm (Figure 8), thus a further distinction of TM from PM2 by means of two-phase partitioning was unnecessary. A previous work has indicated that disruption of *Synechocystis* cells using a French-press leads to a higher portion of inside-out membrane vesicles whereas using glass-beads leads to a majority of right-side out vesicles (Zak et al., 1999). Because of the large culture volumes used in this work, the French-press method was chosen for cell disruption. Therefore, the TM fraction of the sucrose gradient was expected to be composed of more inside-out vesicles (might not contain SynTic22) than right-side out vesicles (should contain SynTic22). Thus, it cannot be excluded that some of the soluble SynTic22 protein was lost into the sucrose gradient after cell disruption. Nevertheless, since not all vesicles are inside-out (Zak et al., 1999) and the majority of SynTic22 was reported to be luminal (Fulda et al., 2002), a signal should have been detected in case of a luminal localization of the protein. YCF48 was supposed to be a marker protein for thylakoid luminal proteins. Since it was detected in PM but not in the periplasm a rather stable than transient attachment to the membrane can be assumed (Figure 8), thus it cannot be used as a control for the existence of luminal proteins. However, data obtained from an endogenous SynTic22-His expressing strain ( $\Delta$ SynTic22::*synTic22-His*) also argues against a localization of SynTic22 within the thylakoid lumen. Periplasm was isolated by cold osmotic shock and the remaining spheroplasts were disrupted using the French-press, followed by sonication. After centrifugation, the membrane fraction was solubilized by detergents and together with the other fractions applied to metal affinity chromatography. SynTic22-His was only observed in stained SDS gels loaded with periplasmic samples but not within any other cell fraction. Data from *Anabaena* sp. PCC 7120 support a dual localization where the majority of AnaTic22 was reported to reside in or associate to the cell wall within the periplasm (Tripp et al., 2012). Taken together I conclude that most of SynTic22 is localized in the periplasm.

PCR analysis on genomic DNA of  $\Delta$ SynTic22::*synTic22-His* strain confirmed that the endogenous *synTic22* gene was completely exchanged by the tagged form (Figure 10). Because SynTic22 is essential for cell survival, this is only possible if the C-terminal His<sub>6</sub>-tag is not interfering with the proteins function. It may, however, interfere with the sorting of the protein.

SynTic22 has a predicted N-terminal Sec signal sequence (PRET-TAT; Bagos et al. 2010). Sec translocon subunits have been shown to be present in the plasma and thylakoid membrane (Nakai et al., 1993). Only an interference of the His<sub>6</sub>-tag with sorting of SynTic22 via the Sec pathway into the thylakoid lumen but not into the periplasm could explain the missing protein. How proteins are sorted in *Synechocystis* is still an unsolved question, thus it is not clear how that could have happened. In any case, it would suggest that only the periplasmic but not the luminal function of SynTic22 is essential for cell survival.

The TM sucrose gradient fraction contains the recently characterized PDM subfraction that was shown to be involved in a PSII biogenesis assembly network (Schottkowski et al., 2008; Rengstl et al., 2011; Nickelsen et al., 2011). SynTic22 was not found in Western analysis of the TM samples. Furthermore, SynTic22 was also not found within the PM that is supposed to be in direct contact with thylakoid membranes and were YCF48 and D1 (Figure 8) and other photosystem II subunits were localized (Pisareva et al., 2011). Thus, an involvement in PM and TM biogenesis processes is unlikely, at least for photosystem II. As a periplasmic protein, SynTic22 could still be involved in outer membrane biogenesis processes. Indeed, this was reported for *Anabaena* Tic22 where a direct interaction was demonstrated with the outer membrane biogenesis protein Omp85 (Tripp et al., 2012).

### 5.3 Initial screen for interaction partners of SynTic22

Data presented in this work has supported the finding that SynTic22 is an essential protein (Figure 9) (Fulda et al., 2002). Since no knockout or knockdown strain was available, efforts were focused on identification of putative interaction partners to characterize SynTic22 protein function. A first indication for a putative interaction partner was obtained from the overexpression of the recombinant protein in *E. coli*, when after purification via Nickel-sepharose matrix a second band at about 23 kDa appeared (Figure 7). Mass spectrometric analysis identified the lower protein band to be the *E. coli* cAMP receptor protein (CRP). Control experiments suggested that the co-purification was not due to unspecific binding to the column (data not shown). Instead, several lines of evidence indicate a direct and strong interaction of both proteins. No separation was achieved using high salt conditions in IEX chromatography even though the isoelectric points of both proteins were predicted to be rather different (Figure 7). In addition, HIC chromatography, which uses different chemical properties for separation of proteins as IEX, was also not successful (data not shown). Hydrogen bonds as well as ionic interactions should have been dramatically destabilized or broken by the high salt concentrations that were applied in those experiments. As this was not observed, a participation of mainly hydrophobic interactions in the binding of SynTic22 with cAMP receptor protein



could be assumed. In parallel, the highest amino acid conservation between Tic22 sequences of nine cyanobacteria strains was found between residues of mainly hydrophobic character like proline, alanine, valine, phenylalanine and isoleucine (Figure 3). Even though the general homology is decreasing from cyanobacteria to higher plants, some of these amino acids were even conserved in *Pisum sativum* and *Arabidopsis thaliana*, underlining a possible importance of those residues for protein-protein interaction. Very recently, the first crystal structure of a Tic22 family member, the *Anabaena* sp. PCC 7120 Tic22 protein, was published (Tripp et al., 2012). Interestingly, the authors could show that the surface of the AnaTic22 displays several functionally important hydrophobic sites (Tripp et al., 2012). The arrangement of those sites resembles substrate binding sites of chaperones like SecB and SurA in *E. coli*, therefore they were proposed to be important for AnaTic22 function. Indeed, the authors could show that a mutation in one of the hydrophobic pockets resulted in a phenotype similar to that of the AnaTic22 knockdown mutant (Tripp et al., 2012).

Even though several relatives with high similarity to the *E. coli* CRP protein exist in *Synechocystis*, none of them was identified in the pull-down experiments. Therefore, the strong interaction that had been observed was rather likely to be of artificial character.

Several proteins identified in the pull-down experiments are supposed to have a common function in chemotaxis, PilT1, PilT2, CheY and McpA (Table 10 and Table 11). *Synechocystis* and other gram-negative bacteria use type IV pili for locomotion in a form called twitching mobility (Henrichsen, 1983). The process of type IV pili assembly in the periplasm involves more than twelve different proteins, which are located in the periplasm, the outer side of the plasma membrane, and the inner side of the outer membrane (Dalbey and Kuhn, 2012). PilB and PilT have been shown to be plasma membrane ATPases that function in the fast polymerization and depolymerization of the pilus, respectively (Jakovljevic et al., 2008; Dalbey and Kuhn, 2012). PilT is the only type IV pili protein that is not involved in extension of the pilus but only in its retraction. *Synechocystis* encodes two proteins similar to PilT of *E. coli*, PilT1 (Slr0161) and PilT2 (Sll1533). The precise mode of function and especially their regulation has so far not been determined (Yoshihara, 2002). In this work, both proteins were identified as possible interaction partners of endogenously expressed SynTic22-His (Table 11), strengthening the significance of the pull-down result. In addition, the molecular weight of PilT1 (40 kDa) or PilT2 (47.9 kDa) in a complex with SynTic22 would nicely fit to the signals of possible higher molecular weight complexes detected in the BN-PAGE (Figure 11). *Synechocystis*  $\Delta pilT1$  mutants were shown to be non-motile and hyperpiliated with a drastically increase in thick pili that were distributed about the entire cell surface (Bhaya et al., 2000). Interestingly, the outer

surface of  $\Delta pilT1$  cells seemed to be less smooth than that of the wild-type strain, probably caused by the changes in pili morphology. Similarly, a Tic22 knockdown strain in *Anabaena* sp. PCC 7120 was recently found to have an altered outer membrane morphology (Tripp et al., 2012). The rippled phenotype was associated with a function of the AnaTic22 in outer membrane biogenesis (Tripp et al., 2012). Nevertheless, a staining method was used for transmission electron microscopy that focused on staining of the outer membrane structure but not on staining of pili structures. Because no pili structures were visible, the changes in outer membrane morphology could have also been caused by differences in pili morphology. Defects in pili subunits or assembly factors usually result in non-motile cells but not in a lethal phenotype (Bhaya et al., 2000; Yoshimura, 2002). If SynTic22 is involved in pili assembly processes there are at least two explanations why it is essential for cell survival. First, it could have an unknown second function, as has been proposed for most of the TIC subunits (Gross and Bhattacharya, 2009; Chan et al., 2011). It is also thinkable that the outer membrane phenotype observed in AnaTic22 knockdown cells is just a primary, still viable stage. The complete disruption of the gene could possibly result in a further loss of membrane integrity that is lethal in the end. This hypothesis is supported by the fact that *E. coli* cells without outer membrane are not viable (Silhavy et al., 2010).

Interestingly, two further proteins were identified in the pull-down experiments that support an association of SynTic22 with pili, Slr1044 (McpA, also known as PilJ) and Slr2024 (CheY) (Table 11). Both are components of a MCP/CheA/CheY system, which constitutes a major signaling pathway for bacterial chemotaxis (Yoshihara, 2002). In *E. coli*, the system is used to switch flagella rotation from counter to clockwise rotation. If no attractant is bound to the methyl-accepting chemotaxis protein (Mcp) the soluble CheA kinase autophosphorylates. CheA-P then donates its phosphoryl group to CheY. CheY-P is then regulating the rotor (Parkinson, 2003). This suggests that the soluble Slr2024 (CheY) might not have been just a cytosolic contamination but rather a component of a pili regulatory complex.

Another possible interaction partner was identified as Sll1951 (HlyA) (Table 11). Outer membranes (OM) consist of a phospholipid monolayer and an outermost leaflet that contains either almost all lipopolysaccharides (LPS) of the envelope (Filip et al., 1973; Osborn et al., 1972) or a protein surface layer (S-layer) or both (Sakiyama et al., 2011). S-layers cover the whole cell surface and are usually composed of only a single protein (Sakiyama et al., 2011). The hemolysin-like protein A (HlyA) of *Synechocystis* has been shown to be an S-layer protein that serves as a barrier to protect cells from osmotic stress and from adsorption of toxic compounds like antibiotics and heavy metals (Sakiyama et al., 2011). If SynTic22 is involved in

transport processes, as a periplasmic protein, it could assist in transport of HlyA from the plasma membrane to the outer membrane. A function in this respect is especially thinkable because the surface of AnaTic22 has been shown to resemble the substrate binding site of the chaperone SurA (Tripp et al., 2012), which has been implicated in transport of outer membrane proteins to their destination (Dalbey and Kuhn, 2012). Moreover, it could also explain the outer membrane phenotype of the AnaTic22 knockdown mutant (Tripp et al., 2012), because the S-layer has been proposed to resemble some sort of exoskeleton necessary for maintaining the cell shape (Engelhardt, 2007). Unfortunately, Sakiyama (2011) failed at taking electron microscopic pictures of outer membranes in  $\Delta hlyA$  mutants. Therefore, a phenotypic comparison with the outer membranes of AnaTic22 knockdown cells is not possible. Besides an interaction between both proteins in the periplasm, there is also the possibility for an interaction outside of the cell, because SynTic22 was one of the proteins that were identified in exudates of *Synechocystis* (Sergeyenko and Los, 2000).

In this work, Slr0114 was found to be a putative SynTic22 interaction partner in three different pull-down experiments (Figure 10 and Figure 11). It is one of eight genes in *Synechocystis* that have been suggested to encode for prospective members of the  $Mg^{2+}/Mn^{2+}$ -dependent PP2C family of phosphatases (Irmeler, 2001). The most intensively studied member is the *slr1771* product PhpA, which has been shown to dephosphorylate  $P_{II}$ , a key regulator that plays a central role in nitrogen metabolism (Irmeler, 2001; Osanai and Tanaka, 2007). The physiological substrate and function of Slr0114 is not known but it was demonstrated not to be important for  $P_{II}$  dephosphorylation (Irmeler, 2001). The precise subcellular localization of Slr0114 is also not known. In general, periplasmic phosphatases exist in cyanobacteria like PhoA, an alkaline phosphatase in *Synechococcus* sp. PC7924 (Ray et al., 1991). However, Slr0114 is unlikely to be a periplasmic or luminal protein, since it has no predicted Sec or Tat signal sequence. In contrast, it could be a membrane protein because it possesses several predicted transmembrane domains. Phosphorylation and dephosphorylation of proteins plays an important role in regulation of protein functions or during the assembly of proteins into complexes (Taiz, 2006). In this respect, dephosphorylation on Ser/Thr and/or Tyr residues, a mechanism that has been shown to be carried out by several members of the *Synechocystis* PP2C family, is increasingly recognized as an important mechanism for signal transduction processes in prokaryotes (Li et al., 2005; Irmeler, 2001; Deutscher et al., 2005). If that is the case, one could speculate it to function with the periplasmic SynTic22 in transmitting environmental signals into the cell. It might also be involved in the post-translational modification of SynTic22. Western analysis of total cell extracts and BN-PAGE analysis identified two possible SynTic22 proteins (Figure 6B

and Figure 11). Moreover, pull-down of SynTic22-His from periplasm of the  $J\Delta_{synTic22::synTic22-His}$  strain revealed two bands that were clearly below the 24 kDa marker and more importantly showed a considerably different running behavior from the recombinant SynTic22 protein that is expressed including the N-terminal signal peptide. Different phosphorylation states of the protein might explain the observed running behavior and the putative interaction with the Slr0114 phosphatase. Of course, further experiments confirming an interaction between SynTic22 and Slr0144 need to be performed. Moreover, the questions should be addressed where Slr0114 is exactly localized and if SynTic22 is undergoing different phosphorylation states because apart from phosphorylation also other types of post-translational modification have been shown to occur in prokaryotes that might have caused a different running behavior e.g. acetylation or glycosylation (Soppa, 2010; Tabish et al., 2011).

#### 5.4 Proving of potential SynTic22 interaction partners

The initial screening for SynTic22 interaction partners by pull-down experiments did not establish any evidence for a connection to other TOC-TIC translocase subunit homologs in *Synechocystis*.

Nevertheless, a split-ubiquitin analysis was performed using SynToc75 (Slr1227) and Slr1841. Several reasons indicate both proteins to be potential SynTic22 interaction partners. First, in this work, Slr1841 was identified in pull-down experiments using endogenously expressed SynTic22-His (Table 11). Second, Slr1841 is also predicted to be an S-layer protein. Since SynTic22 has been found within the periplasm (Figure 8; Fulda et al., 2002) and in secretes of *Synechocystis* outside of the cell (Sergeyenko and Los, 2000) it may either interact with Slr1841 during transport to its destination at the outer membrane and/or afterwards. Third, SynToc75 and Slr1841 proteins are predicted to be  $\beta$ -barrel proteins. In *Pisum sativum* crosslinking and immune precipitation experiments suggested Tic22 to interact with several proteins of the general import pathway that are predicted  $\beta$ -barrel proteins, e.g. Toc75 (Kouranov and Schnell, 1997). Moreover, AnaTic22 has recently been shown *in vitro* and *in vivo* to interact with the outer membrane biogenesis factor Omp85 in *Anabaena* sp. PCC 7120 (Tripp et al., 2012). Omp85 is C-terminally embedded into the membrane, thereby forming a  $\beta$ -barrel structure (Koenig et al., 2010). PsToc75 has a homolog in *Synechocystis* that shares a rather high similarity (Bölter et al., 1998) but an interaction with SynTic22 had not been investigated.

The split-ubiquitin system is supposed to be suitable for membrane proteins. However, controls suggested that SynToc75 and Slr1841 were not properly expressed and/or not inserted into the yeast membrane (Table 12). A problem could have been the size and extremely hydrophobic character of both proteins. Other multi-spanning membrane proteins of similar molecular weight

like *Arabidopsis thaliana* Alb3, D1 and SecY have been shown to be compatible with the system (Pasch et al., 2005), although this were not  $\beta$ -barrel proteins. A possible solution could be the application of smaller fragments of the proteins to test for an interaction in the split-ubiquitin system. Although the split-ubiquitin system does not definitely exclude one of the tested proteins to be soluble, the control experiments showed autonomous activation when SynTic22 without the predicted N-terminal signal peptide/transmembrane domain was used as bait (Table 12). Thus, when SynTic22 is used as bait in future experiments, a fusion of the protein to a membrane anchor protein that can be used in such an assay like e.g. Ost4p (Möckli, 2007) should be considered. Since *Synechocystis* is amenable to transformation and homologous recombination, other *in vivo* methods like BiFC are interesting alternatives to the split-ubiquitin system (Kerppola, 2008). In BiFC two parts of a fluorescent molecule are fused to the putative interaction partners. Upon interaction, both parts complement to the functional molecule that can be detected under the microscope (Kerppola, 2008). Slr1841 and SynToc75 could be tested for interaction with SynTic22 in their natural environment. Furthermore, the fluorescence emitted is proportional to the strength of interaction thereby conclusions about a direct interaction or interaction within a complex could be made (Kerppola, 2008).

BN-PAGE of soluble periplasmic proteins followed by Western analysis showed two SynTic22 spots of similar molecular weight. Weak signals that almost perfectly overlapped spread from those spots to higher molecular weight (~90 kDa) (Figure 11), suggesting either that both forms participate in complex formation with other proteins or that they interact with each other. In order to test for oligomeric SynTic22, a yeast two-hybrid assay suitable for testing soluble proteins was performed. The control experiment showed that transport into the nucleus was achieved (Figure 16). However, interaction between SynTic22 proteins could not be observed in the assay, neither with *Leu2* nutritional reporter nor by monitoring  $\beta$ -galactosidase activity (Figure 17). This suggests that SynTic22 does not form homo-oligomers in yeast. The finding is thus inconsistent with data from cross-linking experiments in *Anabaena* where AnaTic22 was shown to form dimers (Tripp et al., 2012). Whether the observed dimerization is an *Anabaena* specific characteristic, a crosslinking artifact or if the SynTic22 dimerization is just too weak to be detected in the Y2H needs to be investigated in further experiments.

The yeast two-hybrid system was also used to confirm the interaction with the soluble Sll1784 protein that has been observed in initial pull-down experiments. Controls showed Sll1784 to exert autonomous activation of the *Leu2* reporter gene, both as bait and as prey protein. Using the  $\beta$ -galactosidase as reporter for protein-protein interaction did not result in autonomous activation of the reporter gene. However, an interaction with SynTic22 was also not confirmed.

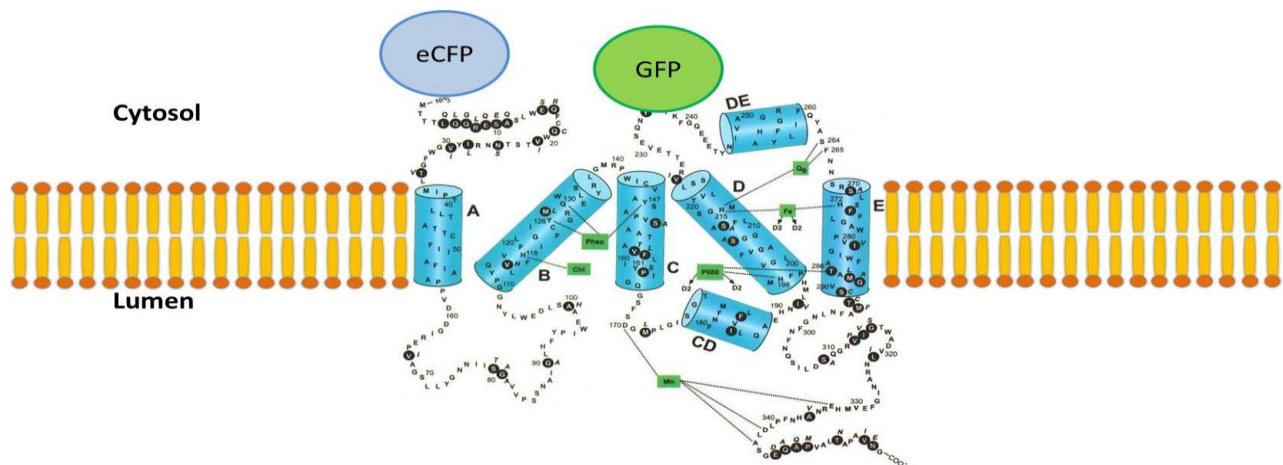
Since the LexA-lacZ reporters are not as sensitive as the *Leu2* nutritional reporter, it is possible for a weak interaction to not result in blue coloring of the yeast cells on X-gal plates. Therefore, pull-down assays with overexpressed proteins might lead to data that are more reliable.

## 5.5 PrataA - visualization of membrane biogenesis processes

In the present work, an inducible construct for regulation of PrataA protein expression was designed, assembled and successfully introduced into *Synechocystis* wild-type Big cells. Biochemical analysis showed that PrataA expression, which is controlled by the *nirA* promoter, is indeed tightly repressed when ammonium was applied to the medium (Figure 21). Using this condition, no PrataA protein could be detected in the inducible strains, which therefore resembled the Big $\Delta$ prataA knockout strain. This is a prerequisite to follow eCFP-D1 processing during PSII biogenesis from its start at the plasma membrane to the thylakoid membranes (Zak, 2001). Induction of the *nirA* promoter by application of nitrate to the medium led to an expression and accumulation of PrataA protein approximately to wild-type levels. Therefore, although all endogenous *prataA* genes were substituted by the inducible *prataA*, the *nirA* promoter did not result in overexpression, which is in opposition to previous reports (Qi et al., 2005; Desplancq et al., 2005). However, this was the first time a *nirA* controlled gene was stably integrated into the genome. The gene dosage number might have been lower compared to *nirA*-controlled genes that are encoded on plasmids. PrataA protein was detected about 30 min after induction with a maximum after 24 h of incubation. The experiment aims on a visual examination using a confocal laser scanning microscope, thus 30 min are enough time to prepare the living cells for microscopy (e.g. embedding of cells in agar solution). Expression of eCFP-D1 encoded on the pVZ322 extrachromosomal vector failed. Most likely, homologous recombination has occurred, because the promoter and the D1 sequence of the construct could serve as left and right borders. Thereby, the eCFP could have transferred into the endogenous D1 gene, exchanging the tagged D1 gene of the vector with the untagged endogenous one. Since the resistance gene of the vector would not be transferred into the genomic DNA in the process, the strain will still show resistance to the antibiotic. However, there is no selection pressure on the genomic D1 genes that have inserted eCFP by homologous recombination, thus those will ultimately get lost. This problem has not occurred when the construct was used with the wild-type HP strain (Schottkowski et al., 2008). An explanation could be the different number of genome copies available in the wild-type Big and HP strains. It is not clear why the Big strain is about one third bigger in size. However, a strong correlation exists between genome copy number (polyploidy) and cell size. E.g., *Epulopiscium* a large bacterium that attains lengths of up to 300  $\mu$ m has tens of thousands of copies of its genome (Mendell et al., 2008). Even the genome copy number

within *Synechocystis* strain sp. PCC 6803 has been shown to differ dramatically with up to 225 copies during exponential phase (Griese et al., 2011). Therefore, one could speculate the size of the Big cells might be due to a higher genome copy number, which eventually increases the chance for homologous recombination to occur.

To circumvent unintended recombination, a construct was made for stable integration into the genome. A C-terminal label was not possible because pD1 is processed to its mature form by removal of the last 16 AA of the protein (Inagaki et al., 2001). For this reason, an internal GFP-label was chosen. Hence, GFP was introduced into a cytosolic loop, which is neither involved in coordination or binding of any known photosystem II subunit nor with PratA protein (Figure 24; Salih and Jansson, 1997; Schottkowski et al., 2008).



**Figure 24: Predicted membrane topology of *Synechocystis* D1 (modified from Salih and Jansson, 1997).** The protein integrates into the membrane via five transmembrane domains. To follow D1 membrane flow during PSII biogenesis, it is labeled either with eCFP at the N-terminus (blue) or with an internal GFP (green). Green boxes indicate amino acid residues which are involved in coordination or binding of PSII subunits.

The application of a stable, internally GFP-labeled D1 protein was expected to have several advantages compared to the extrachromosomal approach. Since several copies of the *D1* gene exist in *Synechocystis* as potential target sites for homologous recombination, in total a higher expression of the labeled protein was expected in comparison to expression from the low copy pVZ322 vector. Moreover, since the endogenous *D1* gene will be replaced by the labeled *D1* less competing unlabeled D1 is expected. This should finally result in a stronger fluorescent signal of GFP-D1 in the membranes compared to the previous approach (Schottkowski et al., 2008).

In future experiments, those strains will be a fascinating tool to visualize subcellular membrane flow in a time-resolved manner. Using high-resolution microscopy could even help to visualize the thylakoid and plasma membrane connecting structures.

## 6 References

- Agne B, Kessler F** (2009) Protein transport in organelles: The Toc complex way of preprotein import. *The FEBS journal* **276**: 1156–1165.
- Alami M, Lüke I, Deitermann S, Eisner G, Koch H, Brunner J, Müller M** (2003) Differential interactions between a twin-arginine signal peptide and its translocase in *Escherichia coli*. *Molecular cell* **12**: 937–946.
- Albiniak AM, Baglieri J, Robinson C** (2012) Targeting of luminal proteins across the thylakoid membrane. *Journal of Experimental Botany* **63**: 1689–1698.
- Aldridge C, Spence E, Kirkilionis MA, Frigerio L, Robinson C** (2008) Tat-dependent targeting of Rieske iron-sulphur proteins to both the plasma and thylakoid membranes in the cyanobacterium *Synechocystis* PCC6803. *Molecular Microbiology* **70**: 140–150.
- Allen JF, Paula WB de, Puthiyaveetil S, Nield J** (2011) A structural phylogenetic map for chloroplast photosynthesis. *Trends in Plant Science* **16**: 645–655.
- Anbudurai PR, Mor TS, Ohad I, Shestakov SV, Pakrasi HB** (1994) The *ctpA* gene encodes the C-terminal processing protease for the D1 protein of the photosystem II reaction center complex. *Proceedings of the National Academy of Sciences of the United States of America* **91**: 8082–8086.
- Armbruster U, Zühlke J, Rengstl B, Kreller R, Makarenko E, Rühle T, Schünemann D, Jahns P, Weisshaar B, Nickelsen J, Leister D** (2010) The *Arabidopsis* thylakoid protein PAM68 is required for efficient D1 biogenesis and photosystem II assembly. *The Plant cell* **22**: 3439–3460.
- Aronsson H, Boij P, Patel R, Wardle A, Töpel M, Jarvis P** (2007) Toc64/OEP64 is not essential for the efficient import of proteins into chloroplasts in *Arabidopsis thaliana*. *The Plant journal : for cell and molecular biology* **52**: 53–68.
- Bageshwar UK, Musser SM** (2007) Two electrical potential-dependent steps are required for transport by the *Escherichia coli* Tat machinery. *The Journal of cell biology* **179**: 87–99.
- Bagos PG, Nikolaou EP, Liakopoulos TD, Tsirigos KD** (2010) Combined prediction of Tat and Sec signal peptides with hidden Markov models. *Bioinformatics (Oxford, England)* **26**: 2811–2817.
- Barnett JP, Robinson C, Scanlan DJ, Blindauer CA** (2011) The Tat protein export pathway and its role in cyanobacterial metalloprotein biosynthesis. *FEMS Microbiology Letters* **325**: 1–9.
- Becker T** (2004) Toc12, a Novel Subunit of the Intermembrane Space Preprotein Translocon of Chloroplasts. *Molecular Biology of the Cell* **15**: 5130–5144.
- Benz M, Bals T, Gugel IL, Piotrowski M, Kuhn A, Schunemann D, Soll J, Ankele E** (2009) Alb4 of *Arabidopsis* Promotes Assembly and Stabilization of a Non Chlorophyll-Binding Photosynthetic Complex, the CF1CF0-ATP Synthase. *Molecular Plant* **2**: 1410–1424.



- Bhaya D, Bianco NR, Bryant D, Grossman A** (2000) Type IV pilus biogenesis and motility in the cyanobacterium *Synechocystis* sp. PCC6803. *Molecular microbiology* **37**: 941–951.
- Blair DF** (2003) Flagellar movement driven by proton translocation. *FEBS Letters* **545**: 86–95.
- Blatch GL, Lässle M** (1999) The tetratricopeptide repeat: a structural motif mediating protein-protein interactions. *BioEssays* **21**: 932–939.
- Blum H, Beier H, Gross HJ** (1987) Improved silver staining of plant proteins, RNA and DNA in polyacrylamide gels. *Electrophoresis* **8**: 93–99.
- Bohnsack MT, Schleiff E** (2010) The evolution of protein targeting and translocation systems. *Biochimica et Biophysica Acta (BBA) - Molecular Cell Research* **1803**: 1115–1130.
- Bölter B, Soll J, Schulz A, Hinnah S, Wagner R** (1998) Origin of a chloroplast protein importer. *Proc. Natl. Acad. Sci. USA* **95**: 15831–15836.
- Boudreau E** (2000) The Nac2 gene of *Chlamydomonas* encodes a chloroplast TPR-like protein involved in psbD mRNA stability. *The EMBO Journal* **19**: 3366–3376.
- Chaddock AM, Mant A, Karnauchov I, Brink S, Herrmann RG, Klösgen RB, Robinson C** (1995) A new type of signal peptide: central role of a twin-arginine motif in transfer signals for the  $\Delta$ pH-dependent thylakoidal protein translocase. *The EMBO Journal* **14**: 2715–2722.
- Chan CX, Gross J, Yoon HS, Bhattacharya D** (2011) Plastid Origin and Evolution: New Models Provide Insights into Old Problems. *PLANT PHYSIOLOGY* **155**: 1552–1560.
- Chiu C, Chen L, Li H** (2010) Pea Chloroplast DnaJ-J8 and Toc12 Are Encoded by the Same Gene and Localized in the Stroma. *PLANT PHYSIOLOGY* **154**: 1172–1182.
- Dalbey RE, Kuhn A** (2012) Protein Traffic in Gram-negative bacteria - how exported and secreted proteins find their way. *FEMS Microbiology Reviews* doi: 10.1111/j.1574-6976.2012.00327.x.
- Dalbey RE, Robinson C** (1999) Protein translocation into and across the bacterial plasma membrane and the plant thylakoid membrane. *Trends in biochemical sciences* **24**: 17–22.
- Dalbey RE, Wang P, Kuhn A** (2011) Assembly of Bacterial Inner Membrane Proteins. *Annual Review of Biochemistry* **80**: 161–187.
- Daley D** (2008) The assembly of membrane proteins into complexes. *Current Opinion in Structural Biology* **18**: 420–424.
- D'Andrea L** (2003) TPR proteins: the versatile helix. *Trends in Biochemical Sciences* **28**: 655–662.
- Das AK** (1998) The structure of the tetratricopeptide repeats of protein phosphatase 5: implications for TPR-mediated protein-protein interactions. *The EMBO Journal* **17**: 1192–1199.

- Desplancq D, Bernard C, Sibler A, Kieffer B, Miguet L, Potier N, van Dorselaer A, Weiss E** (2005) Combining inducible protein overexpression with NMR-grade triple isotope labeling in the cyanobacterium *Anabaena* sp. PCC 7120. *Biotechniques* **39**: 405–411.
- Deutscher J, Saier M.H.** (2005) Ser/Thr/Tyr protein phosphorylation in bacteria – for long time neglected, now well established. *J Mol Microbiol Biotechnol* **9**: 125–131.
- Elanskaya IV, Karandashova IV, Bogachev AV, Hagemann M** (2002) Functional Analysis of the Na<sup>+</sup>/H<sup>+</sup> Antiporter Encoding Genes of the Cyanobacterium *Synechocystis* PCC 6803. *Biochemistry (Moscow)* **67**: 432–440.
- Engelhardt H** (2007) Are S-layers exoskeletons? The basic function of protein surface layers revisited. *Journal of structural biology* **160**: 115–124.
- Ermakova SY, Elanskaya IV, Kallies KU, Weihe A, Börner T, Shestakov SV** (1993) Cloning and sequencing of mutant *psbB* genes of the cyanobacterium *Synechocystis* PCC 6803. *Photosynthesis Research* **37**: 139–146.
- Espinosa J, Forchhammer K, Contreras A** (2007) Role of the *Synechococcus* PCC 7942 nitrogen regulator protein PipX in NtcA-controlled processes. *Microbiology* **153**: 711–718.
- Estojak J, Brent R, Golemis EA** (1995) Correlation of Two-Hybrid Affinity Data with In Vitro Measurements. *Molecular and cellular biology* **15**: 5820–5829.
- Felder S, Meierhoff K, Sane AP, Meurer J, Driemel C, Pluecken H, Klaff P** (2001) The nucleus-encoded HCF107 gene of *Arabidopsis* provides a link between inter-cistronic RNA processing and the accumulation of translation-competent *psbH* transcripts in chloroplasts. *THE PLANT CELL ONLINE* **13**: 2127–2141.
- Fellerer C, Schweiger R, Schongrubner K, Soll J, Schwenkert S** (2011) Cytosolic HSP90 Cochaperones HOP and FKBP Interact with Freshly Synthesized Chloroplast Preproteins of *Arabidopsis*. *Molecular Plant* **4**: 1133–1145.
- Ferreira KN, Iverson TM, Maghlaoui K, Barber J, Iwata S** (2004) Architecture of the Photosynthetic Oxygen-Evolving Center. *Science* **303**: 1831–1838.
- Filip C, Fletcher G, Wulff JL, Earhart CF** (1973) Solubilization of the Cytoplasmic Membrane of *Escherichia coli* by the Ionic Detergent Sodium-Lauryl Sarcosinate. *Journal of Bacteriology* **115**: 717–722.
- Flores-Pérez Ú, Jarvis P** (2012) Molecular chaperone involvement in chloroplast protein import. *Biochimica et Biophysica Acta (BBA) - Molecular Cell Research* **1541**: 102–113.
- Frank M** (2012) Protocadherine als Adhäsions- und Signalmoleküle. *BIOspektrum* **18**: 257–259.
- Fulda S, Huang F, Nilsson F, Hagemann M, Norling B** (2000) Proteomics of *Synechocystis* sp. strain PCC 6803. Identification of periplasmic proteins in cells grown at low and high salt concentrations. *European journal of biochemistry / FEBS* **267**: 5900–5907.

- Fulda S, Mikkat S, Schröder W, Hagemann M** (1999) Isolation of salt-induced periplasmic proteins from *Synechocystis* sp. strain PCC 6803. *Arch Microbiol* **171**: 214–217.
- Fulda S, Norling B, Schoor A, Hagemann M** (2002) The Slr0924 protein of *Synechocystis* sp. strain PCC 6803 resembles a subunit of the chloroplast protein import complex and is mainly localized in the thylakoid lumen. *Plant Molecular Biology* **49**: 107–118.
- Gietz D, St. Jean A, Woods RA, Schiestl RH** (1992) Improved method for high efficiency transformation of intact yeast cells. *Nucleic Acids Research* **20**: 1425.
- Gietz DR, Woods RA** (2002) Transformation of yeast by lithium acetate/single-stranded carrier DNA/polyethylene glycol method, *Methods in Enzymology*. Elsevier, pp. 87–96.
- Golemis EA, Gyuris J, Brent R** (1996) Analysis of protein interactions; and Interaction trap/two-hybrid systems to identify interacting proteins. John Wiley & Sons, Inc.
- Gonen T, Walz T** (2006) The structure of aquaporins. *Quarterly reviews of biophysics* **39**: 361–396.
- Gould SB, Waller RF, McFadden GI** (2008) Plastid Evolution. *Annual Review of Plant Biology* **59**: 491–517.
- Gouridis G, Karamanou S, Gelis I, Kalodimos CG, Economou A** (2009) Signal peptides are allosteric activators of the protein translocase. *Nature* **462**: 363–367.
- Grainger DC** (2005) Studies of the distribution of *Escherichia coli* cAMP-receptor protein and RNA polymerase along the E. coli chromosome. *Proceedings of the National Academy of Sciences* **102**: 17693–17698.
- Griese M, Lange C, Soppa J** (2011) Ploidy in cyanobacteria. *FEMS Microbiology Letters* **323**: 124–131.
- Gross J, Bhattacharya D** (2009) Reevaluating the evolution of the Toc and Tic protein translocons. *Trends in Plant Science* **14**: 13–20.
- Guskov A, Kern J, Gabdulkhakov A, Broser M, Zouni A, Saenger W** (2009) Cyanobacterial photosystem II at 2.9-Å resolution and the role of quinones, lipids, channels and chloride. *Nature Structural & Molecular Biology* **16**: 334–342.
- Gyuris J, Golemis EA, Chertkov H, Brent R** (1993) Cdi1, a Human G1 and S Phase Protein Phosphatase That Associates with Cdk2. *Cell* **75**: 791–803.
- Hanahan D** (1983) Studies on transformation of *Escherichia coli* with plasmids. *Journal of Molecular Biology* **166**: 557–580.
- Hatefi Y** (1985) The Mitochondrial Electron Transport and Oxidative Phosphorylation System. *Annual Review of Biochemistry* **54**: 1015–1069.
- Heijne G von** (1992) Membrane Protein Structure Prediction: Hydrophobicity Analysis and the 'Positive Inside' Rule. *J. Mol. Biol.* **225**: 487–494.
- Henrichsen J** (1983) Twitching Motility. *Annual Review of Microbiology* **37**: 81–93.

- Hörmann F, Küchler M, Sveshnikow D, Oppermann U, Li Y, Soll J** (2004) Tic32, an Essential Component in Chloroplast Biogenesis. *Journal of Biological Chemistry* **279**: 34756–34762.
- Huang F** (2002) Proteomics of *Synechocystis* sp. Strain PCC 6803: Identification of Plasma Membrane Proteins. *Molecular & Cellular Proteomics* **1**: 956–966.
- Hunter S, Jones P, Mitchell A, Apweiler R, Attwood TK, Bateman A, Bernard T, Binns D, Bork P, Burge S, Castro E de, Coggill P, Corbett M, Das U, Daugherty L, Duquenne L, Finn RD, Fraser M, Gough J, Haft D, Hulo N, Kahn D, Kelly E, Letunic I, Lonsdale D, Lopez R, Madera M, Maslen J, McAnulla C, McDowall J, McMenamin C, Mi H, Mutowo-Muellenet P, Mulder N, Natale D, Orengo C, Pesseat S, Punta M, Quinn AF, Rivoire C, Sangrador-Vegas A, Selengut JD, Sigrist CJA, Scheremetjew M, Tate J, Thimmajananthan M, Thomas PD, Wu CH, Yeats C, Yong S** (2011) InterPro in 2011: new developments in the family and domain prediction database. *Nucleic Acids Research* **40**: D306.
- Inagaki N, Yamamoto Y, Satoh K** (2001) A sequential two-step proteolytic process in the carboxyl-terminal truncation of precursor D1 protein in *Synechocystis* sp. PCC6803. *FEBS letters* **509**: 197–201.
- Irmeler A** (2001) A PP2C-type phosphatase dephosphorylates the P<sub>II</sub> signaling protein in the cyanobacterium *Synechocystis* PCC 6803. *Proceedings of the National Academy of Sciences* **98**: 12978–12983.
- Jakovljevic V, Leonardy S, Hoppert M, Sogaard-Andersen L** (2008) PilB and PilT Are ATPases Acting Antagonistically in Type IV Pilus Function in *Myxococcus xanthus*. *Journal of Bacteriology* **190**: 2411–2421.
- Jansén T, Kanervo E, Aro E, Mäenpää P** (2002) Localisation and processing of the precursor form of photosystem II protein D1 in *Synechocystis* 6803. *Journal of Plant Physiology* **159**: 1205–1211.
- Jarvis P** (2008) Targeting of nucleus-encoded proteins to chloroplasts in plants. *New Phytologist* **179**: 257–285.
- Johnsson N, Varshavsky A** (1994) Split ubiquitin as a sensor of protein interactions *in vivo*. *Proc. Natl. Acad. Sci. USA* **91**: 10340–10344.
- Kalanon M, Tonkin CJ, McFadden GI** (2009) Characterization of Two Putative Protein Translocation Components in the Apicoplast of *Plasmodium falciparum*. *Eukaryotic Cell* **8**: 1146–1154.
- Kaneko T** (1996) Sequence Analysis of the Genome of the Unicellular Cyanobacterium *Synechocystis* sp. Strain PCC6803. II. Sequence Determination of the Entire Genome and Assignment of Potential Protein-coding Regions. *DNA Research* **3**: 109–136.
- Kerppola TK** (2008) Bimolecular Fluorescence Complementation (BiFC) Analysis as a Probe of Protein Interactions in Living Cells. *Annual Review of Biophysics* **37**: 465–487.
- Klinkert B** (2004) PratA, a Periplasmic Tetratricopeptide Repeat Protein Involved in Biogenesis of Photosystem II in *Synechocystis* sp. PCC 6803. *Journal of Biological Chemistry* **279**: 44639–44644.

- Kloft N** (2005) Protein phosphatase PphA from *Synechocystis* sp. PCC 6803: the physiological framework of PII-P dephosphorylation. *Microbiology* **151**: 1275–1283.
- Knowles JR** (1980) Enzyme-Catalyzed Phosphoryl Transfer Reactions. *Annual Review of Biochemistry* **49**: 877–919.
- Koenig P, Mirus O, Haarmann R, Sommer MS, Sinning I, Schleiff E, Tews I** (2010) Conserved Properties of Polypeptide Transport-associated (POTRA) Domains Derived from Cyanobacterial Omp85. *Journal of Biological Chemistry* **285**: 18016–18024.
- Komenda J** (2004) Accumulation of the D2 Protein Is a Key Regulatory Step for Assembly of the Photosystem II Reaction Center Complex in *Synechocystis* PCC 6803. *Journal of Biological Chemistry* **279**: 48620–48629.
- Komenda J, Barker M, Kuviková S, Vries R de, Mullineaux CW, Tichý M, Nixon PJ** (2005) The FtsH Protease slr0228 Is Important for Quality Control of Photosystem II in the Thylakoid Membrane of *Synechocystis* sp. PCC 6803. *Journal of Biological Chemistry* **281**: 1145–1151.
- Komenda J, Kuvikova S, Granvogel B, Eichacker L, Diner B, Nixon P** (2007) Cleavage after residue Ala352 in the C-terminal extension is an early step in the maturation of the D1 subunit of Photosystem II in *Synechocystis* PCC 6803. *Biochimica et Biophysica Acta (BBA) - Bioenergetics* **1767**: 829–837.
- Komenda J, Nickelsen J, Tichý M, Prásl O, Eichacker LA, Nixon PJ** (2008) The cyanobacterial homologue of HCF136/YCF48 is a component of an early photosystem II assembly complex and is important for both the efficient assembly and repair of photosystem II in *Synechocystis* sp. PCC 6803. *The Journal of biological chemistry* **283**: 22390–22399.
- Komenda J, Sobotka R, Nixon PJ** (2012) Assembling and maintaining the Photosystem II complex in chloroplasts and cyanobacteria. *Current Opinion in Plant Biology* **15**:1-7.
- Kouranov A, Chen X, Fuks B, Schnell DJ** (1998) Tic20 and Tic22 Are New Components of the Protein Import Apparatus at the Chloroplast Inner Envelope Membrane. *The Journal of Cell Biology* **143**: 991–1002.
- Kouranov A, Schnell DJ** (1997) Analysis of the Interactions of Preproteins with the Import Machinery over the Course of Protein Import into Chloroplasts. *The Journal of Cell Biology* **139**: 1677–1685.
- Kouranov A, Wang H, Schnell DJ** (1999) Tic22 Is Targeted to the Intermembrane Space of Chloroplasts by a Novel Pathway. *The Journal of Biological Chemistry* **274**: 25181–25186.
- Kovács-Bogdán E, Soll J, Bölder B** (2010) Protein import into chloroplasts: The Tic complex and its regulation. *Biochimica et Biophysica Acta (BBA) - Molecular Cell Research* **1803**: 740–747.
- Kroll D** (2001) From the Cover: VIPP1, a nuclear gene of *Arabidopsis thaliana* essential for thylakoid membrane formation. *Proceedings of the National Academy of Sciences* **98**: 4238–4242.

- Kuhn A, Stuart R, Henry R, Dalbey RE** (2003) The Alb3/Oxa1/YidC protein family: membrane-localized chaperones facilitating membrane protein insertion? *Trends in cell biology* **13**: 510–516.
- Kunkel DD** (1982) Thylakoid centers: Structures associated with the cyanobacterial photosynthetic membrane system. *Archives of Microbiology* **133**: 97–99.
- Kuviková S, Tichý M, Komenda J** (2005) A role of the C-terminal extension of the photosystem II D1 protein in sensitivity of the cyanobacterium *Synechocystis* PCC 6803 to photoinhibition. *Photochemical & Photobiological Sciences* **4**: 1044.
- Laemmli UK** (1970) Cleavage of Structural Proteins during the Assembly of the Head of Bacteriophage T4 **227**: 680–685.
- Lane N** (2005) *Power, sex, suicide. Mitochondria and the meaning of life.* Oxford University Press, Oxford ;, New York.
- Liberton M, Howard Berg R, Heuser J, Roth R, Pakrasi HB** (2006) Ultrastructure of the membrane systems in the unicellular cyanobacterium *Synechocystis* sp. strain PCC 6803. *Protoplasma* **227**: 129–138.
- Li R, Potters MB, Shi L, Kennelly PJ.** (2005) The protein phosphatases of *Synechocystis* sp. strain PCC 6803: open reading frames sll1033 and sll1387 encode enzymes that exhibit both protein-serine and protein-tyrosine phosphatase activity in vitro. *J Bacteriol.*; **187**:5877-84.
- Luirink J, Sinning I** (2004) SRP-mediated protein targeting: structure and function revisited. *Biochimica et biophysica acta* **1694**: 17–35.
- Marder JB, Goloubinoff P, Edelman M** (1984) Molecular Architecture of the Rapidly Metabolized 32-kilodalton Protein of Photosystem II. *The Journal of biological chemistry* **259**: 3900–3908.
- Mardis ER** (2008) The impact of next-generation sequencing technology on genetics. *Trends in Genetics* **24**: 133–141.
- Margulis L** (1970) *Origin of eukaryotic cells*; Evidence and research implications for a theory of the origin and evolution of microbial, plant, and animal cells on the Precambrian earth. Yale University Press, New Haven.
- Mendell JE, Clements KD, Choat JH, Angert ER** (2008) From the Cover: Extreme polyploidy in a large bacterium. *Proceedings of the National Academy of Sciences* **105**: 6730–6734.
- Meurer J, Plücker H, Kowallik KV, Westhoff P** (1998) A nuclear-encoded protein of prokaryotic origin is essential for the stability of photosystem II in *Arabidopsis thaliana*. *The EMBO journal* **17**: 5286–5297.
- Mitchell P** (1961) Coupling of phosphorylation to electron and hydrogen transfer by a chemi-osmotic type of mechanism. *Nature* **191**: 144–148.

- Miyadai H** (2004) Effects of Lipoprotein Overproduction on the Induction of DegP (HtrA) Involved in Quality Control in the *Escherichia coli* Periplasm. *Journal of Biological Chemistry* **279**: 39807–39813.
- Möckli N** (2007) Development of a split-ubiquitin based, cytosolic yeast two-hybrid system and its application to the structure-function analysis of scUri1p, Zürich.
- Moghadam MA, Schleiff E** (2005) Analysis of expression patterns of translocon subunits of chloroplasts and mitochondria. *Plant Science* **168**: 1533–1539.
- Mohoj M, Degan FD** (2004) Leader sequences are not signal peptides. *Nature Biotechnology* **22**: 1502.
- Muro-Pastor MI, Reyes JC, Florencio FJ** (2005) Ammonium assimilation in cyanobacteria. *Photosynthesis research* **83**: 135–150.
- Nakai M, Sugita D, Omata T, Endo T** (1993) Sec-Y Protein Is Localized in Both the Cytoplasmic and Thylakoid Membranes in the Cyanobacterium *Synechococcus* PCC7942. *Biochemical and Biophysical Research Communications* **193**: 228–234.
- Natale P, Brüser T, Driessen AJ** (2008) Sec- and Tat-mediated protein secretion across the bacterial cytoplasmic membrane—Distinct translocases and mechanisms. *Biochimica et Biophysica Acta (BBA) - Biomembranes* **1778**: 1735–1756.
- Nevo R, Charuvi D, Shimoni E, Schwarz R, Kaplan A, Ohad I, Reich Z** (2007) Thylakoid membrane perforations and connectivity enable intracellular traffic in cyanobacteria. *The EMBO Journal* **26**: 1467–1473.
- Nickelsen J, Rengstl B, Stengel A, Schottkowski M, Soll J, Ankele E** (2011) Biogenesis of the cyanobacterial thylakoid membrane system - an update. *FEMS Microbiology Letters* **315**: 1–5.
- Nixon PJ, Michoux F, Yu J, Boehm M, Komenda J** (2010) Recent advances in understanding the assembly and repair of photosystem II. *Annals of botany* **106**: 1–16.
- Norling B, Zak E, Andersson B, Pakrasi HB** (1998) 2D-isolation of pure plasma and thylakoid membranes from the cyanobacterium *Synechocystis* sp. PCC 6803. *FEBS Letters* **436**: 189–192.
- Oreb M, Tews I, Schleiff E** (2008) Policing Tic ‘n’ Toc, the doorway to chloroplasts. *Trends in Cell Biology* **18**: 19–27.
- Osanai T, Tanaka K** (2007) Keeping in Touch with PII: PII-Interacting Proteins in Unicellular Cyanobacteria. *Plant and Cell Physiology* **48**: 908–914.
- Osborn MJ, Gander JE, Parisi E, Carson J** (1972) Mechanism of Assembly of the Outer Membrane of *Salmonella typhimurium*. Isolation and characterization of cytoplasmic and outer membrane. *The Journal of Biological Chemistry* **247**: 3962–3972.
- Ossenbühl F, Inaba-Sulpice M, Meurer J, Soll J, Eichacker LA** (2006) The *Synechocystis* sp PCC 6803 Oxa1 Homolog Is Essential for Membrane Integration of Reaction Center Precursor Protein pD1. *THE PLANT CELL ONLINE* **18**: 2236–2246.

- Overton E** (1895) On the osmotic properties of living plants and animals. *Vierteljahrsschrift der Naturforschenden Gesellschaft in Zürich* **40**: 159–201.
- Paetzel M, Karla A, Strynadka NCJ, Dalbey RE** (2002) Signal peptidases. *Chemical reviews* **102**: 4549–4580.
- Parkinson JS** (2003) Bacterial Chemotaxis: a New Player in Response Regulator Dephosphorylation. *Journal of Bacteriology* **185**: 1492–1494.
- Pasch JC, Nickelsen J, Schünemann D** (2005) The yeast split-ubiquitin system to study chloroplast membrane protein interactions. *Applied Microbiology and Biotechnology* **69**: 440–447.
- Peng L** (2006) LOW PSII ACCUMULATION1 Is Involved in Efficient Assembly of Photosystem II in *Arabidopsis thaliana*. *THE PLANT CELL ONLINE* **18**: 955–969.
- Peschek GA, Obinger C, Paumann M** (2004) The respiratory chain of blue-green algae (cyanobacteria). *Physiologia plantarum* **120**: 358–369.
- Petersen TN, Brunak S, Heijne G von, Nielsen H** (2011) SignalP 4.0: discriminating signal peptides from transmembrane regions. *Nature Methods* **8**: 785–786.
- Pike LJ** (2008) The challenge of lipid rafts. *The Journal of Lipid Research* **50**: S323.
- Pisareva T, Kwon J, Oh J, Kim S, Ge C, Wieslander Å, Choi J, Norling B** (2011) Model for Membrane Organization and Protein Sorting in the Cyanobacterium *Synechocystis* sp. PCC 6803 Inferred from Proteomics and Multivariate Sequence Analyses. *Journal of Proteome Research* **10**: 3617–3631.
- Pollard TD, Earnshaw WC** (2007) *Cell Biology. Das Original mit Übersetzungshilfen*, Ed. 2. Spektrum, Akad. Verl., Heidelberg.
- Qbadou S, Becker T, Mirus O, Tews I, Soll J, Schleiff E** (2006) The molecular chaperone Hsp90 delivers precursor proteins to the chloroplast import receptor Toc64. *The EMBO Journal* **25**: 1836–1847.
- Qi Q, Hao M, Ng W, Slater SC, Baszis SR, Weiss JD, Valentin HE** (2005) Application of the *Synechococcus nirA* Promoter To Establish an Inducible Expression System for Engineering the *Synechocystis* Tocopherol Pathway. *Applied and Environmental Microbiology* **71**: 5678–5684.
- Rajalahti T, Huang F, Klement MR, Pisareva T, Edman M, Sjöström M, Wieslander A, Norling B** (2007) Proteins in different *Synechocystis* compartments have distinguishing N-terminal features: a combined proteomics and multivariate sequence analysis. *Journal of Proteome Research* **6**: 2420–2434.
- Rappaport F, Diner B** (2008) Primary photochemistry and energetics leading to the oxidation of the (Mn)<sub>4</sub>Ca cluster and to the evolution of molecular oxygen in Photosystem II. *Coordination Chemistry Reviews* **252**: 259–272.
- Rengstl B, Oster U, Stengel A, Nickelsen J** (2011) An Intermediate Membrane Subfraction in Cyanobacteria Is Involved in an Assembly Network for Photosystem II Biogenesis. *Journal of Biological Chemistry* **286**: 21944–21951.



- Reski R** (1998) Physcomitrella and Arabidopsis: the David and Goliath of reverse genetics. *Trends in Plant Science* **3**: 209–210.
- Rippka R, Deruelles J, Waterbury JB, Herdman M, Stanier RY** (1979) Generic Assignments, Strain Histories and Properties of Pure Cultures of Cyanobacteria. *Microbiology* **111**: 1–61.
- Robinson C, Bolhuis A** (2004) Tat-dependent protein targeting in prokaryotes and chloroplasts. *Biochimica et Biophysica Acta (BBA) - Molecular Cell Research* **1694**: 135–147.
- Sakiyama T, Araie H, Suzuki I, Shiraiwa Y** (2011) Functions of a hemolysin-like protein in the cyanobacterium *Synechocystis* sp. PCC 6803. *Archives of Microbiology* **193**: 565–571.
- Salih GF, Jansson C** (1997) Activation of the silent psbA1 gene in the cyanobacterium *Synechocystis* sp strain 6803 produces a novel and functional D1 protein. *The Plant cell* **9**: 869–878.
- Sambrook J, Russel DW** (2001) *Molecular cloning. A laboratory manual*, Ed. 3. Cold Spring Harbor Laboratory Press, New York.
- Sankaran K, Wu HC** (1994) Lipid modification of bacterial prolipoprotein. Transfer of diacylglyceryl moiety from phosphatidylglycerol. *The Journal of biological chemistry* **269**: 19701–19706.
- Sato T, Hanada M, Bodrug S, Irie S, Iwama N, Boise, Lawrence H, Thompson CB, Golemis E, Fong L, Wang H, Reed JC** (1994) Interactions among members of the Bcl-2 protein family analyzed with a yeast two-hybrid system. *Proc. Natl. Acad. Sci. USA* **91**: 9238–9242.
- Satoh K, Yamamoto Y** (2007) The carboxyl-terminal processing of precursor D1 protein of the photosystem II reaction center. *Photosynthesis Research* **94**: 203–215.
- Schägger H, Jagow G** (1991) Blue native electrophoresis for isolation of membrane protein complexes in enzymatically active form. *Analytical Biochemistry* **199**: 223–231.
- Schneider D, Fuhrmann E, Scholz I, Hess WR, Graumann PL** (2007) Fluorescence staining of live cyanobacterial cells suggest non-stringent chromosome segregation and absence of a connection between cytoplasmic and thylakoid membranes. *BMC Cell Biology* **8**: 39.
- Schottkowski M, Gkalypoudis S, Tzekova N, Stelljes C, Schunemann D, Ankele E, Nickelsen J** (2008) Interaction of the Periplasmic PrtA Factor and the PsbA (D1) Protein during Biogenesis of Photosystem II in *Synechocystis* sp. PCC 6803. *Journal of Biological Chemistry* **284**: 1813–1819.
- Schwenkert S, Soll J, Bölter B** (2011) Protein import into chloroplasts—How chaperones feature into the game. *Biochimica et Biophysica Acta (BBA) - Biomembranes* **1808**: 901–911.
- Serek J, Bauer-Manz G, Struhalla G, van den Berg L, Kiefer D, Dalbey R, Kuhn A** (2004) *Escherichia coli* YidC is a membrane insertase for Sec-independent proteins. *The EMBO Journal* **23**: 294–301.

- Sergeyenko TV, Los DA** (2000) Identification of secreted proteins of the cyanobacterium *Synechocystis* sp. strain PCC 6803. *FEMS Microbiology Letters* **193**: 213–216.
- Sikorski RS, Boguski MS, Goebel M, Hieter P** (1990) A repeating amino acid motif in CDC23 defines a family of proteins and a new relationship among genes required for mitosis and RNA synthesis. *Cell* **60**: 307–317.
- Silhavy TJ, Kahne D, Walker S** (2010) *The Bacterial Cell Envelope*. Cold Spring Harbor Perspectives in Biology **2**:a000414.
- Singer SJ** (1974) The Molecular Organization of Membranes. *Annual Review of Biochemistry* **43**: 805–833.
- Singer SJ, Nicolson GL** (1972) The fluid mosaic model of the structure of cell membranes. *Science* **175**: 720–731.
- Smith D, Howe CJ** (1993) The distribution of Photosystem I and Photosystem II polypeptides between the cytoplasmic and thylakoid membranes of cyanobacteria. *FEMS Microbiology Letters* **110**: 341–347.
- Soll J, Schleiff E** (2004) Plant cell biology: Protein import into chloroplasts. *Nature Reviews Molecular Cell Biology* **5**: 198–208.
- Sonnhammer EL, Heijne G von, Krogh A** (1998) A hidden Markov model for predicting transmembrane helices in protein sequences. *Proc Int Conf Intell Syst Mol Biol* **6**: 175–182.
- Soppa J** (2010) Protein Acetylation in Archaea, Bacteria, and Eukaryotes. *Archaea* **2010**: 1–9.
- Spence E, Bailey S, Nenninger A, Moller SG, Robinson C** (2004) A Homolog of Albino3/OxaI Is Essential for Thylakoid Biogenesis in the Cyanobacterium *Synechocystis* sp. PCC6803. *Journal of Biological Chemistry* **279**: 55792–55800.
- Spence E, Sarcina M, Ray N, Møller SG, Mullineaux CW, Robinson C** (2003) Membrane-specific targeting of green fluorescent protein by the Tat pathway in the cyanobacterium *Synechocystis* PCC6803. *Molecular Microbiology* **48**: 1481–1489.
- Srivastava R, Pisareva T, Norling B** (2005) Proteomic studies of the thylakoid membrane of *Synechocystis* sp. PCC 6803. *PROTEOMICS* **5**: 4905–4916.
- Stanier RY, Kunisawa R, Mandel M, Cohen-Bazire G** (1971) Purification and Properties of Unicellular Blue-Green Algae (Order *Chroococcales*). *Bacteriological Reviews* **35**: 171–205.
- Stengel A, Gugel IL, Hilger D, Rengstl B, Jung H, Nickelsen J** (2012) Initial Steps of Photosystem II de Novo Assembly and Preloading with Manganese Take Place in Biogenesis Centers in *Synechocystis*. *THE PLANT CELL ONLINE* **24**: 660–675.
- Stiegler N, Dalbey RE, Kuhn A** (2011) M13 Procoat Protein Insertion into YidC and SecYEG Proteoliposomes and Liposomes. *Journal of Molecular Biology* **406**: 362–370.
- Stockel J** (2006) The Evolutionarily Conserved Tetratricopeptide Repeat Protein Pale Yellow Green7 Is Required for Photosystem I Accumulation in Arabidopsis and Copurifies with the Complex. *PLANT PHYSIOLOGY* **141**: 870–878.

- Suzuki I, Sugiyama T., Omata T** (1993) Primary structure and transcriptional regulation of the gene for nitrite reductase from the cyanobacterium *Synechococcus* PCC 7942. *Plant Cell Physiol.* **34**: 1311–1320.
- Swaney KF, Huang C, Devreotes PN** (2010) Eukaryotic Chemotaxis: A Network of Signaling Pathways Controls Motility, Directional Sensing, and Polarity. *Annual Review of Biophysics* **39**: 265–289.
- Tabish S, Raza A, Nasir A, Zafar S, Bokhari H** (2011) Analysis of glycosylation motifs and glycosyltransferases in Bacteria and Archaea. *Bioinformation* **6**: 191–195.
- Tilett D, Neilan BA** (2000) Xanthogenate nucleic acid isolation from cultured and environmental Cyanobacteria. *Journal of Phycology* **36**: 251–258.
- Towbin H, Staehelin T, Gordon J** (1979) Electrophoretic transfer of proteins from polyacrylamide gels to nitrocellulose sheets: Procedure and some applications. *Proc. Natl. Acad. Sci. USA* **76**: 4350–4354.
- Tripp J, Hahn A, Koenig P, Flinner N, Bublak D, Brouwer EM, Ertel F, Mirus O, Sinning I, Tews I, Schleiff E** (2012) Structure and conservation of the periplasmic targeting factor Tic22 from plants and cyanobacteria. *Journal of Biological Chemistry*.
- Van de Meene AM, Hohmann-Marriott MF, Vermaas WF, Roberson RW** (2006) The three-dimensional structure of the cyanobacterium *Synechocystis* sp. PCC 6803. *Archives of Microbiology* **184**: 259–270.
- Vojta L, Soll J, Bölter B** (2007) Protein transport in chloroplasts – targeting to the intermembrane space. *FEBS Journal* **274**: 5043–5054.
- Westphal S** (2001) From the Cover: Vipp1 deletion mutant of *Synechocystis*: A connection between bacterial phage shock and thylakoid biogenesis? *Proceedings of the National Academy of Sciences* **98**: 4243–4248.
- Westphal S, Soll J, Vothknecht UC** (2001) A vesicle transport system inside chloroplasts. *FEBS letters* **506**: 257–261.
- Westphal S, Soll J, Vothknecht UC** (2003) Evolution of chloroplast vesicle transport. *Plant & cell physiology* **44**: 217–222.
- Xie K, Dalbey RE** (2008) Inserting proteins into the bacterial cytoplasmic membrane using the Sec and YidC translocases. *Nature Reviews Microbiology* **6**: 234–244.
- Yi L, Jiang F, Chen M, Cain B, Bolhuis A, Dalbey RE** (2003) YidC Is Strictly Required for Membrane Insertion of Subunits a and c of the F<sub>1</sub>F<sub>0</sub> ATP Synthase and SecE of the SecYEG Translocase †. *Biochemistry* **42**: 10537–10544.
- Yoshihara S** (2002) pilG Gene Cluster and Split pilL Genes Involved in Pilus Biogenesis, Motility and Genetic Transformation in the Cyanobacterium *Synechocystis* sp. PCC 6803. *Plant and Cell Physiology* **43**: 513–521.
- Yoshimura H** (2002) A cAMP Receptor Protein, SYCRP1, is Responsible for the Cell Motility of *Synechocystis* sp. PCC 6803. *Plant and Cell Physiology* **43**: 460–463.

- Yoshimura H, Hisabori T, Yanagisawa S, Ohmori M** (2000) Identification and characterization of a novel cAMP receptor protein in the cyanobacterium *Synechocystis* sp. PCC 6803. *The Journal of biological chemistry* **275**: 6241–6245.
- Zak E** (2001) The initial steps of biogenesis of cyanobacterial photosystems occur in plasma membranes. *Proceedings of the National Academy of Sciences* **98**: 13443–13448.
- Zak E, Norling B, Andersson B, Pakrasi HB** (1999) Subcellular localization of the BtpA protein in the cyanobacterium *Synechocystis* sp. PCC 6803. *FEBS* **261**: 311–316.
- Zang X, Liu B, Liu S, Arunakumara KKIU, Zhang X** (2007) Optimum Conditions for Transformation of *Synechocystis* sp. PCC 6803. *The Journal of Microbiology* **45**: 241–245.
- Zhou C, Yang Y, Jong A** (1990) Mini-Prep in 10 Minutes. *Biotechniques*: 172–173.
- Zhou J, Xu Z** (2005) The structural view of bacterial translocation-specific chaperone SecB: implications for function. *Molecular microbiology* **58**: 349–357.
- Zinchenko VV, Piven IP, Melnik V, Shestakov SV** (1999) Vectors for the complementation of cyanobacterial mutants **35**: 228–232.
- Zouni A, Witt HT, Kern J, Fromme P, Krauß N, Saenger W, Orth P** (2001) Crystal structure of photosystem II from *Synechococcus elongatus* at 3.8 Å resolution. *Nature* **409**: 739–743.

## 7 Danksagung

Ich möchte mich herzlich bei Prof. Dr. Jürgen Soll bedanken, dass ich meine Promotion in seiner Arbeitsgruppe anfertigen konnte.

Weiterer Dank gehört Prof. Dr. Nickelsen, Prof. Dr. Mascher, Prof. Dr. Leonhardt, Prof. Dr. Frank und Prof. Dr. Metzler für ihre Bereitschaft zur Begutachtung dieser Arbeit und für die fordernde aber dennoch angenehme Prüfungsatmosphäre.

Ein besonderes Dankeschön geht an Dr. Elisabeth Ankele für die tolle Betreuung, die nützlichen Ratschläge und anregenden Diskussionen, die eine wirkliche Unterstützung für meine Arbeit waren.

Allen Mitgliedern der AG Soll danke ich für ihre Hilfsbereitschaft und die tolle Arbeitsatmosphäre im Labor.

Ganz besonders herzlich möchte ich mich bei Sabine Nick, meiner zweiten (besseren) Hälfte im Labor, Maxi Richter und Yuanyuan Liang für den Spaß, den interkulturellen Flair und die super Zusammenarbeit bedanken. Ihr wart das beste Team, das ich mir vorstellen kann!

Christine Fellerer, Regina Schweiger und Giorgia Lamberti danke ich für die tolle Zeit in und außerhalb des Labors. Carsten Studte danke ich für seine treue Begleitung während der angenehmsten Zeit des Arbeitsalltags, auch wenn ein Experiment mal 10 Minuten länger dauerte.

Jenny danke ich für ihren Rückhalt und bedingungslose Unterstützung, auf die ich immer zählen konnte.

Meine tiefste Dankbarkeit geht an meine Eltern für ihre Unterstützung und das Vertrauen, das sie in mich setzen. Ihre Ermutigung meine Ziele zu verfolgen hat mich bis hierher geführt. Ohne ihre großartige Unterstützung wäre mein Studium der Biologie nicht möglich gewesen.

## **8 Eidesstattliche Versicherung**

Ich versichere hiermit an Eides statt, dass die vorgelegte Dissertation von mir selbstständig und ohne unerlaubte Hilfe angefertigt ist.

München, den 29.08.2012

Ingo Wolf

## **9 Erklärung**

Hiermit erkläre ich, dass die Dissertation nicht ganz oder in wesentlichen Teilen einer anderen Prüfungskommission vorgelegt worden ist. Außerdem erkläre ich, dass ich mich anderweitig einer Doktorprüfung ohne Erfolg nicht unterzogen habe.

München, den 29.08.2012

Ingo Wolf